



LAWRENCE
LIVERMORE
NATIONAL
LABORATORY

Conversion and optimization of the parameters from an extended form of the ion-interaction model for $\text{Ca}(\text{NO}_3)_2(\text{aq})$ and $\text{NaNO}_3(\text{aq})$ to those of the standard Pitzer model, and an assessment of the accuracy of the parameter temperature representations

A. M. Wijesinghe , J. A. Rard

January 7, 2005

Journal of Chemical Thermodynamics

Disclaimer

This document was prepared as an account of work sponsored by an agency of the United States Government. Neither the United States Government nor the University of California nor any of their employees, makes any warranty, express or implied, or assumes any legal liability or responsibility for the accuracy, completeness, or usefulness of any information, apparatus, product, or process disclosed, or represents that its use would not infringe privately owned rights. Reference herein to any specific commercial product, process, or service by trade name, trademark, manufacturer, or otherwise, does not necessarily constitute or imply its endorsement, recommendation, or favoring by the United States Government or the University of California. The views and opinions of authors expressed herein do not necessarily state or reflect those of the United States Government or the University of California, and shall not be used for advertising or product endorsement purposes.

12/21/2004

Conversion and optimization of the parameters from an extended form of the ion-interaction model for $\text{Ca}(\text{NO}_3)_2(\text{aq})$ and $\text{NaNO}_3(\text{aq})$ to those of the standard Pitzer model, and an assessment of the accuracy of the parameter temperature representations

Ananda M. Wijesinghe and Joseph A. Rard*

Energy and Environment Directorate, Lawrence Livermore National Laboratory,
University of California, Livermore, California 94550, U.S.A.

Send proof to J. A. Rard by email to rard1@llnl.gov

Short title: Pitzer parameter conversion and optimization for $\text{Ca}(\text{NO}_3)_2(\text{aq})$ and $\text{NaNO}_3(\text{aq})$

A. M. Wijesinghe and J. A. Rard

Abstract

The electrolytes $\text{Ca}(\text{NO}_3)_2(\text{aq})$ and $\text{NaNO}_3(\text{aq})$ are both extremely soluble but differ in several important respects. $\text{Ca}(\text{NO}_3)_2(\text{aq})$ has complex behavior at low ionic strengths and forms several thermodynamically stable and metastable solid phases, whereas $\text{NaNO}_3(\text{aq})$ forms only an anhydrous solid phase. The thermodynamic properties of both have previously been modeled using extended Pitzer ion-interaction models that include higher-order virial terms, in addition to those of the standard Pitzer model. The parameters of the original Pitzer model, however, are often needed for thermodynamic modeling calculations. In this paper we convert the parameters of the extended ion-interaction models for $\text{Ca}(\text{NO}_3)_2(\text{aq})$ and $\text{NaNO}_3(\text{aq})$ to the standard Pitzer model using an extension of the methodology previously described by Rard and Wijesinghe [J. Chem. Thermodynamics 35 (2003) 439–473]. In this variant, the exponential coefficient a_1^{P} of Pitzer's model is also optimized to yield the most accurate overall representation of the osmotic coefficients f over the ionic strength and temperature ranges of interest. The optimal values of $a_1^{\text{P}} = 0.87 \text{ kg}^{1/2}\cdot\text{mol}^{-1/2}$ for $\text{Ca}(\text{NO}_3)_2(\text{aq})$ and $a_1^{\text{P}} = 1.43 \text{ kg}^{1/2}\cdot\text{mol}^{-1/2}$ for $\text{NaNO}_3(\text{aq})$ are smaller than the value $a_1^{\text{P}} = 2.00 \text{ kg}^{1/2}\cdot\text{mol}^{-1/2}$ normally used for electrolytes of these valence types. In both cases, the accuracy of the osmotic coefficients predicted by the standard Pitzer model was nearly equal to that of the extended Pitzer model up to the solubility limit for $T = (298.15 \text{ to } 423.15) \text{ K}$. This result is consistent with the findings of Rard, Wijesinghe, and Wolery [J. Chem. Eng. Data 49 (2004) 1127–1140] who obtained a substantial improvement in model accuracy for $\text{Mg}(\text{NO}_3)_2(\text{aq})$ at $T = 298.15 \text{ K}$ by optimizing this parameter. The use of a temperature dependent a_1^{P} that is optimal at each temperature did not yield a significant improvement in accuracy over

using a constant optimal value. We also investigated the impact of choosing different temperature functions to develop temperature correlations for the Pitzer parameters. Higher-order temperature functions were needed for evaluations with solubility limited maximum ionic strength compared to evaluations performed at constant maximum ionic strength over the temperature range, especially for $\text{Ca}(\text{NO}_3)_2(\text{aq})$ because of its more complex thermodynamic behavior. Accurate temperature correlations are presented for both $\text{Ca}(\text{NO}_3)_2(\text{aq})$ and $\text{NaNO}_3(\text{aq})$.

KEYWORDS: Pitzer's model, Archer's model, ion-interaction model, aqueous electrolyte, calcium nitrate, sodium nitrate, parameter optimization, parameter correlations

1. Introduction

The standard form of Pitzer's ion-interaction model for electrolyte solutions [1,2], which contains three empirically determined parameters $b_{M,X}^{(0)}$, $b_{M,X}^{(1)}$, and $C_{M,X}^f$, has been used extensively for representing the thermodynamic properties of aqueous electrolytes, with an additional term containing the $b_{M,X}^{(2)}$ parameter for aqueous divalent metal sulfates and other higher-valence electrolytes that have significant ionic association at low molalities followed by redissociation at higher molalities [2–4].

Weare and co-workers [5,6] showed that Pitzer's model could be used to reliably model the solubilities of solutes present in complex, highly concentrated, natural brines and their precipitation sequences as solvent is evaporated. Pitzer's ion-interaction model is included in several geochemical modeling codes [7–9]. Extended forms of Pitzer's model with ionic-strength dependent third virial terms [10–13] have been used to represent thermodynamic data for highly soluble electrolytes, when the standard (three parameter) Pitzer model is not able to represent these data with sufficient accuracy. Rard and Wijesinghe [14] listed studies published up to 2002 that reported parameters for these extended models. Many of these studies used the extended ion-interaction model described by Archer [10,11]. Parameters for the Archer model were subsequently evaluated for $\text{Na}_2\text{SO}_4(\text{aq})$ [15], $\text{NdCl}_3(\text{aq})$ [16], and $\text{Mg}(\text{NO}_3)_2(\text{aq})$ [17].

Databases are available [2,5,6,18–21] for the parameters of the original or standard Pitzer model [1–4]. However, the equations of the extended models [10–13] have not been incorporated in most geochemical modeling codes, and thus there is a continuing need for expanding the parameter databases for the standard Pitzer model.

The electrolyte $\text{Ca}(\text{NO}_3)_2$ is soluble in H_2O to about $m = 8.4 \text{ mol}\cdot\text{kg}^{-1}$ at $T = 298.15 \text{ K}$, but the solubility increases rapidly with temperature reaching values of $m \approx (22 \text{ to } 23) \text{ mol}\cdot\text{kg}^{-1}$ for the temperature range $T = (348.15 \text{ to } 423.15) \text{ K}$ where anhydrous $\text{Ca}(\text{NO}_3)_2(\text{cr})$ is the thermodynamically stable solid phase [22]. However, as observed by Stokes and Robinson at $T = 298.15 \text{ K}$ [23], $\text{Ca}(\text{NO}_3)_2(\text{aq})$ solutions readily supersaturate when evaporated isothermally. When the solution is concentrated sufficiently, the supersaturated solution transforms into a semi-solid gel. Stokes and Robinson further noted that the curve of vapor pressures against molality is continuous for both the fluid and gel phases. They also reported isopiestic molalities at $T = 298.15 \text{ K}$ for supersaturated solutions ranging up to $m = 21.58 \text{ mol}\cdot\text{kg}^{-1}$. Oakes et al. [13] summarized published thermodynamic studies for $\text{Ca}(\text{NO}_3)_2(\text{aq})$ in their table 2, which includes isopiestic results at $T = (373 \text{ to } 423) \text{ K}$ extending nearly to the saturated solution molalities [24].

A molality of $m = 21.58 \text{ mol}\cdot\text{kg}^{-1}$ corresponds to an ionic molality of $3m = 3(21.58 \text{ mol}\cdot\text{kg}^{-1}) = 64.74 \text{ mol}\cdot\text{kg}^{-1}$, or 0.857 water molecules per ion. Clearly, at this very high molality there is insufficient water present to fulfill the hydration requirements of the individual ions, extensive ion pairing or complex formation must be present, and the basic assumptions of Debye-Hückel type electrostatic models are no longer valid. The Brunauer-Emmett-Teller (BET) absorption model [25] has been used to represent the water activities of such highly concentrated solutions. Although the BET model generally represents the water activities fairly well at very high molalities, the quality of representation at low molalities is significantly poorer than at higher molalities. This failure to accurately represent the low molality behavior can result in large systematic errors in the derived mean activity coefficients for electrolytes with large but finite

solubilities, because the mean activity coefficients are based on the infinite dilution reference state by way of a standard state defined in terms of Henry's law.

Clegg et al. [26] represented the osmotic coefficients of $\text{Ca}(\text{NO}_3)_2(\text{aq})$ at $T = 298.15 \text{ K}$ with a mole-fraction based thermodynamic model. The mole-fraction composition scale is a more appropriate composition scale than molality for thermodynamic models at very high concentrations, where the molality varies rapidly with the amount of solvent and can become infinite for completely miscible systems. They were able to represent the available osmotic coefficients of $\text{Ca}(\text{NO}_3)_2(\text{aq})$ fairly accurately to $m \approx 15 \text{ mol}\cdot\text{kg}^{-1}$ with four model parameters. However, their model is restricted to $T = 298.15 \text{ K}$.

In Archer's model [10,11] the constant $C_{M,X}^f$ term of Pitzer's standard model is replaced by a two-parameter ionic strength-dependent function, and this extended model is able to accurately represent the thermodynamic properties of most soluble electrolytes over wide ranges of molality and temperature. However, the thermodynamic data for $\text{Ca}(\text{NO}_3)_2(\text{aq})$ extend to such high molalities that Oakes et al. [13] found it was necessary to extend the Archer model by adding a second ionic-strength dependent third virial term. Oakes et al. were able to represent the available thermodynamic data for $\text{Ca}(\text{NO}_3)_2(\text{aq})$ to $m \approx 20 \text{ mol}\cdot\text{kg}^{-1}$ for $T \approx (298 \text{ to } 373) \text{ K}$ without explicitly considering ionic association. However, it is likely that the additional third virial terms, in part, are indirectly representing the effects both this ionic association and the breakdown of the assumptions of the Debye-Hückel model. Their parameterized model represents the available osmotic coefficients f fairly accurately up to $m \approx 10 \text{ mol}\cdot\text{kg}^{-1}$, and to $\Delta f \approx 0.03$ at the highest molalities.

The most rigorous way to obtain the parameters of Pitzer's standard model is to evaluate the parameters using the same critically-assessed database that was used for

evaluating the parameters of the extended ion-interaction model. However, the original, critically-assessed database is not always available. Rard and Wijesinghe [14] proposed an alternative approach in which the available model parameters for the extended ion-interaction model are directly converted to those of the standard Pitzer model. They reported the Pitzer model parameters for four aqueous electrolytes, including $\text{Ca}(\text{NO}_3)_2(\text{aq})$ and $\text{NaNO}_3(\text{aq})$, that were derived by this method. Unfortunately, there was a significant degradation of the quality of representation of the thermodynamic behavior for $\text{Ca}(\text{NO}_3)_2(\text{aq})$, and to a lesser extent for $\text{NaNO}_3(\text{aq})$, when the 5-parameter and 4-parameter extended models were transformed into 3-parameter standard Pitzer models.

Rard et al. [17] subsequently modeled the thermodynamic properties for the $\text{Mg}(\text{NO}_3)_2(\text{aq})$ system with Pitzer's standard model [1,2] and with Archer's model [10,11]. Isopiestic data for this system extend to $m = 5.123 \text{ mol}\cdot\text{kg}^{-1}$ but are restricted to $T = 298.15 \text{ K}$. Rard et al. found that optimizing the a_1 exponential coefficient to $a_1 = 1.55 \text{ kg}^{1/2}\cdot\text{mol}^{-1/2}$ for the $b_{\text{M,X}}^{(1)}$ term of Pitzer's standard model improved the standard deviation of the model fit by more than a factor of two relative to the fit with the usual value of $a_1 = 2.0 \text{ kg}^{1/2}\cdot\text{mol}^{-1/2}$, and gave an excellent representation of the available thermodynamic data that was essentially equal in quality to the fit with Archer's model. They suggested that a significant improvement might also be achieved for the standard Pitzer model for $\text{Ca}(\text{NO}_3)_2(\text{aq})$ if the a_1 exponential coefficient was similarly optimized.

The method of Rard and Wijesinghe [14] is based on determining the integral over the ionic strength range of the square of the differences between osmotic coefficients evaluated from two different ion-interaction models. Simultaneously setting equal to zero the partial derivatives of this cumulative square difference function with respect to

each of the parameters of standard Pitzer model $\{b_{M,X}^{(0)}, b_{M,X}^{(1)}, b_{M,X}^{(2)}, \text{ and } C_{M,X}^f\}$ yields the conditions necessary to obtain the optimum values of these parameters. However, they assumed that the exponential coefficients a_1 and a_2 of the $b_{M,X}^{(1)}$ and $b_{M,X}^{(2)}$ terms, respectively, were the same for both standard and extended ion-interaction models. In the present report we extend this method to the more general case where $a_1^P \neq a_1^{EA}$ and $a_2^P \neq a_2^{EA}$, where the superscripts P denote Pitzer and EA denote extended Archer models, and apply it to improving the representation of the $\text{Ca}(\text{NO}_3)_2(\text{aq})$ and $\text{NaNO}_3(\text{aq})$ systems with the standard Pitzer model.

2. The standard and extended ion-interaction models for strong electrolytes

Pitzer's original ion-interaction equation [1–4] for the molality-based osmotic coefficient f of a binary solution of a dissociated electrolyte of stoichiometry $M_{\nu_M}X_{\nu_X}$ in a single solvent may be written as:

$$f^P = 1 - |z_M z_X| A_\phi \cdot I^{1/2} / (1 + bI^{1/2}) + (2\nu_M \nu_X / \nu) m \{ b_{M,X}^{(0,P)} + b_{M,X}^{(1,P)} \cdot \exp(-a_1^P I^{1/2}) + b_{M,X}^{(2,P)} \cdot \exp(-a_2^P I^{1/2}) \} + \{ 2(\nu_M \nu_X)^{3/2} / \nu \} m^2 \cdot C_{M,X}^{(f,P)}, \quad (1)$$

where M denotes the cation and X the anion; m is the stoichiometric molality; $b = 1.2 \text{ kg}^{1/2} \cdot \text{mol}^{-1/2}$; A_ϕ is the Debye-Hückel limiting law slope for f ; I is the stoichiometric, molality-based, ionic strength; z_M and z_X are the valences (with sign) of ions M and X; ν_M and ν_X are the number of M and X ions formed by complete dissociation of one molecule of $M_{\nu_M}X_{\nu_X}$; and $\nu = \nu_M + \nu_X$ is the stoichiometric ionization number of the total

electrolyte. The exponential coefficient a_1^P is usually fixed at $a_1^P = 2.0 \text{ kg}^{1/2} \cdot \text{mol}^{-1/2}$, except for the divalent metal sulfates and for other higher-charge-type electrolytes with both ions having valences $|z_i| \geq 2$, where $a_1^P = 1.4 \text{ kg}^{1/2} \cdot \text{mol}^{-1/2}$ is the usual choice [2,3]. The $b_{M,X}^{(2,P)}$ term is normally included only for higher charge type electrolytes, and thus would not be used for electrolytes such as $\text{Ca}(\text{NO}_3)_2(\text{aq})$ and $\text{NaNO}_3(\text{aq})$.

For Pitzer's model, mean activity coefficients g_{\pm} of a single electrolyte are given by

$$\begin{aligned} \ln g_{\pm}^P = & -|z_M z_X| A_{\phi} \{ I^{1/2} / (1 + b I^{1/2}) + (2/b) \ln(1 + b I^{1/2}) \} + (2\nu_M \nu_X / \nu) m [2 b_{M,X}^{(0,P)} + \\ & 2 \{ b_{M,X}^{(1,P)} / (a_1^P)^2 I \} \{ 1 - \{ 1 + (a_1^P) I^{1/2} - (a_1^P)^2 I / 2 \} \exp(-a_1^P I^{1/2}) \} + \\ & 2 \{ b_{M,X}^{(2,P)} / (a_2^P)^2 I \} \{ 1 - \{ 1 + (a_2^P) I^{1/2} - (a_2^P)^2 I / 2 \} \exp(-a_2^P I^{1/2}) \}] + \\ & \{ 3(\nu_M \nu_X)^{3/2} / \nu \} m^2 \cdot C_{M,X}^{(f,P)}. \end{aligned} \quad (2)$$

We now recast these two equations solely in terms of the stoichiometric ionic strength I , rather than using both ionic strength and molality. For a single electrolyte, that is either completely or partially associated, the stoichiometric ionic strength is related to the molality by equation (11) of Rard and Wijesinghe [14]:

$$m = 2I / \{ \nu |z_M z_X| \}. \quad (3)$$

Using this relationship to eliminate the molality m in favor of the ionic strength I in equations (1) and (2) we obtain the expressions:

$$f^P = 1 - |z_M z_X| A_\phi \cdot I^{1/2} / (1 + bI^{1/2}) + \lambda_3 I \{ b_{M,X}^{(0,P)} + b_{M,X}^{(1,P)} \cdot \exp(-a_1^P I^{1/2}) + b_{M,X}^{(2,P)} \cdot \exp(-a_2^P I^{1/2}) + \lambda_1 IC_{M,X}^{(f,P)} \} \quad (4)$$

and

$$\ln g_{\pm}^P = -|z_M z_X| A_\phi \{ I^{1/2} / (1 + bI^{1/2}) + (2/b) \ln(1 + bI^{1/2}) \} + 2\lambda_3 I [b_{M,X}^{(0,P)} + \{ b_{M,X}^{(1,P)} / (a_1^P)^2 I \} \{ 1 - \{ 1 + (a_1^P) I^{1/2} - (a_1^P)^2 I / 2 \} \exp(-a_1^P I^{1/2}) \} + \{ b_{M,X}^{(2,P)} / (a_2^P)^2 I \} \{ 1 - \{ 1 + (a_2^P) I^{1/2} - (a_2^P)^2 I / 2 \} \exp(-a_2^P I^{1/2}) \} + (3/4) \lambda_1 IC_{M,X}^{(f,P)}], \quad (5)$$

where the charge-type dependent constants λ_1 and λ_3 are defined by

$$\lambda_1 \equiv 2(v_M v_X)^{1/2} / (v |z_M z_X|) \quad (6)$$

and

$$\lambda_3 \equiv (4v_M v_X) / (v^2 |z_M z_X|). \quad (7)$$

The Oakes et al. [13] equation for f will first be converted to a form analogous to equation (1) by recognizing that their anion molality m_a and cation molality m_c are related to the stoichiometric molality by $m_a = v_X \cdot m$ and $m_c = v_M \cdot m$, and by making the following composition scale transformations:

$$(2I / \hat{a}_i m_i) = |z_M z_X| \quad (8)$$

and

$$(2m_a m_c / \hat{a}_i m_i) = (2v_M v_X / v) m. \quad (9)$$

The equations of Oakes et al. [13] for the osmotic and mean activity coefficients then become:

$$\begin{aligned} f^{\text{EA}} = & 1 - |z_M z_X| A_\phi \cdot I^{1/2} / (1 + bI^{1/2}) + (2v_M v_X / v) m \{ b_{M,X}^{(0,\text{EA})} + \\ & b_{M,X}^{(1,\text{EA})} \cdot \exp(-a_1^{\text{EA}} I^{1/2}) + b_{M,X}^{(2,\text{EA})} \cdot \exp(-a_2^{\text{EA}} I^{1/2}) \} + \\ & (4v_M^2 v_X z_M / v) m^2 \{ C_{M,X}^{(0,\text{EA})} + C_{M,X}^{(1,\text{EA})} \cdot \exp(-w_1^{\text{EA}} I^{1/2}) + C_{M,X}^{(2,\text{EA})} \cdot \exp(-w_2^{\text{EA}} I^{1/2}) \} \end{aligned} \quad (10)$$

and

$$\begin{aligned} \ln g_{\pm}^{\text{EA}} = & -|z_M z_X| A_\phi \{ I^{1/2} / (1 + bI^{1/2}) + (2/b) \ln(1 + bI^{1/2}) \} + (2n_M n_X / n) m [2b_{M,X}^{(0,\text{EA})} + \\ & 2 \{ b_{M,X}^{(1,\text{EA})} / (a_1^{\text{EA}})^2 I \} \{ 1 - \{ 1 + (a_1^{\text{EA}})^2 I \} \exp(-a_1^{\text{EA}} I^{1/2}) \} + \\ & 2 \{ b_{M,X}^{(2,\text{EA})} / (a_2^{\text{EA}})^2 I \} \{ 1 - \{ 1 + (a_2^{\text{EA}})^2 I \} \exp(-a_2^{\text{EA}} I^{1/2}) \}] + \\ & (2n_M^2 n_X z_M / n) m^2 [3C_{M,X}^{(0,\text{EA})} + 4 \{ C_{M,X}^{(1,\text{EA})} / (w_1^{\text{EA}})^4 I^2 \} \{ 6 - \{ 6 + 6(w_1^{\text{EA}})^2 I \} \exp(-w_1^{\text{EA}} I^{1/2}) + \\ & 3(w_1^{\text{EA}})^2 I + (w_1^{\text{EA}})^3 I^{3/2} - (w_1^{\text{EA}})^4 I^2 / 2 \} \} + \\ & 4 \{ C_{M,X}^{(2,\text{EA})} / (w_2^{\text{EA}})^4 I^2 \} \{ 6 - \{ 6 + 6(w_2^{\text{EA}})^2 I \} \exp(-w_2^{\text{EA}} I^{1/2}) + 3(w_2^{\text{EA}})^2 I + (w_2^{\text{EA}})^3 I^{3/2} - \\ & (w_2^{\text{EA}})^4 I^2 / 2 \} \exp(-w_2^{\text{EA}} I^{1/2}) \}]. \end{aligned} \quad (11)$$

When these equations for the extended Archer model are recast solely in terms of the ionic strength I , as was done for the standard Pitzer model, we obtain

$$f^{\text{EA}} = 1 - |z_M z_X| A_\phi \cdot I^{1/2} / (1 + bI^{1/2}) + \lambda_3 I [b_{M,X}^{(0,\text{EA})} +$$

$$\begin{aligned}
& b_{M,X}^{(1,EA)} \cdot \exp(-a_1^{EA} I^{1/2}) + b_{M,X}^{(2,EA)} \cdot \exp(-a_2^{EA} I^{1/2}) \} + \\
& \lambda_1 \lambda_2 I \{ C_{M,X}^{(0,EA)} + C_{M,X}^{(1,EA)} \cdot \exp(-w_1^{EA} I^{1/2}) + C_{M,X}^{(2,EA)} \cdot \exp(-w_2^{EA} I^{1/2}) \}] \quad (12)
\end{aligned}$$

and

$$\begin{aligned}
\ln g_{\pm}^{EA} = & -|z_M z_X| A_{\phi} \{ I^{1/2} / (1 + b I^{1/2}) + (2/b) \ln(1 + b I^{1/2}) \} + 2\lambda_3 I [b_{M,X}^{(0,EA)} + \\
& \{ b_{M,X}^{(1,EA)} / (a_1^{EA})^2 I \} \{ 1 - \{ 1 + (a_1^{EA}) I^{1/2} - (a_1^{EA})^2 I / 2 \} \exp(-a_1^{EA} I^{1/2}) \} + \\
& \{ b_{M,X}^{(2,EA)} / (a_2^{EA})^2 I \} \{ 1 - \{ 1 + (a_2^{EA}) I^{1/2} - (a_2^{EA})^2 I / 2 \} \exp(-a_2^{EA} I^{1/2}) \}] + \\
& 2\lambda_1 \lambda_2 \lambda_3 I^2 [(3/4) C_{M,X}^{(0,EA)} + \{ C_{M,X}^{(1,EA)} / (w_1^{EA})^4 I^2 \} \{ 6 - \{ 6 + 6(w_1^{EA}) I^{1/2} + \\
& 3(w_1^{EA})^2 I + (w_1^{EA})^3 I^{3/2} - (w_1^{EA})^4 I^2 / 2 \} \exp(-w_1^{EA} I^{1/2}) \} + \\
& \{ C_{M,X}^{(2,EA)} / (w_2^{EA})^4 I^2 \} \{ 6 - \{ 6 + 6(w_2^{EA}) I^{1/2} + 3(w_2^{EA})^2 I + (w_2^{EA})^3 I^{3/2} - \\
& (w_2^{EA})^4 I^2 / 2 \} \exp(-w_2^{EA} I^{1/2}) \}], \quad (13)
\end{aligned}$$

where

$$\lambda_2 \equiv 2(|z_M z_X|)^{1/2}. \quad (14)$$

The $b_{M,X}^{(0)}$ and $b_{M,X}^{(1)}$ parameters are intended to represent exactly the same two-ion interactions in the Pitzer [1–4], Archer [10,11], and Oakes et al. [13] models, and thus, in principle, the numerical values of each of these equivalent parameters should be the same in the two formulations. Similarly, the parameter $C_{M,X}^{(f,P)}$ of Pitzer's equation is equivalent to Archer's $C_{M,X}^{(0,EA)}$ parameter, because $C_{M,X}^{(f,P)} = 2z_M(n_M/n_X)^{1/2} C_{M,X}^{(0,A)}$ when $C_{M,X}^{(1,EA)} = C_{M,X}^{(2,EA)} = 0$. However, the numerical values of the equivalent parameters will not be identical

unless the $C_{M,X}^{(1,EA)}$ and $C_{M,X}^{(2,EA)}$ parameters are set equal to zero and $a_1^P = a_1^{EA}$ and $a_2^P = a_2^{EA}$. In the present paper we consider the more general case where a_1^P and a_2^P , respectively, may differ from a_1^{EA} and a_2^{EA} . Thus, the model parameters, osmotic coefficients, and mean activity coefficients are identified by either a superscript "P" for Pitzer or superscript "EA" for extended Archer, in order to distinguish between the two source model equations.

3. Methods of Analysis: Conversion of the model parameters of the extended ion-interaction model of Oakes et al. to those of the standard Pitzer model with the simultaneous optimization of $b_{M,X}^{(0,P)}$, $b_{M,X}^{(1,P)}$, $b_{M,X}^{(2,P)}$, $C_{M,X}^{(f,P)}$, a_1^P , and a_2^P

The general method we use for converting parameters from the extended ion-interaction model of Oakes et al. [13] to those of the standard Pitzer model [1-4], is based on minimizing, in a least-squares sense, the difference (or "error") between the osmotic coefficients predicted by these two models. The equations of Oakes et al. [13] reduce to the equations of Archer [10,11] when $C_{M,X}^{(2,EA)} = 0$, and consequently the methodology described below is applicable to Archer's model by setting $C_{M,X}^{(2,EA)}$ and its derivatives equal to zero.

For simplicity, we shall assume that identical values of the Debye-Hückel model limiting law slopes A_ϕ , and their temperature and pressure derivatives, are to be used in both the Pitzer and the extended Archer forms of the ion-interaction model. Archer [27] described how to adjust the Pitzer model parameters if the value of A_ϕ is changed. We use the same value of the constant $b = 1.2 \text{ kg}^{1/2} \cdot \text{mol}^{-1/2}$ in both forms of the ion-interaction model, following Pitzer's recommendation [1].

We minimize the mean square difference function $E_1^2\{X^P(T, p)\}$ defined by:

$$E_I^2 \equiv \left\{ \int_{I_{\min}=0}^{I_{\max}(T)} (f^P - f^{EA})^2 dI \right\} / \int_{I_{\min}=0}^{I_{\max}(T)} dI, \quad (15a)$$

$$= \{I / I_{\max}(T)\} \left\{ \int_{I_{\min}=0}^{I_{\max}(T)} (f^P - f^{EA})^2 dI \right\}, \quad (15b)$$

over the ionic-strength range of interest $\{I_{\min} = 0 \text{ to } I_{\max}(T)\}$.

Examination of equations (4) and (12), and (5) and (13), indicates that the Debye-Hückel terms are identical for f^{EA} and f^P , and also for $\ln g_{\pm}^{EA}$ and $\ln g_{\pm}^P$, and thus they will cancel exactly when the differences $(f^P - f^{EA})$ and $(\ln g_{\pm}^P - \ln g_{\pm}^{EA})$, are taken. The choice of one difference function over the other will not influence the results that follow.

The parameters and exponential coefficients of the extended Archer ion-interaction model {i.e, $b_{MX}^{(0,EA)}$, $b_{MX}^{(1,EA)}$, $b_{MX}^{(2,EA)}$, $C_{M,X}^{(0,EA)}$, $C_{M,X}^{(1,EA)}$, $C_{M,X}^{(2,EA)}$, a_1^{EA} , and a_2^{EA} } are assumed to be known, and those of Pitzer's standard model $\{b_{M,X}^{(0,P)}$, $b_{M,X}^{(1,P)}$, $b_{M,X}^{(2,P)}$, $C_{M,X}^{(f,P)}$, a_1^P , and $a_2^P\}$ are unknown quantities whose values are to be determined from the parameters of the extended ion-interaction model.

The method that we will use, as described by Rard and Wijesinghe [14], is to evaluate the optimum values of the parameters of the original Pitzer model [1–4] from those of extended Archer model [13], by determining the unknown standard Pitzer parameter set $X^P(T, p)$ that minimizes the values of the difference function $(f^P - f^{EA})$ over the full ionic-strength range $I_{\min} = 0$ to some maximum value $I_{\max}(T)$. The selected Pitzer model parameter set is denoted by $X^P(T, p) \equiv \{b_{M,X}^{(0,P)}$, $b_{M,X}^{(1,P)}$, $b_{M,X}^{(2,P)}$, $C_{M,X}^{(f,P)}$, a_1^P , and $a_2^P\}$, and an element of this parameter set is denoted by X_i^P ($i = 1, 2, \dots, 6$). Similarly, we define the extended Archer model parameter set as $X^{EA}(T, p) \equiv \{b_{MX}^{(0,EA)}$, $b_{MX}^{(1,EA)}$, $b_{MX}^{(2,EA)}$, $C_{M,X}^{(0,EA)}$, $C_{M,X}^{(1,EA)}$, $C_{M,X}^{(2,EA)}$, a_1^{EA} , a_2^{EA} , w_1^{EA} , and $w_2^{EA}\}$, where X_i^{EA} ($i = 1, 2, \dots, 10$) is an element of the

extended Archer model parameter set. Therefore, the mean square error E_I^2 defined by equation (15) can be viewed as a function $E_I^2\{X_i^P(T, p)\}$ of the unknown temperature and pressure dependent standard Pitzer parameters $X_i^P(T, p)$.

The advantages of using $E_I^2\{X^P(T, p)\}$ as the measure of “goodness of fit” is that its values will be identically zero only if $(f^P - f^{EA})$ is identically zero at all values of I , and it has positive values for all finite positive or negative differences $(f^P - f^{EA})$. More specifically, $E_I^2\{X^P(T, p)\}$ is a positive definite function with a quadratic form in the unknown $\{b_{M,X}^{(0,P)}, b_{M,X}^{(1,P)}, b_{M,X}^{(2,P)}, \text{ and } C_{M,X}^{(f,P)}\}$ parameters because $(f^P - f^{EA})$ is a continuous linear function of these four parameters, although it is nonlinear in the two exponential coefficients $\{a_1^P, a_2^P\}$. Our approach, applied here to continuous functions, is analogous to the traditional least-squares method applied to sets of discrete experimental information.

The upper integration limit $I_{\max}(T)$ may be the same as the maximum ionic strength used for evaluation of the parameters for the extended Archer model at the temperature under consideration. Alternatively, if the extended Archer model parameters are based in part on thermodynamic measurements for highly supersaturated solutions, it may be desirable to restrict I_{\max} to the ionic strength of the saturated solutions I_{sat} , in order to optimize the representation for solubility calculations. The minimum ionic strength I_{\min} has been set equal to zero, to simplify the analysis and because this is the reference state for mean activity coefficients.

The values of the X_i^P parameters that minimize the values of $E_I^2\{X^P(T, p)\}$ can be found by simultaneously setting equal to zero the derivatives of this function with respect to all of the Pitzer model parameters X_i^P . Integration of the complicated expression resulting from direct evaluation of the $(f^P - f^{EA})^2$ term in equation (15) can be avoided

and simplified by first differentiating the integrand under the integral sign, and then analytically integrating the resulting simpler integrands:

$$\partial E_i^2 / \partial X_i^P = (2 / I_{\max}) \left\{ \int_{I_{\min}=0}^{I_{\max}(\tau)} (f^P - f^{EA}) (\partial f^P / \partial X_i^P) dI \right\} = 0, \quad (16)$$

The subsequent mathematical development can be considerably simplified and streamlined by recasting equations (4) and (12) for the osmotic coefficient of the standard Pitzer and extended Archer models in forms that exploit the linearity of these expressions in the coefficients X_i^P ($i = 1, \dots, 4$) = $\{b_{M,X}^{(0,P)}, b_{M,X}^{(1,P)}, b_{M,X}^{(2,P)}, \text{ and } C_{M,X}^{(f,P)}\}$ of the standard Pitzer model, and in the coefficients X_i^{EA} ($i = 1, \dots, 6$) = $\{b_{M,X}^{(0,EA)}, b_{M,X}^{(1,EA)}, b_{M,X}^{(2,EA)}, C_{M,X}^{(0,EA)}, C_{M,X}^{(1,EA)}, \text{ and } C_{M,X}^{(2,EA)}\}$ of the extended Archer model:

$$f^P = f_{DH}^P + \sum_{j=1}^4 (\partial f^P / \partial X_j^P) X_j^P \quad (17)$$

$$f^{EA} = f_{DH}^{EA} + \sum_{j=1}^6 (\partial f^{EA} / \partial X_j^{EA}) X_j^{EA} \quad (18)$$

where:

$$f_{DH}^P = 1 - |z_M z_X| A_\phi \cdot I^{1/2} / (1 + bI^{1/2}) \quad (19)$$

$$\partial f^P / \partial b_{M,X}^{(0,P)} = \lambda_3 I \quad (20)$$

$$\partial f^P / \partial b_{M,X}^{(1,P)} = \lambda_3 I \cdot \exp(-a_1^P I^{1/2}) \quad (21)$$

$$\partial f^P / \partial b_{M,X}^{(2,P)} = \lambda_3 I \cdot \exp(-a_2^P I^{1/2}) \quad (22)$$

$$\partial f^P / \partial C_{M,X}^{(f,P)} = \lambda_1 \lambda_3 I^2 \quad (23)$$

$$f_{DH}^{EA} = 1 - |z_M z_X| A_\phi \cdot I^{1/2} / (1 + bI^{1/2}) \quad (24)$$

$$\partial f^{EA} / \partial b_{M,X}^{(0,EA)} = \lambda_3 I \quad (25)$$

$$\partial f^{EA}/\partial b_{M,X}^{(1,EA)} = \lambda_3 I \cdot \exp(-a_1^{EA} I^{1/2}) \quad (26)$$

$$\partial f^{EA}/\partial b_{MX}^{(2,EA)} = \lambda_3 I \cdot \exp(-a_2^{EA} I^{1/2}) \quad (27)$$

$$\partial f^{EA}/\partial C_{M,X}^{(0,EA)} = \lambda_1 \lambda_2 \lambda_3 I^2 \quad (28)$$

$$\partial f^{EA}/\partial C_{M,X}^{(1,EA)} = \lambda_1 \lambda_2 \lambda_3 I^2 \cdot \exp(-w_1^{EA} I^{1/2}) \quad (29)$$

$$\partial f^{EA}/\partial C_{M,X}^{(2,EA)} = \lambda_1 \lambda_2 \lambda_3 I^2 \cdot \exp(-w_2^{EA} I^{1/2}) \}.$$

(30)

All of the extended Archer model parameters, the ionic strength, the temperature, and the pressure are held constant when these partial derivatives are evaluated.

Inserting expressions (17) and (18) into equation (16), and rearranging the terms and defining new matrix arrays, we obtain

$$\sum_{j=1}^4 A_{ij} \cdot X_j^P = B_i \quad i = 1, \dots, 4 \quad (31)$$

where

$$B_i = \sum_{k=1}^6 C_{ik} \cdot X_k^{EA} - D_i \quad i = 1, \dots, 4 \quad (32)$$

The coefficient matrices A_{ij} , C_{ik} , and the Debye-Hückel vector D_i are given by

$$A_{ij} \equiv \int_{I_{\min}=0}^{I_{\max}(T)} (\partial f^P / \partial X_i^P) (\partial f^P / \partial X_j^P) dI \quad i, j = 1, \dots, 4 \quad (33)$$

$$C_{ik} \equiv \int_{I_{\min}=0}^{I_{\max}(T)} (\partial f^P / \partial X_i^P) (\partial f^{EA} / \partial X_k^{EA}) dI \quad i = 1, \dots, 4 ; k = 1, \dots, 6 \quad (34)$$

$$D_i \equiv \int_{I_{\min}=0}^{I_{\max}(T)} (\partial f^P / \partial X_i^P) (f_{DH}^P - f_{DH}^{EA}) dI \quad i = 1, \dots, 4 \quad (35)$$

It can be seen from equation (33) that the coefficient matrix A_{ij} is a symmetric (i.e, $A_{ij} = A_{ji}$) square ($i, j = 1, \dots, 4$) matrix whose size is determined by the number of unknown Pitzer parameters (excluding the a_1^P and a_2^P exponential coefficients), and it depends solely on the properties of the standard Pitzer model and the maximum ionic strength $I_{\max}(T)$. In contrast, the coefficient matrix C_{ik} is, in general, neither square nor symmetric. The number of rows of this matrix is equal to the number of unknown parameters of the standard Pitzer model (excluding its a_1^P and a_2^P exponential coefficients) and the number of columns is equal to the number of extended Archer model parameters (excluding the a_1^{EA} and a_2^{EA} exponential coefficients), and it is a function of the properties of both the standard Pitzer and the extended Archer models. The Debye-Hückel vector D_i will be set equal to zero because the Debye-Hückel limiting-law slope A_ϕ and b were assumed to be the same for the standard Pitzer and extended Archer models, so that $f_{DH}^P = f_{DH}^{EA}$. The integrations required to evaluate the coefficient matrix A_{ij} and the right hand side vector B_i can be performed analytically, and the results are given in Appendix A. The values of the resulting expressions for A_{ij} and B_i can be evaluated numerically if the values of the exponents $\{a_1^P, a_2^P\}$ are specified, and all of the extended Archer model parameters $X^{EA}(T, p) \equiv \{b_{MX}^{(0,EA)}, b_{MX}^{(1,EA)}, b_{MX}^{(2,EA)}, C_{MX}^{(0,EA)}, C_{MX}^{(1,EA)}, C_{MX}^{(2,EA)}, a_1^{EA}, a_2^{EA}, w_1^{EA}, \text{ and } w_2^{EA}\}$ are known. The matrix equation (31), which is linear in the parameters $X_i^P (i = 1, \dots, 4) = \{b_{M,X}^{(0,P)}, b_{M,X}^{(1,P)}, b_{M,X}^{(2,P)}, \text{ and } C_{M,X}^{(f,P)}\}$, can then be easily solved for these parameters by standard matrix solution methods.

The condition expressed by equation (16) is a necessary condition for the solution $X^P(T, p)$ of the matrix equation (31) to be a local extremum of the function $E_I^2\{X^P(T, p)\}$. However, equation (16) alone is not sufficient to ensure that the resulting solution $X^P(T, p)$ represents a minimum, rather than a maximum or a point of inflection. Therefore, the goodness of fit of the model representation obtained by this approach should be evaluated by directly calculating, and then comparing the f values obtained by using the original extended Archer model parameters to those calculated using the derived Pitzer parameters.

Determination of the optimum exponents a_1^P, a_2^P

The two equations that determine the optimum values of the exponential coefficients a_1^P, a_2^P that minimize the mean square error E_I^2 can be formulated in a similar fashion by setting the derivatives of E_I^2 with respect to each exponential coefficient equal to zero:

$$\partial E_I^2 / \partial a_n^P = (2/I_{\max}) \left\{ \int_{I_{\min}=0}^{I_{\max}(T)} (f^P - f^{EA}) (\partial f^P / \partial a_n^P) dI \right\} = 0, \quad (36)$$

where $a_n^P = \{a_1^P, a_2^P\}$ for $n = 1, 2$ and

$$\partial f^P / \partial a_1^P = -\lambda_3 b_{M,X}^{(1,P)} \cdot I^{3/2} \cdot \exp(-a_1^P I^{1/2}) \quad (37)$$

$$\partial f^P / \partial a_2^P = -\lambda_3 b_{M,X}^{(2,P)} \cdot I^{3/2} \cdot \exp(-a_2^P I^{1/2}). \quad (38)$$

Inserting the expressions (17) and (18) for the osmotic coefficients f^P and f^{EA} into equation (36) and rearranging the terms and defining new variables, we obtain

$$\sum_{j=1}^4 A_{nj}^a \cdot X_j^P = B_n^a, \quad n = 1, 2 \quad (39)$$

where,

$$\mathbf{B}_n^a = \sum_{k=1}^6 \mathbf{C}_{nk}^a \cdot \mathbf{X}_k^{\text{EA}} - \mathbf{D}_n^a, \quad n = 1, \dots, 4 \quad (40)$$

The exponential coefficient matrices \mathbf{A}_{nj}^a , \mathbf{C}_{nk}^a , and the Debye-Hückel vector \mathbf{D}_n^a are given by

$$\mathbf{A}_{nj}^a \equiv -(1/b_{M,X}^{(n,P)}) \int_{I_{\min}=0}^{I_{\max}(T)} (\partial f^P / \partial a_n^P) (\partial f^P / \partial X_j^P) dI, \quad n = 1, 2; j = 1, \dots, 4 \quad (41)$$

$$\mathbf{C}_{nk}^a \equiv -(1/b_{M,X}^{(n,P)}) \int_{I_{\min}=0}^{I_{\max}(T)} (\partial f^P / \partial a_n^P) (\partial f^{\text{EA}} / \partial X_k^{\text{EA}}) dI, \quad n = 1, 2; k = 1, \dots, 6 \quad (42)$$

$$\mathbf{D}_n^a \equiv -(1/b_{M,X}^{(n,P)}) \int_{I_{\min}=0}^{I_{\max}(T)} (\partial f^P / \partial a_n^P) (f_{\text{DH}}^P - f_{\text{DH}}^{\text{EA}}) dI, \quad n = 1, 2 \quad (43)$$

The integrations required to evaluate the exponential coefficient matrices \mathbf{A}_{nj}^a and \mathbf{C}_{nk}^a can be performed analytically, and the results are given in Appendix A. As before, the associated Debye-Hückel vector \mathbf{D}_n^a vanishes because the Debye-Hückel limiting-law slope A_ϕ and b were assumed to be the same for the standard Pitzer and extended Archer models. The factor of $b_{M,X}^{(n,P)}$ that is common to all terms of equation (39) has been eliminated from the definitions given by equations (41)–(43).

Upon examining equation (39) for the unknown exponents $\{a_1^P, a_2^P\}$ and the previously obtained equation (31) for the parameters $\{b_{M,X}^{(0,P)}, b_{M,X}^{(1,P)}, b_{M,X}^{(2,P)}, \text{ and } C_{M,X}^{(f,P)}\}$ of the standard Pitzer model, we see that coefficient matrices of these two equations are themselves functions of the unknown exponential coefficients, yielding a system of matrix equations that is non-linear with respect to a_1^P and a_2^P . This non-linear system of six simultaneous equations can be solved by non-linear iterative matrix solution methods

such as the Newton-Raphson iterative technique, but this is usually much more difficult than solving the system of linear simultaneous equations, given by equation (31), for the parameter sub-set $\{b_{M,X}^{(0,P)}, b_{M,X}^{(1,P)}, b_{M,X}^{(2,P)}, \text{ and } C_{M,X}^{(f,P)}\}$ for given values of a_1^P and a_2^P .

4. Methods of Analysis: Alternative approach for conversion of the model parameters for model equations with only one non-linear exponent coefficient

In the previous section, a general non-linear procedure for determining all parameters of the standard Pitzer model, including the exponential coefficients, was presented. There is, however, a more direct alternative approach that is more convenient when there is only one exponential coefficient with respect to which the problem is non-linear. For $\text{Ca}(\text{NO}_3)_2(\text{aq})$ and $\text{NaNO}_3(\text{aq})$ the terms involving $b_{MX}^{(2,EA)}$ and a_2^{EA} , and thus $b_{M,X}^{(2,P)}$ and a_2^P , are absent, so that there is only one non-linear unknown a_1^P . Therefore, instead of simultaneously solving the full non-linear set of equations (31) and (39) for the optimal values of all five unknowns, it is more convenient to only solve the linear matrix equation (31) for the four unknowns, $(b_{M,X}^{(0,P)}, b_{M,X}^{(1,P)}, b_{M,X}^{(2,P)}, \text{ and } C_{M,X}^{(f,P)})$ while keeping the value of a_1^P fixed, and then to numerically evaluate the mean square difference function E_I^2 given by equation (15) at each temperature T for a series of assumed values of a_1^P . The optimum value of a_1^P that minimizes E_I^2 may then be determined at a particular temperature by examining the tabulated values of E_I^2 . This procedure yields a different value of a_1^P that is optimum at each different temperature. Thus, in effect, we have replaced the non-linear least-squares parameter evaluation with a series of linear least-squares parameter evaluations.

The determination of an “average” optimal value of a_1^P that is constant for all ionic strength and temperature ranges is also of great interest because it can be used directly in the standard Pitzer model, which has traditionally employed a temperature independent value of a_1^P . For determining this temperature-average optimum value of a_1^P , we define the temperature averaged mean square error $E_{I,T}^2$ resulting from converting the extended Archer model to the standard Pitzer model by

$$E_{I,T}^2 \equiv \left\{ \int_{T_{\min}}^{T_{\max}} \int_{I_{\min}=0}^{I_{\max}(T)} (\bar{f}^P - \bar{f}^{EA})^2 dI dT \right\} / \left\{ \int_{T_{\min}}^{T_{\max}} \int_{I_{\min}=0}^{I_{\max}(T)} dI dT \right\} \quad (46a)$$

$$= \left[\int_{T_{\min}}^{T_{\max}} I_{\max}(T) \cdot \{E_I(T)\}^2 dT \right] / \left[\int_{T_{\min}}^{T_{\max}} I_{\max}(T) dT \right] \quad (46b)$$

The optimal average value of a_1^P over the entire ionic strength range $\{I_{\min}, I_{\max}(T)\}$ and temperature range (T_{\min}, T_{\max}) is determined by examining calculated values of the root mean square error (RMSE) measure $E_{I,T}$ for a series of fixed (temperature-independent) values of a_1^P , and then selecting the value of a_1^P for which $E_{I,T}$ is a minimum.

Rard et al. [17] found that optimizing the Archer model parameters for $\text{Mg}(\text{NO}_3)_2(\text{aq})$, by a least-squares fitting method applied to experimentally determined values of \bar{f} , resulted in three minima (two local, one absolute) in the RMSE $E_{I,T}$ evaluated as a function of a_1 and w_1 . Similarly, Albright et al. [28] found three minima (two local, one absolute) in the RMSE for an extended Archer model for $\text{ZnSO}_4(\text{aq})$. It is possible that even more local minima may be encountered if we attempted to simultaneously optimize the values of $\{b_{M,X}^{(0,P)}, b_{M,X}^{(1,P)}, b_{M,X}^{(2,P)}, C_{M,X}^{(f,P)}, a_1^P, \text{ and } a_2^P\}$.

Our parameter conversion procedure is based on minimizing the difference (or “error”) between the osmotic coefficients predicted by the two models. This choice was

motivated by the simpler form of the difference function for the osmotic coefficient compared to those of the activity coefficients or the excess Gibbs free energies, and because all of the input activity data for the $\text{Ca}(\text{NO}_3)_2(\text{aq})$ source model [13] are osmotic coefficients. There are other electrolyte systems where the majority of the thermodynamic data are values of mean activity coefficients from e.m.f. measurements using reversible electrochemical cells. For these systems the use of conversion equations based on minimizing the difference between activity coefficients calculated from the different models may be more appropriate.

The values of the RMSE measure E_I over the ionic strength range $\{I_{\min}, I_{\max}(T)\}$, and the overall RMSE measure $E_{I,T}$ over the combined ionic strength and temperature range $\{I_{\min} \text{ to } I_{\max}(T) \text{ and } T_{\min} \text{ to } T_{\max}\}$ are necessary both for determining the optimum exponential coefficients by inspection and for subsequent evaluation of the accuracy of the optimized results. The values of the Pitzer parameters $X_i^P(T)$ were computed at regularly spaced temperature values from equations (31) and (39) for iteratively determined values of the exponential coefficients. In the case of one exponential term, the value of a_1^P that minimizes the error $E_{I,T}$ was determined by inspection of the results from these fits as described previously. The integrals over ionic strength of the osmotic coefficient in the definitions of the square error measure $E_I^2(T)$, given by equation (15), was numerically evaluated by dividing the ionic-strength range of integration at each temperature into equal intervals and approximating the integrals using the trapezoidal

integration rule [i.e., $\int_{x_1}^{x_2} y(x) dx \approx (1/2)\{y(x_1) + y(x_2)\}(x_2 - x_1)$] within each ionic-

strength interval. The RMSE measure $E_{I,T}$ was next computed in a similar manner from

equation (46b) by using these values of $E_i^2(T)$ and the trapezoidal integration rule within each temperature interval.

5. Methods of Analysis: Fitting of temperature functions to the standard Pitzer model parameters $b_{M,X}^{(0,P)}$, $b_{M,X}^{(1,P)}$, $b_{M,X}^{(2,P)}$, $C_{M,X}^{(f,P)}$, a_1^P , and a_2^P obtained by converting the parameters of the extended ion-interaction model

The method of determining the parameters $X_i^P(T) = \{b_{M,X}^{(0,P)}(T), b_{M,X}^{(1,P)}(T), b_{M,X}^{(2,P)}(T), C_{M,X}^{(f,P)}(T), a_1^P(T), \text{ and } a_2^P(T)\}$ of the standard Pitzer model at a given value of the temperature T , and of determining optimal constant average values for a_1^P and a_2^P over the entire temperature range, was described previously in Sections 3 and 4. In this section we present the method that we used to fit standard temperature functions to the values of these parameters computed over the desired range of temperatures, so that they can be described over this temperature range with a small number of constant temperature coefficients. To this end, we represent each Pitzer parameter $X_i^P(T)$ by the linear sum of a finite series of terms of the form

$$X_i^P(T) = \sum_{j=1}^8 a_{ij} \cdot g_j(T), \quad i = 1, \dots, 4; j = 1, \dots, 8 \quad (47)$$

where the $g_j(T)$ ($j = 1, \dots, 8$) are a standard set of pre-defined temperature basis functions, and the a_{ij} are the constant temperature coefficients corresponding to each Pitzer parameter $X_i^P(T)$ and temperature basis function $g_j(T)$.

We selected the temperature basis functions to represent all integer powers T^n of the absolute temperature T , where n ranged from -3 to $+3$. The natural logarithm $\ln(T)$ was also included as a term in this series because it is intermediate in power law behavior

between T and T^{-1} . This choice of basis functions allows the temperature dependencies typical of thermodynamic properties of electrolytes to be accommodated. Thus, we adopted the set of temperature basis functions given by

$$g_1(T) = 1 \quad (48)$$

$$g_2(T) = T - T_{\text{ref}} \quad (49)$$

$$g_3(T) = T^2 - T_{\text{ref}}^2 \quad (50)$$

$$g_4(T) = T^{-1} - T_{\text{ref}}^{-1} \quad (51)$$

$$g_5(T) = \ln(T/T_{\text{ref}}) \quad (52)$$

$$g_6(T) = T^3 - T_{\text{ref}}^3 \quad (53)$$

$$g_7(T) = T^{-2} - T_{\text{ref}}^{-2} \quad (54)$$

$$g_8(T) = T^{-3} - T_{\text{ref}}^{-3} \quad (55)$$

where each basis function $g_{j \neq 1}(T_{\text{ref}}) = 0$ to yield $a_{i1} = X_i^{\text{P}}(T_{\text{ref}})$. Therefore, the first temperature coefficient a_{i1} is equal to the value of the Pitzer parameter at the reference temperature T_{ref} , which we fix at $T_{\text{ref}} = 298.15$ K.

The temperature coefficients a_{ij} of each Pitzer parameter $X_i^{\text{P}}(T)$ are determined by minimizing the mean square error between the values of $X_i^{\text{P}}(T)$ determined from the model conversion step described in Sections 3 and 4, and its value calculated using equation (47). That is, we minimize the mean square error

$$E_T^2 \equiv \left[\int_{T_{\text{min}}}^{T_{\text{max}}} \{ X_i^{\text{P}}(T) - \sum_{j=1}^8 a_{ij} \cdot g_j(T) \}^2 dT \right] / \left[\int_{T_{\text{min}}}^{T_{\text{max}}} dT \right], \quad (56a)$$

$$= [1/(T_{\text{max}} - T_{\text{min}})] \left[\int_{T_{\text{min}}}^{T_{\text{max}}} \{ X_i^{\text{P}}(T) - \sum_{j=1}^8 a_{ij} \cdot g_j(T) \}^2 dT \right], \quad (56b)$$

over the temperature range of interest (T_{min} , T_{max}) by setting its derivatives with respect to the unknown temperature coefficients a_{ij} equal to zero. Thus, we have

$$\partial E_T^2 / \partial a_{ij} = [2 / (T_{\max} - T_{\min})] \left[\int_{T_{\min}=0}^{T_{\max}(T)} \{ X_i^P(T) - \sum_{k=1}^8 a_{ik} \cdot g_k(T) \} g_j(T) dT \right] = 0, \quad (57)$$

Rearranging equation (57) and defining new matrix arrays, we obtain the matrix equation

$$\sum_{k=1}^8 A_{jk}^{\dagger} \cdot a_{ik} = B_{ij}^{\dagger} \quad i = 1, \dots, 4; j = 1, \dots, 8 \quad (58)$$

where

$$A_{jk}^{\dagger} \equiv \int_{T_{\min}=0}^{T_{\max}(T)} g_j(T) \cdot g_k(T) dT \quad j, k = 1, \dots, 8 \quad (59)$$

$$B_{ij}^{\dagger} \equiv \int_{T_{\min}=0}^{T_{\max}(T)} X_i^P(T) \cdot g_j(T) dT \quad i = 1, \dots, 4; j = 1, \dots, 8 \quad (60)$$

Note that the index i of the generic Pitzer parameters $X_i^P(T)$, of the temperature coefficients a_{ij} , and of the vector B_{ij}^{\dagger} is effectively a dummy index that can be ignored when solving the linear matrix equation (58) for the temperature coefficient vector, because each Pitzer parameter is fitted to the temperature functions independently of the other Pitzer parameters.

The values of the Pitzer parameters $X_i^P(T)$ were obtained from the model conversion step in Section 3 at regularly spaced temperature values. Therefore, the integrals in the definitions (59) and (60) of the matrix coefficients A_{jk}^{\dagger} and the right-hand side vector B_{ij}^{\dagger} were numerically evaluated by dividing the range of integration into equal intervals and approximating the integral within each temperature interval using the trapezoidal integration rule for a linear variation of the integrand within that interval. The linear matrix equation (58) is then solved for the temperature coefficients a_{ik} by Gaussian elimination.

The impact of the overall error incurred, including both the error due model conversion and the error due to fitting the temperature functions, is evaluated through the difference between the osmotic coefficients calculated using the fitted temperature coefficients for the standard Pitzer model and the osmotic coefficient calculated using the input temperature dependent parameters of the extended Archer model. This is compared against the error in the osmotic coefficient due to model conversion only through the difference between the osmotic coefficient from the standard Pitzer model computed using the parameters calculated from the model conversion step only, and the osmotic coefficient calculated using the input temperature dependent parameters of the extended Archer model.

Temperature function representations

In this paper we present the results for two different choices of the temperature basis functions for representing the temperature dependence of the standard Pitzer model.

Four-term temperature function representation: This 4-term choice of temperature basis functions was selected by evaluating the accuracy of test calculations made using several different thermodynamic properties. The set consists of constant, linear, inverse temperature and logarithmic basis functions {i.e., $1, T, T^{-1}, \ln(T)$ }. Thus, the standard Pitzer model parameters $X_i^P (i = 1, \dots, 4) = \{b_{M,X}^{(0,P)}, b_{M,X}^{(1,P)}, b_{M,X}^{(2,P)}, \text{ and } C_{M,X}^{(f,P)}\}$ are represented by 4-term temperature functions of the form

$$X_i(T) = a_{i1} + a_{i2}(T - T_{\text{ref}}) + a_{i4}(T^{-1} - T_{\text{ref}}^{-1}) + a_{i5} \ln(T/T_{\text{ref}}) \quad (61a)$$

$$= a_{i1} + a_{i2} \cdot g_2(T) + a_{i4} \cdot g_4(T) + a_{i5} \cdot g_5(T) \quad (61b)$$

Seven-term temperature function representation: This set of temperature basis functions supplements the basis functions of the 4-term set with four more basis functions to overcome observed deficiencies in the performance of the 4-term basis function set. This selection was made on the basis of exploratory evaluations of the temperature function fitting error in the osmotic coefficient for $\text{Ca}(\text{NO}_3)_2(\text{aq})$ with solubility constrained maximum ionic strength, and represents an optimal choice for this electrolyte under these conditions. It consists of the basis functions given by equations (48)–(54), excluding the $g_8(T)$ term that was not required. Thus, the standard Pitzer parameters $X_i^p (i = 1, \dots, 4) = \{b_{M,X}^{(0,P)}(T), b_{M,X}^{(1,P)}(T), b_{M,X}^{(2,P)}(T), \text{ and } C_{M,X}^{(f,P)}(T)\}$ are represented by 7-term temperature functions of the form,

$$X_i^p(T) = a_{i1} + a_{i2}(T - T_{\text{ref}}) + a_{i3}(T^2 - T_{\text{ref}}^2) + a_{i4}(T^{-1} - T_{\text{ref}}^{-1}) + a_{i5} \ln(T/T_{\text{ref}}) + a_{i6}(T^3 - T_{\text{ref}}^3) + a_{i7}(T^{-2} - T_{\text{ref}}^{-2}) \quad (62a)$$

$$= a_{i1} + a_{i2} \cdot g_2(T) + a_{i3} \cdot g_3(T) + a_{i4} \cdot g_4(T) + a_{i5} \cdot g_5(T) + a_{i6} \cdot g_6(T) + a_{i7} \cdot g_7(T) \quad (62b)$$

6. Activity of water and solubility product

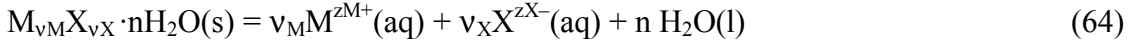
The activity of water in aqueous electrolyte solutions and the solubility products for solid phases in equilibrium with the saturated solutions are often needed to calculate the saturated solution molalities. The activity of water a_w may be computed from the osmotic coefficient f using the equation

$$a_w \equiv \exp(-n \cdot M_w \cdot m \cdot f)$$

(63)

where M_w is the molar mass of water ($0.0180153 \text{ kg}\cdot\text{mol}^{-1}$).

The dissolution reaction describing the equilibrium between a solid phase $M_{v_M}X_{v_X}\cdot n\text{H}_2\text{O}(\text{s})$ that has n waters of hydration and its saturated solution is



Therefore, the standard (thermodynamic) solubility product K_{sp} can be computed from the activity of water a_w and the mean activity coefficient g_{\pm} of the saturated solution using the equation

$$K_{\text{sp}} \equiv \{m(M^{z_{M^+}}, \text{sat})^{v_M} \cdot m(X^{z_{X^-}}, \text{sat})^{v_X} / (m^\circ)^v\} \cdot g(M^{z_{M^+}}, \text{sat})^{v_M} \cdot g(X^{z_{X^-}}, \text{sat})^{v_X} \cdot a_w(\text{sat})^n \quad (65a)$$

$$= v_M^{v_M} \cdot v_X^{v_X} \cdot \{m(\text{sat})/m^\circ\}^v \cdot g_{\pm}(\text{sat})^v \cdot a_w(\text{sat})^n \quad (65b)$$

where the stoichiometric coefficients v_M , v_X , and v have been introduced previously, and $m^\circ = 1 \text{ mol}\cdot\text{kg}^{-1}$. The molality $m(\text{sat})$ and the corresponding ionic strength I_{sat} used in computing the solubility product from equation (65) correspond to those of the saturated solution.

7. Computer code for model conversion and fitting temperature functions

A Microsoft ExcelTM spreadsheet was programmed, using both cell formulae and macros written in the Visual Basic language, to compute the parameter conversion and

exponential coefficient optimization procedures described in Sections 3 and 4, the temperature function fitting procedure described in Section 5, and the water activity, mean activity coefficient, and solubility product calculations described in Section 6.

The parameter conversion part of the program was developed to permit different combinations of unknown model parameters to be activated and determined by deleting the unneeded equations from the full set of matrix equations and function evaluations, and renumbering the remaining equations and variables. For example, the $b_{M,X}^{(2,P)}$, a_2^P , $b_{MX}^{(2,EA)}$, and a_2^{EA} parameters are not used in the standard Pitzer and extended Archer models of the aqueous $\text{Ca}(\text{NO}_3)_2(\text{aq})$ and $\text{NaNO}_3(\text{aq})$ electrolyte systems presented in this paper, and removing these terms reduces the number of equations in matrix equation (31) from 4 to 3, and in the exponential matrix equation (39) from 2 to 1.

Similarly, the temperature function fitting part of the program was developed to permit any sub-set of the full suite of temperature basis functions to be activated, and the temperature coefficients for only that particular sub-set to be calculated from equation (58). As a result, it was possible to easily examine the impact of different choices of the temperature basis functions on the accuracy of evaluation of any thermodynamic property (e.g, osmotic coefficient, activity coefficients, water activity, or solubility product) based on the standard Pitzer model.

8. Results: Pitzer parameters for the standard Pitzer model for $\text{Ca}(\text{NO}_3)_2(\text{aq})$ and $\text{NaNO}_3(\text{aq})$

In this section we present values of the $b_{M,X}^{(0,P)}$, $b_{M,X}^{(1,P)}$, and $C_{M,X}^{(f,P)}$ parameters of the standard Pitzer model derived from the extended Archer-type model parameters given by Oakes et al. [13] for $\text{Ca}(\text{NO}_3)_2(\text{aq})$ and by Archer [29] for $\text{NaNO}_3(\text{aq})$, and examine the impact of

optimizing the selection of the exponential coefficient a_1^P on the accuracy of the derived standard Pitzer model.

Ca(NO₃)₂(aq) Pitzer parameters

Oakes et al. [13] have critically evaluated the thermodynamic properties of the Ca(NO₃)₂ + H₂O system and provide evaluated parameters of a 5-parameter model $\{b_{MX}^{(0,EA)}$, $b_{MX}^{(1,EA)}$, $C_{M,X}^{(0,EA)}$, $C_{M,X}^{(1,EA)}$, and $C_{M,X}^{(2,EA)}\}$ valid for $T = (298 \text{ to } 373) \text{ K}$. The molalities of saturated Ca(NO₃)₂(aq) solutions [22] are very high, e.g., $I_{\text{sat}} = 3 \cdot m \approx 18.7 \text{ mol} \cdot \text{kg}^{-1}$ at $T = 273.15 \text{ K}$; $I_{\text{sat}} \approx 51.5 \text{ mol} \cdot \text{kg}^{-1}$ at $T = 323.15 \text{ K}$; $I_{\text{sat}} \approx 66.5 \text{ mol} \cdot \text{kg}^{-1}$ at $T = 373.15 \text{ K}$; and $I_{\text{sat}} \approx 68.5 \text{ mol} \cdot \text{kg}^{-1}$ at $T = 423.15 \text{ K}$. Oakes et al. [13] included some thermodynamic measurements for supersaturated solutions when evaluating the values of their model parameters.

The variation of the average root mean square error (RMSE) $E_{I,T}$ with the a_1^P parameter for the solubility limited maximum ionic strength, $I_{\text{max}} = I_{\text{sat}}(T)$, and a constant maximum ionic strength, $I_{\text{max}} = 68.5 \text{ mol} \cdot \text{kg}^{-1}$, are given in figures 1 and 2, respectively. The plot in figure 1 for the solubility limited maximum ionic strength case shows a minimum RMSE of $6.0964 \cdot 10^{-3}$ at $a_1^P = 0.87 \text{ kg}^{1/2} \cdot \text{mol}^{-1/2}$ with the RMSE increasing to $7.2456 \cdot 10^{-2}$ at $a_1^P = 2.0 \text{ kg}^{1/2} \cdot \text{mol}^{-1/2}$. Using the optimal value of $a_1^P = 0.87 \text{ kg}^{1/2} \cdot \text{mol}^{-1/2}$ yields a factor of 11.9 improvement in the accuracy of the osmotic coefficient calculated by the standard Pitzer model, over that obtained when using the standard value of $a_1^P = 2.0 \text{ kg}^{1/2} \cdot \text{mol}^{-1/2}$. The optimal value of a_1^P for the evaluation with constant $I_{\text{max}} = 68.5 \text{ mol} \cdot \text{kg}^{-1}$ is also $a_1^P = 0.87 \text{ kg}^{1/2} \cdot \text{mol}^{-1/2}$ and this model yields a factor of 11.5 improvement in accuracy over that obtained for $a_1^P = 2.0 \text{ kg}^{1/2} \cdot \text{mol}^{-1/2}$.

Tables 1 and 2 list the values of $b_{M,X}^{(0,P)}$, $b_{M,X}^{(1,P)}$, and $C_{M,X}^{(f,P)}$ for $\text{Ca}(\text{NO}_3)_2(\text{aq})$ that were obtained from the extended Archer model parameters by minimizing E_1^2 . Two sets of Pitzer parameter values, corresponding to the constant optimized value of $a_1^P = 0.87 \text{ kg}^{1/2}\cdot\text{mol}^{-1/2}$ and the standard value of $a_1^P = 2.0 \text{ kg}^{1/2}\cdot\text{mol}^{-1/2}$, are presented in these tables. The maximum ionic strengths I_{max} used for these parameter evaluations in table 1 were those of the saturated solutions, whereas a constant value of $I_{\text{max}} = 68.5 \text{ mol}\cdot\text{kg}^{-1}$ was used for table 2. It was possible to evaluate these Pitzer model parameters for both constraints on I_{max} , because data for supersaturated solutions were included in the Oakes et al. model [13].

The quality of the osmotic coefficient predicted by the standard Pitzer model using the above parameter sets can be assessed from the plots of the osmotic coefficient as a function of ionic strength and temperature given in figures 3 to 5 for the solubility limited maximum ionic strength, and in figures 6 to 8 for constant maximum ionic strength, at values of $a_1^P = (0.20, 0.87, \text{ and } 2.0) \text{ kg}^{1/2}\cdot\text{mol}^{-1/2}$, respectively. It can be seen from these figures that the use of the optimal value $a_1^P = 0.87 \text{ kg}^{1/2}\cdot\text{mol}^{-1/2}$ gives a nearly perfect agreement between the standard and extended Pitzer models over most of the ionic strength range, whereas the standard value $a_1^P = 2.0 \text{ kg}^{1/2}\cdot\text{mol}^{-1/2}$ yields significantly poorer agreement, particularly at low ionic strengths and high temperatures. Comparing the plots of figures 3 to 5 with those of figures 6 to 8 we see that there are no significant differences in accuracy between the results for solubility limited maximum ionic strength and those for constant maximum ionic strength. The Pitzer model fits with $a_1^P = 2.0 \text{ kg}^{1/2}\cdot\text{mol}^{-1/2}$ have deviations from the extended Archer model [13] of ca. 10 per cent at certain ionic strengths and temperatures (see figure 9 of Rard and Wijesinghe [14]),

whereas those obtained with the optimized value $a_1^P = 0.87 \text{ kg}^{1/2} \cdot \text{mol}^{-1/2}$ have maximum deviations of ca. 1 per cent.

NaNO₃(aq) Pitzer parameters

Archer [29] has critically evaluated the thermodynamic properties of the NaNO₃ + H₂O system and provided evaluated parameters of a 4-parameter model $\{b_{MX}^{(0,EA)}, b_{MX}^{(1,EA)}, C_{M,X}^{(0,EA)}, \text{ and } C_{M,X}^{(1,EA)}\}$ valid for temperatures from $T = (273 \text{ to } 373) \text{ K}$. The molalities of saturated NaNO₃(aq) solutions [22] are high, e.g., $I_{\text{sat}} = m \approx 8.59 \text{ mol} \cdot \text{kg}^{-1}$ at $T = 273.15 \text{ K}$; $I_{\text{sat}} \approx 13.16 \text{ mol} \cdot \text{kg}^{-1}$ at $T = 323.15 \text{ K}$; $I_{\text{sat}} \approx 21.19 \text{ mol} \cdot \text{kg}^{-1}$ at $T = 373.15 \text{ K}$; and $I_{\text{sat}} \approx 33.07 \text{ mol} \cdot \text{kg}^{-1}$ at $T = 423.15 \text{ K}$, but are not as high on an ionic strength basis as in the case of Ca(NO₃)₂(aq).

The variation of the average root mean square error (RMSE) $E_{I,T}$ with the a_1^P parameter for the solubility limited maximum ionic strength $\{\text{i.e., } I_{\text{max}} = I_{\text{sat}}(T)\}$ is given in figure 9. This plot shows a minimum RMSE of $2.0340 \cdot 10^{-3}$ at $a_1^P = 1.43 \text{ kg}^{1/2} \cdot \text{mol}^{-1/2}$ with the RMSE increasing to $7.9871 \cdot 10^{-3}$ at $a_1^P = 2.0 \text{ kg}^{1/2} \cdot \text{mol}^{-1/2}$. Therefore, using the optimal value of $a_1^P = 1.43 \text{ kg}^{1/2} \cdot \text{mol}^{-1/2}$ yields a factor of 3.93 increase in the accuracy of the osmotic coefficient calculated by the standard Pitzer model, over that obtained when using the standard value of $a_1^P = 2.0 \text{ kg}^{1/2} \cdot \text{mol}^{-1/2}$.

Table 3 lists the values of $b_{M,X}^{(0,P)}$, $b_{M,X}^{(1,P)}$, and $C_{M,X}^{(f,P)}$ for NaNO₃(aq) that were obtained from the Archer model parameters by minimizing E_I^2 . Two sets of parameter values, corresponding to the constant optimized value of $a_1^P = 1.43 \text{ kg}^{1/2} \cdot \text{mol}^{-1/2}$ and the standard value of $a_1^P = 2.0 \text{ kg}^{1/2} \cdot \text{mol}^{-1/2}$ are presented in this table at various temperatures. The

maximum ionic strength I_{\max} used for these parameter evaluations in table 3 were those of the saturated solutions.

The quality of the osmotic coefficient predicted by the standard Pitzer model using the above parameter set can be assessed from the plots of the osmotic coefficient as a function of ionic strength and temperature given in figures 10–12, for values of $a_1^P = (0.20, 1.43, \text{ and } 2.0) \text{ kg}^{1/2} \cdot \text{mol}^{-1/2}$, respectively. It can be seen from these figures that the use of the optimal value of a_1^P gives excellent agreement, whereas the standard value of $a_1^P = 2.0 \text{ kg}^{1/2} \cdot \text{mol}^{-1/2}$ yields significantly poorer agreement, particularly at low ionic strengths and high temperatures.

Pitzer parameters when $a_1^P(T)$ is optimized separately at each temperature

Tables 4 and 5 give the corresponding values of $b_{M,X}^{(0,P)}$, $b_{M,X}^{(1,P)}$, and $C_{M,X}^{(f,P)}$ for $\text{Ca}(\text{NO}_3)_2(\text{aq})$ and $\text{NaNO}_3(\text{aq})$, respectively, using values of $a_1^P(T)$ that have been optimized at each reported temperature. It can be seen that the values of $a_1^P(T)$ for $\text{Ca}(\text{NO}_3)_2(\text{aq})$ are nearly constant at $T \geq 353.15 \text{ K}$ as are those for $\text{NaNO}_3(\text{aq})$ at $T \geq 333.15 \text{ K}$.

9. Results: temperature functions for parameters of the standard Pitzer model for $\text{Ca}(\text{NO}_3)_2(\text{aq})$ and $\text{NaNO}_3(\text{aq})$

$\text{Ca}(\text{NO}_3)_2(\text{aq})$ temperature functions

The coefficients of the temperature functions were fitted to the standard Pitzer model parameters presented for $\text{Ca}(\text{NO}_3)_2(\text{aq})$ in tables 1 and 2 as described in Section 5. The accuracy of the 4-term temperature functions given by equation (61) and the extended 7-term temperature functions given by equation (62) were evaluated. The average RMSE

between the osmotic coefficients calculated using the temperature functions for the temperature dependent Pitzer parameters and the input osmotic coefficients calculated from the extended Archer model of Oakes et al. [13] for the solubility limited maximum ionic strength and constant maximum ionic strength cases are given in figures 1 and 2, respectively. From figure 1, for the solubility limited maximum ionic strength case, it can be seen that the choice of the temperature functions fitted to the standard Pitzer model parameters has a very significant impact on the accuracy of the calculated osmotic coefficients. The accuracy of the fit is seen to be unacceptable in the case of the 4-term temperature functions, whereas the 7-term temperature functions yields accurate values of the osmotic coefficient, for $a_1^p \geq 0.75 \text{ kg}^{1/2} \cdot \text{mol}^{-1/2}$.

From the corresponding results in figure 2 for the constant maximum ionic strength case, it can be seen that the choice between the 4- and 7-term temperature functions for the standard Pitzer model parameters has a much smaller impact on the accuracy of the calculated osmotic coefficients compared to the case of solubility limited maximum ionic strength. In this case, while the 7-term temperature functions give a nearly perfect representation for all values of a_1^p , the 4-term temperature functions gives acceptable results for most values of a_1^p with the least accuracy occurring around the optimal value of $a_1^p = 0.87 \text{ kg}^{1/2} \cdot \text{mol}^{-1/2}$, where the 7-term functions perform much better. Clearly, the solubility limited maximum ionic strength fit requires more temperature functions to achieve acceptable accuracy, particularly if the solubility behavior is complicated by the many different solid phases that are formed in the case of $\text{Ca}(\text{NO}_3)_2(\text{aq})$. In both of these cases, the 7-term temperature functions yielded accurate values of the Pitzer parameters as a function of temperature for the optimal values of a_1^p .

The quality of the temperature function fits to the standard Pitzer model parameters $b_{M,X}^{(0,P)}$, $b_{M,X}^{(1,P)}$, and $C_{M,X}^{(f,P)}$ for $\text{Ca}(\text{NO}_3)_2(\text{aq})$ can be assessed from the plots of these parameters against temperature given in figures 13–15 for the case of solubility limited maximum ionic strength. It can be seen from these figures that while both 4-term and 7-term temperature functions represent $b_{M,X}^{(1,P)}$ adequately, the 4-term functions have difficulty in representing both $b_{M,X}^{(0,P)}$ and $C_{M,X}^{(f,P)}$ with sufficient accuracy. The temperature coefficients calculated for the 7-term temperature functions for the optimal and standard values of the exponential coefficient a_1^P are given for $\text{Ca}(\text{NO}_3)_2(\text{aq})$ in tables 6 and 7 for the cases of solubility limited maximum ionic strength and constant $I_{\max} = 68.5 \text{ mol}\cdot\text{kg}^{-1}$, respectively.

The $b_{M,X}^{(0,P)}$ and $C_{M,X}^{(f,P)}$ parameters for $\text{Ca}(\text{NO}_3)_2(\text{aq})$ are more difficult to represent as functions of temperature for the solubility limited maximum ionic strength model as a result of abrupt changes in slope around 327 K, and shown in figures 13 and 15. The thermodynamically stable solid phase is $\text{Ca}(\text{NO}_3)_2\cdot 4\text{H}_2\text{O}(\text{s})$ from about 244 K to 321 K where it melts congruently to form a solution of the same composition, with $\text{Ca}(\text{NO}_3)_2\cdot 3\text{H}_2\text{O}(\text{s})$ and $\text{Ca}(\text{NO}_3)_2\cdot 2\text{H}_2\text{O}(\text{s})$ occurring up to $\approx 324 \text{ K}$ [22]. The slope changes observed in figures 13 and 15 directly reflect slope changes in I_{sat} as a function of temperature as the stable hydrate changes.

$\text{NaNO}_3(\text{aq})$ temperature functions

Temperature functions were fitted to the standard Pitzer model parameters for $\text{NaNO}_3(\text{aq})$ presented in table 3, and the accuracy of the 4-term temperature functions given by equation (61) and the 7-term temperature functions given by equation (62) were evaluated for $\text{NaNO}_3(\text{aq})$ as in the case of $\text{Ca}(\text{NO}_3)_2(\text{aq})$. The average RMSE between the

osmotic coefficient calculated using the temperature functions for the standard Pitzer model parameters and the input osmotic coefficient values calculated from the extended model of Archer [29] for the solubility limited maximum ionic strength case are given for $\text{NaNO}_3(\text{aq})$ in figure 9. It can be seen from this figure that the choice of the temperature functions fitted to the standard Pitzer parameters has a very significant impact on the accuracy of the calculated osmotic coefficient. In the case of the 4-term temperature functions, the accuracy of the fit is seen to be acceptable only over a limited range of $a_1^P = (0.8 \text{ to } 1.2) \text{ kg}^{1/2} \cdot \text{mol}^{-1/2}$, whereas the 7-term temperature functions yield accurate values of the osmotic coefficient for all values of a_1^P , including its optimal value of $a_1^P = 1.43 \text{ kg}^{1/2} \cdot \text{mol}^{-1/2}$.

Figure 9 clearly indicates that the 4-term temperature functions perform better in the case of $\text{NaNO}_3(\text{aq})$ that has lower solubility and only one stable solid phase, compared to $\text{Ca}(\text{NO}_3)_2(\text{aq})$ which is much more soluble and has a complex solubility behavior.

The quality of the temperature function fits to the standard Pitzer model parameters $b_{M,X}^{(0,P)}$, $b_{M,X}^{(1,P)}$, and $C_{M,X}^{(f,P)}$ for $\text{NaNO}_3(\text{aq})$ can be assessed from the plots of these parameters against temperature given in figures 16–18 for the case of solubility limited maximum ionic strength. It can be seen from these figures that while both 4-term and 7-term temperature functions represent all three parameters adequately, the 7-term function fit is more accurate at all temperatures. The temperature coefficients calculated for the 7-term temperature functions for the constant optimal and standard values of the exponential coefficient a_1^P for $\text{NaNO}_3(\text{aq})$ are given in table 8 for calculations with the solubility limited maximum ionic strengths.

10. Results: temperature dependent optimal a_1^P for the standard Pitzer model for $\text{Ca}(\text{NO}_3)_2(\text{aq})$ and $\text{NaNO}_3(\text{aq})$

In this study, we also investigated the potential benefit of using a temperature dependent a_1^P that is optimal at each temperature, compared to the use of a temperature independent constant optimal value in minimizing the error in the osmotic coefficient calculated by the standard Pitzer model. To determine this value of $a_1^P(T)$, we computed the RMSE E_I in the osmotic coefficient over the ionic strength range as defined by equation (15b), for a range of assumed values of a_1^P , and determined the optimal value of a_1^P that minimized E_I . The temperature dependent values of a_1^P , and the corresponding minimum value of E_I computed in this way, are listed in table 9 for each temperature T . It can be seen from table 9 that the optimal values of $a_1^P(T)$ for both $\text{Ca}(\text{NO}_3)_2(\text{aq})$ and $\text{NaNO}_3(\text{aq})$ are quite close to the corresponding temperature-independent optimal values of $a_1^P = (0.87 \text{ and } 1.43) \text{ kg}^{1/2}\cdot\text{mol}^{-1/2}$, respectively, when $T > \approx 340 \text{ K}$. For comparison, the corresponding values of a_1^P and the RMSE are also given for $\text{Mg}(\text{NO}_3)_2(\text{aq})$ at $T = 298.15 \text{ K}$ [17].

The accuracy of the osmotic coefficient computed using these values of $a_1^P(T)$ from the standard Pitzer model are compared against the input osmotic coefficients calculated from the extended Archer model of Oakes et al. [13] for $\text{Ca}(\text{NO}_3)_2(\text{aq})$ in figure 19 and for $\text{NaNO}_3(\text{aq})$ in figure 20. It can be seen from these figures that the accuracy of this approach is comparable to that achieved previously for $\text{Ca}(\text{NO}_3)_2(\text{aq})$ in figure 4 using the constant optimal value of $a_1^P = 0.87 \text{ kg}^{1/2}\cdot\text{mol}^{-1/2}$, and for $\text{NaNO}_3(\text{aq})$ in figure 11 using the constant optimal value of $a_1^P = 1.43 \text{ kg}^{1/2}\cdot\text{mol}^{-1/2}$. Therefore, we recommend the use of the constant optimal values of this exponential coefficient instead of more

complicated temperature dependent values, which would also require re-derivation of the expressions for the temperature derivatives of the excess Gibbs energy such as the relative enthalpy and heat capacity.

11. Results: Thermodynamic properties of saturated solutions of $\text{Ca}(\text{NO}_3)_2(\text{aq})$ and $\text{NaNO}_3(\text{aq})$

In this section we use the previously determined standard Pitzer model parameters to calculate the osmotic coefficient, water activity, mean activity coefficient, and solubility product of saturated solutions of $\text{Ca}(\text{NO}_3)_2(\text{aq})$ and $\text{NaNO}_3(\text{aq})$ as a function of temperature.

The solubilities of $\text{Ca}(\text{NO}_3)_2(\text{aq})$ and $\text{NaNO}_3(\text{aq})$, reported by Linke [22], are reproduced in tables 10 and 11, respectively, together the chemical composition of each solid phase that is in equilibrium with the saturated solution at each temperature. The osmotic coefficient and mean activity coefficient of each of these solutions were then computed from equations (4) and (5) using the standard Pitzer model parameters evaluated with the optimal constant exponential coefficients α_1^P and the solubility limited maximum ionic strengths $I_{\text{max}}(T)$. The standard Pitzer model parameters were calculated as functions of temperature using the accurate 7-term temperature functions given in table 6 for $\text{Ca}(\text{NO}_3)_2(\text{aq})$, and in table 8 for $\text{NaNO}_3(\text{aq})$. The water activity and the solubility product were then evaluated at each temperature using equations (63) and (65), respectively.

The osmotic coefficient, water activity, mean activity coefficient, and the solubility product calculated as described above for saturated solutions as a function of temperature, are summarized in table 10 and figures 21 and 22 for $\text{Ca}(\text{NO}_3)_2(\text{aq})$, and in

table 11 and figures 23 and 24 for $\text{NaNO}_3(\text{aq})$. The results for $\text{Ca}(\text{NO}_3)_2(\text{aq})$ are plotted in three discontinuous segments for the thermodynamically stable single-hydrate solid phases of $\text{Ca}(\text{NO}_3)_2 \cdot 4\text{H}_2\text{O}(\text{s})$, $\text{Ca}(\text{NO}_3)_2 \cdot 3\text{H}_2\text{O}(\text{s})$, and $\text{Ca}(\text{NO}_3)_2(\text{s})$ with increasing temperature, excluding the metastable solid phases included by Linke [22]. The results for $\text{NaNO}_3(\text{aq})$ are much simpler and consist of a single continuous segment, because it forms only the anhydrous solid phase over this temperature range.

12. Conclusions

A general error minimization method was presented for converting the temperature dependent parameters of extended forms of Pitzer's ion-interaction model to those of the standard Pitzer model. It was further shown that the error minimization criterion could be fruitfully exploited to optimize the value of the exponential coefficient a_1^P of the standard Pitzer model, with the result that the accuracy of the standard Pitzer model was improved to the point where it may no be longer necessary to use extended Pitzer models for both $\text{Ca}(\text{NO}_3)_2(\text{aq})$ and $\text{NaNO}_3(\text{aq})$ over the full ionic strength range up to the solubility limit for $T = (298.15 \text{ to } 423.15) \text{ K}$. Instead of the standard value of $a_1^P = 2.0 \text{ kg}^{1/2} \cdot \text{mol}^{-1/2}$, the optimum constant values for the exponential coefficient were found to be $a_1^P = 0.87 \text{ kg}^{1/2} \cdot \text{mol}^{-1/2}$ for $\text{Ca}(\text{NO}_3)_2(\text{aq})$ and $a_1^P = 1.43 \text{ kg}^{1/2} \cdot \text{mol}^{-1/2}$ $\text{NaNO}_3(\text{aq})$, respectively. The accuracies of the standard Pitzer model representations using these optimized values of a_1^P are also comparable to or better than commonly achieved with the more complex mole-fraction based thermodynamic models [26,30].

An exploratory study performed to determine whether the use of an optimal temperature dependent a_1^P exponential coefficient would improve the accuracy of the standard Pitzer model showed that no significant increase in accuracy could be realized

over that obtained using a constant optimal value of the exponential coefficient.

Therefore, it is recommended that the constant optimal exponential coefficient values given above be used for these two aqueous electrolytes.

A general error minimization method of fitting temperature functions to the parameters of the standard Pitzer model, previously determined through the model conversion process, was developed. The impact of different selections of temperature functions on the accuracy of the osmotic coefficient calculated using these temperature functions to represent the variation with temperature of the Pitzer parameters, was investigated. It was found that while 4-term temperature functions were adequate for $\text{NaNO}_3(\text{aq})$, 7-term temperature functions were required to accurately represent the Pitzer parameters for $\text{Ca}(\text{NO}_3)_2(\text{aq})$. We recommend the use of the 7-term temperature functions given in the paper together with the constant optimized values of the exponential coefficient a_1^P .

Finally, these Pitzer parameter temperature coefficients and optimized a_1^P exponential coefficient values were used to compute the osmotic coefficient, water activity, mean activity coefficient, and solubility product of saturated solutions of $\text{Ca}(\text{NO}_3)_2(\text{aq})$ and $\text{NaNO}_3(\text{aq})$ over the temperature range of $T = (273.15 \text{ K to } 423.15) \text{ K}$ as presented in tables 10 and 11.

Our success in representing the osmotic coefficients of $\text{Ca}(\text{NO}_3)_2(\text{aq})$ and $\text{NaNO}_3(\text{aq})$ with the standard Pitzer model when the a_1^P values are optimized leads us to believe that thermodynamic data for other highly-soluble metal nitrate salts such as $\text{LiNO}_3(\text{aq})$, $\text{KNO}_3(\text{aq})$, $\text{Cu}(\text{NO}_3)_2(\text{aq})$, etc., may also be accurately represented with the standard Pitzer model using this approach.

Acknowledgments

This work was performed under the auspices of the U. S. Department of Energy by University of California, Lawrence Livermore National Laboratory under contract No. W-7405-ENG-48.

References

- [1] K. S. Pitzer, *J. Phys. Chem.* 77 (1973) 268–277.
- [2] K. S. Pitzer, in K.S. Pitzer (Ed.) *Activity Coefficients in Electrolyte Solutions*, 2nd edition, CRC Press, Boca Raton, FL, 1991, pp. 75–153.
- [3] K. S. Pitzer, G. Mayorga, *J. Solution Chem.* 3 (1974) 539–546.
- [4] K. S. Pitzer, L. F. Silvester, *J. Phys. Chem.* 82 (1978) 1239–1242.
- [5] C. E. Harvie, J. H. Weare, *Geochim. Cosmochim. Acta* 44 (1980) 981–997.
- [6] C. E. Harvie, H. P. Eugster, J. H. Weare, *Geochim. Cosmochim. Acta* 46 (1982) 1603–1618.
- [7] L. N. Plummer, D. L. Parkhurst, G. W. Fleming, S. A. Dunkel, U. S. Geological Survey Water-Resources Investigations Report 88-4153, 1988.
- [8] T. J. Wolery, EQ3NR, A Computer Program for Geochemical Aqueous Speciation-Solubility Calculations: Theoretical Manual, User's Guide, and Related Documentation (Version 7.0), UCRL-MA-110662 Pt. III, Lawrence Livermore National Laboratory, Livermore, California, 1992.
- [9] G. M. Marion, S. A. Grant, FREZCHEM: A Chemical-Thermodynamic Model for Aqueous Solutions at Subzero Temperatures. Special Report 94-18, U. S. Army Corps of Engineers, Cold Regions Research & Engineering Laboratory, 1994.
- [10] D. G. Archer, *J. Phys. Chem. Ref. Data* 20 (1991) 509–555.
- [11] D. G. Archer, *J. Phys. Chem. Ref. Data* 21 (1992) 793–829.
- [12] K. S. Pitzer, P. Wang, J. A. Rard, S. L. Clegg, *J. Solution Chem.* 28 (1999) 265–282.
- [13] C. S. Oakes, A. R. Felmy, S. M. Sterner, *J. Chem. Thermodyn.* 32 (2000) 29–54.
- [14] J. A. Rard, A. M. Wijesinghe, *J. Chem. Thermodyn.* 35 (2003) 439–473.
- [15] J. A. Rard, S. L. Clegg, R. F. Platford, *J. Chem. Thermodyn.* 35 (2003) 967–1008.

- [16] C. S. Oakes, J. A. Rard, D. G. Archer, *J. Chem. Eng. Data* 49 (2004) 313–325.
- [17] J. A. Rard, A. M. Wijesinghe, T. J. Wolery, *J. Chem. Eng. Data* 49 (2004) 1127–1140.
- [18] C. Christov, N. Møller, *Geochim. Cosmochim. Acta* 68 (2004) 1309–1331.
- [19] R. T. Pabalan, K. S. Pitzer, *Geochim. Cosmochim. Acta* 51 (1987) 2429–2443.
- [20] A. R. Felmy, D. Rai, *J. Solution Chem.* 28 (1999) 533–553.
- [21] F. J. Millero, D. Pierrot, *Aquatic Geochem.* 4 (1998) 153–199.
- [22] W. F. Linke, *Solubilities: Inorganic and Metal-Organic Compounds*, vol. I, 4th ed., American Chemical Society, Washington, DC, 1958, pp. 615–616; vol. II, 4th ed., American Chemical Society, Washington, DC, 1965, p. 250.
- [23] R. H. Stokes, R. A. Robinson, *J. Am. Chem. Soc.* 70 (1948) 1870–1878.
- [24] H. Braunstein, J. Braunstein, *J. Chem. Thermodyn.* 3 (1971) 419–431.
- [25] M. R. Ally, J. Braunstein, *Fluid Phase Equil.* 120 (1996) 131–141.
- [26] S. L. Clegg, K. S. Pitzer, P. Brimblecombe, *J. Phys. Chem.* 96 (1992) 9470–9479.
- [27] D. G. Archer, *J. Chem. Eng. Data* 35 (1990) 340–344.
- [28] J. G. Albright, J. A. Rard, S. Serna, E. E. Summers, M. C. Yang, *J. Chem. Thermodyn.* 32 (2000) 1447–1487.
- [29] D. G. Archer, *J. Phys. Chem. Ref. Data* 29 (2000) 1141–1156.
- [30] J. M. Simonson, K. S. Pitzer, *J. Phys. Chem.* 90 (1986) 3009–3013.

TABLE 1. Parameters for the standard Pitzer ion-interaction model for $\text{Ca}(\text{NO}_3)_2(\text{aq})$ converted from the extended Archer ion-interaction model of Oakes et al. [13], with temperature independent optimal and standard values of the exponential coefficients a_i^p and maximum ionic strengths $I_{\max}(T)$ equal to those of the saturated solutions^a

T/K	$b_{\text{MX}}^{(0,\text{P})} \cdot m^\circ$	$b_{\text{MX}}^{(1,\text{P})} \cdot m^\circ$	$C_{\text{M,X}}^{(\text{f},\text{P})} \cdot (m^\circ)^2$	I_{\max}/m°	I_{sat}/m°
$a_i^p = 0.87 \text{ kg}^{1/2} \cdot \text{mol}^{-1/2}$ (optimum value); average RMSE ($E_{i,T}$) = $6.0964 \cdot 10^{-3}$					
273.15	$8.9288 \cdot 10^{-2}$	0.41957	$1.5814 \cdot 10^{-3}$	18.651	18.651
283.15	0.10216	0.45835	$-1.3534 \cdot 10^{-4}$	21.078	21.078
293.15	0.10978	0.49995	$-1.1700 \cdot 10^{-3}$	23.640	23.640
298.15	0.11256	0.51995	$-1.5540 \cdot 10^{-3}$	25.227	25.227
303.15	0.11534	0.53501	$-1.9213 \cdot 10^{-3}$	27.897	27.897
313.15	0.11828	0.57057	$-2.3499 \cdot 10^{-3}$	35.841	35.841
323.15	0.11813	0.61606	$-2.4774 \cdot 10^{-3}$	51.480	51.480
333.15	0.11612	0.67152	$-2.4685 \cdot 10^{-3}$	56.180	56.180
343.15	0.11419	0.72067	$-2.4599 \cdot 10^{-3}$	60.880	60.880
353.15	0.11243	0.76350	$-2.4555 \cdot 10^{-3}$	65.580	65.580
363.15	0.11092	0.79955	$-2.4583 \cdot 10^{-3}$	66.030	66.030
373.15	0.10963	0.82985	$-2.4659 \cdot 10^{-3}$	66.480	66.480
383.15	0.10853	0.85433	$-2.4746 \cdot 10^{-3}$	66.696	66.696
393.15	0.10762	0.87454	$-2.4845 \cdot 10^{-3}$	66.912	66.912
403.15	0.10686	0.89030	$-2.4913 \cdot 10^{-3}$	67.227	67.227
413.15	0.10623	0.90214	$-2.4932 \cdot 10^{-3}$	67.640	67.640
423.15	0.10571	0.91022	$-2.4873 \cdot 10^{-3}$	68.486	68.486

$$a_i^p = 2.0 \text{ kg}^{1/2} \cdot \text{mol}^{-1/2} \text{ (optimum value); average RMSE } (E_{I,T}) = 7.2456 \cdot 10^{-2}$$

273.15	0.13520	1.5222	$-2.8248 \cdot 10^{-3}$	18.651	18.651
283.15	0.14720	1.7892	$-4.1041 \cdot 10^{-3}$	21.078	21.078
293.15	0.15390	2.0779	$-4.7514 \cdot 10^{-3}$	23.640	23.640
298.15	0.15557	2.2387	$-4.8824 \cdot 10^{-3}$	25.227	25.227
303.15	0.15509	2.4417	$-4.7737 \cdot 10^{-3}$	27.897	27.897
313.15	0.14983	2.9650	$-4.2132 \cdot 10^{-3}$	35.841	35.841
323.15	0.13866	3.7113	$-3.3784 \cdot 10^{-3}$	51.480	51.480
333.15	0.13567	4.1053	$-3.2655 \cdot 10^{-3}$	56.180	56.180
343.15	0.13262	4.4680	$-3.1608 \cdot 10^{-3}$	60.880	60.880
353.15	0.12965	4.7979	$-3.0696 \cdot 10^{-3}$	65.580	65.580
363.15	0.12875	5.0051	$-3.0906 \cdot 10^{-3}$	66.030	66.030
373.15	0.12793	5.1878	$-3.1109 \cdot 10^{-3}$	66.480	66.480
383.15	0.12727	5.3414	$-3.1331 \cdot 10^{-3}$	66.696	66.696
393.15	0.12669	5.4785	$-3.1527 \cdot 10^{-3}$	66.912	66.912
403.15	0.12610	5.6016	$-3.1629 \cdot 10^{-3}$	67.227	67.227
413.15	0.12550	5.7140	$-3.1624 \cdot 10^{-3}$	67.640	67.640
423.15	0.12471	5.8250	$-3.1400 \cdot 10^{-3}$	68.486	68.486

^a These parameter values were obtained by using matrix equation (31) to determine the standard Pitzer model parameters at $\Delta T = 10$ K temperature intervals from $T = (273.15$ to $423.15)$ K. Values of $I_{\text{sat}}(T)$, used to evaluate the coefficients of matrix equation (31), were calculated from the information tabulated by Linke [22], or estimated by interpolation when the temperatures reported by Linke did not correspond to those in this

table. The highest ionic strengths are those of the saturated solution, with $I_{\max}(T) = I_{\text{sat}}(T)$.

$$m^{\circ} = 1 \text{ mol}\cdot\text{kg}^{-1}.$$

TABLE 2. Parameters for the standard Pitzer ion-interaction model for $\text{Ca}(\text{NO}_3)_2(\text{aq})$ converted from the extended Archer ion-interaction model of Oakes et al. [13], with temperature independent optimal and standard values of exponential coefficients a_1^p and constant maximum ionic strengths $I_{\max}(T) = 68.5 \text{ mol}\cdot\text{kg}^{-1}$ ^a

T/K	$b_{\text{MX}}^{(0,P)} \cdot m^\circ$	$b_{\text{MX}}^{(1,P)} \cdot m^\circ$	$C_{\text{MX}}^{(f,P)} \cdot (m^\circ)^2$	I_{\max}/m°	I_{sat}/m°
$a_1^p = 0.87 \text{ kg}^{1/2} \cdot \text{mol}^{-1/2}$ (optimum value); average RMSE ($E_{I,T}$) = $6.6666 \cdot 10^{-3}$					
273.15	0.13608	$9.5318 \cdot 10^{-2}$	$-2.9299 \cdot 10^{-3}$	68.5	18.651
283.15	0.13180	0.23936	$-2.7991 \cdot 10^{-3}$	68.5	21.078
293.15	0.12790	0.35729	$-2.6920 \cdot 10^{-3}$	68.5	23.640
298.15	0.12611	0.40910	$-2.6480 \cdot 10^{-3}$	68.5	25.227
303.15	0.12441	0.45588	$-2.6084 \cdot 10^{-3}$	68.5	27.897
313.15	0.12132	0.53913	$-2.5463 \cdot 10^{-3}$	68.5	35.841
323.15	0.11861	0.60975	$-2.5027 \cdot 10^{-3}$	68.5	51.480
333.15	0.11625	0.66976	$-2.4748 \cdot 10^{-3}$	68.5	56.180
343.15	0.11419	0.72069	$-2.4598 \cdot 10^{-3}$	68.5	60.880
353.15	0.11242	0.76376	$-2.4547 \cdot 10^{-3}$	68.5	65.580
363.15	0.11090	0.79997	$-2.4570 \cdot 10^{-3}$	68.5	66.030
373.15	0.10960	0.83029	$-2.4645 \cdot 10^{-3}$	68.5	66.480
383.15	0.10850	0.85477	$-2.4732 \cdot 10^{-3}$	68.5	66.696
393.15	0.10760	0.87494	$-2.4832 \cdot 10^{-3}$	68.5	66.912
403.15	0.10684	0.89059	$-2.4904 \cdot 10^{-3}$	68.5	67.227
413.15	0.10622	0.90230	$-2.4927 \cdot 10^{-3}$	68.5	67.640
423.15	0.10571	0.91022	$-2.4873 \cdot 10^{-3}$	68.5	68.486

$$a_i^p = 2.0 \text{ kg}^{1/2} \cdot \text{mol}^{-1/2} \text{ (optimum value); average RMSE (E}_{I,T}) = 7.5730 \cdot 10^{-2}$$

273.15	0.13771	1.4144	$-2.9843 \cdot 10^{-3}$	68.5	18.651
283.15	0.13652	2.1478	$-2.9600 \cdot 10^{-3}$	68.5	21.078
293.15	0.13515	2.7497	$-2.9400 \cdot 10^{-3}$	68.5	23.640
298.15	0.13447	3.0143	$-2.9344 \cdot 10^{-3}$	68.5	25.227
303.15	0.13377	3.2540	$-2.9293 \cdot 10^{-3}$	68.5	27.897
313.15	0.13247	3.6813	$-2.9286 \cdot 10^{-3}$	68.5	35.841
323.15	0.13128	4.0458	$-2.9372 \cdot 10^{-3}$	68.5	51.480
333.15	0.13019	4.3582	$-2.9536 \cdot 10^{-3}$	68.5	56.180
343.15	0.12923	4.6269	$-2.9760 \cdot 10^{-3}$	68.5	60.880
353.15	0.12837	4.8586	$-3.0025 \cdot 10^{-3}$	68.5	65.580
363.15	0.12762	5.0590	$-3.0313 \cdot 10^{-3}$	68.5	66.030
373.15	0.12697	5.2335	$-3.0609 \cdot 10^{-3}$	68.5	66.480
383.15	0.12639	5.3834	$-3.0873 \cdot 10^{-3}$	68.5	66.696
393.15	0.12590	5.5162	$-3.1117 \cdot 10^{-3}$	68.5	66.912
403.15	0.12546	5.6321	$-3.1298 \cdot 10^{-3}$	68.5	67.227
413.15	0.12507	5.7346	$-3.1400 \cdot 10^{-3}$	68.5	67.640
423.15	0.12470	5.8253	$-3.1396 \cdot 10^{-3}$	68.5	68.486

^a These parameter values were obtained by using matrix equation (31) to determine the standard Pitzer model parameters at $\Delta T = 10$ K temperature intervals from $T = (273.15$ to $423.15)$ K. Values of $I_{\text{sat}}(T)$, used to evaluate the coefficients of matrix equation (31), were calculated from the information tabulated by Linke [22], or estimated by

interpolation when the temperatures reported by Linke did not correspond to those in this table. The maximum ionic strength $I_{\max}(T) = 68.5 \text{ mol}\cdot\text{kg}^{-1}$. $m^{\circ} = 1 \text{ mol}\cdot\text{kg}^{-1}$.

TABLE 3. Parameters for the standard Pitzer ion-interaction model for $\text{NaNO}_3(\text{aq})$ converted from the extended ion-interaction model of Archer [29], with temperature independent optimal and standard values of exponential coefficient a_i^p and maximum ionic strengths $I_{\max}(T)$ equal to those of the saturated solutions ^a

T/K	$b_{\text{MX}}^{(0,P)} \cdot m^\circ$	$b_{\text{MX}}^{(1,P)} \cdot m^\circ$	$C_{\text{MX}}^{(f,P)} \cdot (m^\circ)^2$	I_{\max}/m°	I_{sat}/m°
$a_i^p = 1.43 \text{ kg}^{1/2} \cdot \text{mol}^{-1/2}$ (optimum value); average RMSE ($E_{I,T}$) = $2.0340 \cdot 10^{-3}$					
273.15	$-1.8283 \cdot 10^{-2}$	$3.6990 \cdot 10^{-3}$	$1.6561 \cdot 10^{-3}$	8.584	8.584
283.15	$-1.0998 \cdot 10^{-2}$	$7.1311 \cdot 10^{-2}$	$1.0319 \cdot 10^{-3}$	9.454	9.454
293.15	$-4.6944 \cdot 10^{-3}$	0.12367	$5.3708 \cdot 10^{-4}$	10.365	10.365
298.15	$-1.8888 \cdot 10^{-3}$	0.14594	$3.3095 \cdot 10^{-4}$	10.839	10.839
303.15	$6.9924 \cdot 10^{-4}$	0.16622	$1.4906 \cdot 10^{-4}$	11.327	11.327
313.15	$5.2627 \cdot 10^{-3}$	0.20219	$-1.5053 \cdot 10^{-4}$	12.352	12.352
323.15	$9.0742 \cdot 10^{-3}$	0.23361	$-3.7671 \cdot 10^{-4}$	13.453	13.453
333.15	$1.2209 \cdot 10^{-2}$	0.26184	$-5.4193 \cdot 10^{-4}$	14.644	14.644
343.15	$1.4738 \cdot 10^{-2}$	0.28778	$-6.5670 \cdot 10^{-4}$	15.944	15.944
353.15	$1.6732 \cdot 10^{-2}$	0.31204	$-7.2995 \cdot 10^{-4}$	17.372	17.372
363.15	$1.8255 \cdot 10^{-2}$	0.33506	$-7.6939 \cdot 10^{-4}$	18.950	18.950
373.15	$1.9373 \cdot 10^{-2}$	0.35715	$-7.8169 \cdot 10^{-4}$	20.701	20.701
383.15	$2.0136 \cdot 10^{-2}$	0.37865	$-7.7206 \cdot 10^{-4}$	22.547	22.547
393.15	$2.0629 \cdot 10^{-2}$	0.39936	$-7.4740 \cdot 10^{-4}$	24.805	24.805
403.15	$2.0879 \cdot 10^{-2}$	0.41986	$-7.1031 \cdot 10^{-4}$	27.169	27.169
413.15	$2.0952 \cdot 10^{-2}$	0.44008	$-6.6576 \cdot 10^{-4}$	29.810	29.810
423.15	$2.0924 \cdot 10^{-2}$	0.45974	$-6.1857 \cdot 10^{-4}$	33.069	33.069

$$a_1^p = 2.0 \text{ kg}^{1/2} \cdot \text{mol}^{-1/2} \text{ (optimum value); average RMSE (E}_{I,T}) = 7.9871 \cdot 10^{-3}$$

273.15	$-1.8440 \cdot 10^{-2}$	$1.2425 \cdot 10^{-2}$	$1.6810 \cdot 10^{-3}$	8.584	8.584
283.15	$-8.1391 \cdot 10^{-3}$	0.11486	$7.8419 \cdot 10^{-4}$	9.454	9.454
293.15	$9.1337 \cdot 10^{-6}$	0.19958	$1.4950 \cdot 10^{-4}$	10.365	10.365
298.15	$3.4443 \cdot 10^{-3}$	0.23750	$-9.5861 \cdot 10^{-5}$	10.839	10.839
303.15	$6.5168 \cdot 10^{-3}$	0.27324	$-3.0280 \cdot 10^{-4}$	11.327	11.327
313.15	$1.1715 \cdot 10^{-2}$	0.33987	$-6.2203 \cdot 10^{-4}$	12.352	12.352
323.15	$1.5832 \cdot 10^{-2}$	0.40213	$-8.4089 \cdot 10^{-4}$	13.453	13.453
333.15	$1.9039 \cdot 10^{-2}$	0.46182	$-9.8248 \cdot 10^{-4}$	14.644	14.644
343.15	$2.1469 \cdot 10^{-2}$	0.52025	$-1.0638 \cdot 10^{-3}$	15.944	15.944
353.15	$2.3235 \cdot 10^{-2}$	0.57834	$-1.0982 \cdot 10^{-3}$	17.372	17.372
363.15	$2.4435 \cdot 10^{-2}$	0.63673	$-1.0962 \cdot 10^{-3}$	18.950	18.950
373.15	$2.5157 \cdot 10^{-2}$	0.69587	$-1.0668 \cdot 10^{-3}$	20.701	20.701
383.15	$2.5515 \cdot 10^{-2}$	0.75524	$-1.0196 \cdot 10^{-3}$	22.547	22.547
393.15	$2.5497 \cdot 10^{-2}$	0.81719	$-9.5460 \cdot 10^{-4}$	24.805	24.805
403.15	$2.5274 \cdot 10^{-2}$	0.87929	$-8.8377 \cdot 10^{-4}$	27.169	27.169
413.15	$2.4872 \cdot 10^{-2}$	0.94260	$-8.0883 \cdot 10^{-4}$	29.810	29.810
423.15	$2.4314 \cdot 10^{-2}$	1.0084	$-7.3183 \cdot 10^{-4}$	33.069	33.069

^a These parameter values were obtained by using matrix equation (31) to determine the standard Pitzer model parameters at $\Delta T = 10$ K temperature intervals from $T = (273.15$ to $423.15)$ K. Values of $I_{\text{sat}}(T)$, used to evaluate the coefficients of matrix equation (31), were calculated from the information tabulated by Linke [22] from the studies of Berkeley and Chretien, after smoothing the combined results as a function of

temperature. The highest ionic strengths are those of the saturated solution, with $I_{\max}(T) = I_{\text{sat}}(T)$. $m^{\circ} = 1 \text{ mol}\cdot\text{kg}^{-1}$.

TABLE 4. Parameters for the standard Pitzer ion-interaction model for $\text{Ca}(\text{NO}_3)_2(\text{aq})$ converted from the extended Archer ion-interaction model of Oakes et al. [13], with temperature dependent optimal exponential coefficient $a_1^{\text{P}}(\text{opt})$ and maximum ionic strengths $I_{\text{max}}(T)$ equal to the ionic strength $I_{\text{sat}}(T)$ of the saturated solutions ^a

T/K	$a_1^{\text{P}}(\text{opt})$	RMSE (E_1)	$b_{\text{MX}}^{(0,\text{P})} \cdot m^\circ$	$b_{\text{MX}}^{(1,\text{P})} \cdot m^\circ$	$C_{\text{MX}}^{(\text{f},\text{P})} \cdot (m^\circ)^2$	I_{max}/m°	I_{sat}/m°
273.15	1.74	$1.4797 \cdot 10^{-3}$	0.12990	1.1300	$-2.1968 \cdot 10^{-3}$	18.651	18.651
283.15	1.56	$1.4143 \cdot 10^{-4}$	0.13746	1.0553	$-3.0828 \cdot 10^{-3}$	21.078	21.078
293.15	1.40	$1.3206 \cdot 10^{-3}$	0.13950	0.98237	$-3.4060 \cdot 10^{-3}$	23.640	23.640
298.15	1.30	$2.0533 \cdot 10^{-3}$	0.13795	0.91424	$-3.3472 \cdot 10^{-3}$	25.227	25.227
303.15	1.25	$2.7466 \cdot 10^{-3}$	0.13699	0.90822	$-3.3335 \cdot 10^{-3}$	27.897	27.897
313.15	1.10	$4.1928 \cdot 10^{-3}$	0.13028	0.82543	$-2.9845 \cdot 10^{-3}$	35.841	35.841
323.15	0.95	$4.8171 \cdot 10^{-3}$	0.12139	0.72113	$-2.6048 \cdot 10^{-3}$	51.480	51.480
333.15	0.90	$4.8545 \cdot 10^{-3}$	0.11737	0.71422	$-2.5136 \cdot 10^{-3}$	56.180	56.180
343.15	0.88	$4.7533 \cdot 10^{-3}$	0.11539	0.76836	$-2.5004 \cdot 10^{-3}$	60.880	60.880
353.15	0.86	$4.6822 \cdot 10^{-3}$	0.11204	0.74673	$-2.4430 \cdot 10^{-3}$	65.580	65.580
363.15	0.86	$4.7743 \cdot 10^{-3}$	0.11051	0.78197	$-2.4454 \cdot 10^{-3}$	66.030	66.030
373.15	0.85	$4.9281 \cdot 10^{-3}$	0.10878	0.79364	$-2.4392 \cdot 10^{-3}$	66.480	66.480
383.15	0.85	$5.1225 \cdot 10^{-3}$	0.10766	0.81700	$-2.4473 \cdot 10^{-3}$	66.696	66.696
393.15	0.85	$5.3845 \cdot 10^{-3}$	0.10673	0.83626	$-2.4568 \cdot 10^{-3}$	66.912	66.912
403.15	0.85	$5.6852 \cdot 10^{-3}$	0.10596	0.85120	$-2.4634 \cdot 10^{-3}$	67.227	67.227
413.15	0.86	$6.0665 \cdot 10^{-3}$	0.10578	0.88204	$-2.4794 \cdot 10^{-3}$	67.640	67.640
423.15	0.87	$6.4759 \cdot 10^{-3}$	0.10571	0.91022	$-2.4873 \cdot 10^{-3}$	68.486	68.486

^a These parameter values are for the optimal value of the exponential coefficient a_1^p that minimizes the RMS error E_I defined by equation (15) and were obtained by using matrix equation (31) to determine the standard Pitzer model parameters at $\Delta T = 10$ K temperature intervals from $T = (273.15$ to $423.15)$ K. Values of $I_{\text{sat}}(T)$, used to evaluate the coefficients of matrix equation (31), were calculated from the information tabulated by Linke [22], or estimated by interpolation when the temperatures reported by Linke did not correspond to those in this table. ^c The highest ionic strengths are those of the saturated solution, with $I_{\text{max}}(T) = I_{\text{sat}}(T)$. $m^\circ = 1 \text{ mol}\cdot\text{kg}^{-1}$.

TABLE 5. Parameters for the standard Pitzer ion-interaction model for $\text{NaNO}_3(\text{aq})$ converted from the extended ion-interaction model of Archer [29], with temperature dependent optimal exponential coefficient $a_1^{\text{P}}(\text{opt})$ and maximum ionic strengths $I_{\text{max}}(T)$ equal to the solubility limit $I_{\text{sat}}(T)$ ^a

T/K	$a_1^{\text{P}}(\text{opt})$	RMSE (E_I)	$b_{\text{MX}}^{(0,\text{P})} \cdot m^\circ$	$b_{\text{MX}}^{(1,\text{P})} \cdot m^\circ$	$C_{\text{M,X}}^{(\text{f},\text{P})} \cdot (m^\circ)^2$	I_{max}/m°	I_{sat}/m°
273.15	n.a.	n.a.	n.a.	n.a.	n.a.	8.584	8.584
283.15	2.60	$2.0005 \cdot 10^{-4}$	$-6.4628 \cdot 10^{-3}$	0.19302	$6.1175 \cdot 10^{-4}$	9.454	9.454
293.15	1.96	$8.8132 \cdot 10^{-6}$	$-2.3091 \cdot 10^{-4}$	0.19277	$1.7124 \cdot 10^{-4}$	10.365	10.365
298.15	1.81	$2.2945 \cdot 10^{-5}$	$2.0449 \cdot 10^{-3}$	0.20107	$2.4427 \cdot 10^{-5}$	10.839	10.839
303.15	1.70	$4.5837 \cdot 10^{-5}$	$3.9495 \cdot 10^{-3}$	0.20933	$-9.2604 \cdot 10^{-5}$	11.327	11.327
313.15	1.57	$1.5174 \cdot 10^{-4}$	$7.2901 \cdot 10^{-3}$	0.22896	$-2.8942 \cdot 10^{-4}$	12.352	12.352
323.15	1.50	$3.1935 \cdot 10^{-4}$	$1.0187 \cdot 10^{-2}$	0.24938	$-4.4757 \cdot 10^{-4}$	13.453	13.453
333.15	1.45	$5.2718 \cdot 10^{-4}$	$1.2541 \cdot 10^{-2}$	0.26705	$-5.6168 \cdot 10^{-4}$	14.644	14.644
343.15	1.43	$7.6164 \cdot 10^{-4}$	$1.4738 \cdot 10^{-2}$	0.28778	$-6.5670 \cdot 10^{-4}$	15.944	15.944
353.15	1.41	$1.0221 \cdot 10^{-3}$	$1.6406 \cdot 10^{-2}$	0.30525	$-7.1300 \cdot 10^{-4}$	17.372	17.372
363.15	1.42	$1.3559 \cdot 10^{-3}$	$1.8102 \cdot 10^{-2}$	0.33119	$-7.6187 \cdot 10^{-4}$	18.950	18.950
373.15	1.41	$1.6397 \cdot 10^{-3}$	$1.9083 \cdot 10^{-2}$	0.34849	$-7.6845 \cdot 10^{-4}$	20.701	20.701
383.15	1.42	$1.9957 \cdot 10^{-3}$	$2.0002 \cdot 10^{-2}$	0.37380	$-7.6632 \cdot 10^{-4}$	22.547	22.547
393.15	1.42	$2.3166 \cdot 10^{-3}$	$2.0508 \cdot 10^{-2}$	0.39397	$-7.4257 \cdot 10^{-4}$	24.805	24.805
403.15	1.43	$2.6761 \cdot 10^{-3}$	$2.0879 \cdot 10^{-2}$	0.41986	$-7.1031 \cdot 10^{-4}$	27.169	27.169
413.15	1.44	$3.0433 \cdot 10^{-3}$	$2.1049 \cdot 10^{-2}$	0.44667	$-6.6910 \cdot 10^{-4}$	29.810	29.810
423.15	1.45	$3.4111 \cdot 10^{-3}$	$2.1091 \cdot 10^{-2}$	0.47426	$-6.2387 \cdot 10^{-4}$	33.069	33.069

^a These parameter values are for the optimal value of the exponential coefficient a_1^{P} that minimizes the RMS error E_I defined by equation (15) and were obtained by using matrix equation (31) to determine the standard Pitzer model parameters at $\Delta T = 10$ K temperature intervals from $T = (273.15 \text{ to } 423.15)$ K. Values of $I_{\text{sat}}(T)$, used to evaluate the coefficients of matrix equation (31), were calculated from the information tabulated

by Linke [22] from the studies of Berkeley and Chretien, after smoothing the combined results as a function of temperature. The highest ionic strengths are those of the saturated solution, with $I_{\max}(T) = I_{\text{sat}}(T)$. $m^\circ = 1 \text{ mol}\cdot\text{kg}^{-1}$. Values of the Pitzer parameters are not reported at $T = 273.15 \text{ K}$ because the source model yield an unrealistic value of $a_1^{\text{P}}(\text{opt})$ at this temperature; n.a. denotes not available.

TABLE 6. Temperature coefficients a_{ij} of parameters for the standard Pitzer ion-interaction model for $\text{Ca}(\text{NO}_3)_2(\text{aq})$, derived from the extended Archer ion-interaction model of Oakes et al. [13], with maximum ionic strengths $I_{\max}(T)$ equal to the ionic strengths $I_{\text{sat}}(T)$ of the saturated solutions ^a

Temperature Coefficient: $\{a_{1j}(b_{\text{MX}}^{(0,P)})\} \cdot (m^\circ)$ $\{a_{2j}(b_{\text{MX}}^{(1,P)})\} \cdot (m^\circ)$ $\{a_{3j}(C_{\text{M,X}}^{(f,P)})\} \cdot (m^\circ)^2$				
$a_1^p = 0.87 \text{ kg}^{1/2} \cdot \text{mol}^{-1/2}$ (optimum value); average RMSE = $8.7357 \cdot 10^{-3}$				
Index j	Basis Function	i = 1	i = 2	i = 3
1	1	0.1131573	0.5151491	$-1.601513 \cdot 10^{-3}$
2	$\{g_2(T)\} \cdot (T^\circ)$	1.492571	$-2.209288 \cdot 10$	$-9.000908 \cdot 10^{-3}$
3	$\{g_3(T)\} \cdot (T^\circ)^2$	$-1.013127 \cdot 10^{-3}$	$1.439130 \cdot 10^{-2}$	$1.244447 \cdot 10^{-5}$
4	$\{g_4(T)\} / (T^\circ)$	$-9.178758 \cdot 10^4$	$1.555944 \cdot 10^6$	$-1.469640 \cdot 10^3$
5	$g_5(T)$	$-5.335195 \cdot 10^2$	$8.357861 \cdot 10^3$	-1.556757
6	$\{g_6(T)\} \cdot (T^\circ)^3$	$3.579341 \cdot 10^{-7}$	$-4.939277 \cdot 10^{-6}$	$-5.932399 \cdot 10^{-9}$
7	$\{g_7(T)\} / (T^\circ)^2$	$3.002336 \cdot 10^6$	$-5.703014 \cdot 10^7$	$1.088473 \cdot 10^5$
8	$\{g_8(T)\} / (T^\circ)^3$	not used	not used	not used
$a_1^p = 2.0 \text{ kg}^{1/2} \cdot \text{mol}^{-1/2}$ (standard value); average RMSE = $7.5993 \cdot 10^{-2}$				
1	1	0.1541224	2.281398	$-4.710317 \cdot 10^{-3}$
2	$\{g_2(T)\} \cdot (T^\circ)$	-5.753712	$1.393891 \cdot 10^2$	0.7664789
3	$\{g_3(T)\} \cdot (T^\circ)^2$	$3.485761 \cdot 10^{-3}$	$-8.218850 \cdot 10^{-2}$	$-4.737426 \cdot 10^{-4}$
4	$\{g_4(T)\} / (T^\circ)$	$4.774220 \cdot 10^5$	$-1.214241 \cdot 10^7$	$-6.114101 \cdot 10^4$
5	$g_5(T)$	$2.354621 \cdot 10^3$	$-5.851593 \cdot 10^4$	$-3.075189 \cdot 10^2$
6	$\{g_6(T)\} \cdot (T^\circ)^3$	$-1.117736 \cdot 10^{-6}$	$2.562256 \cdot 10^{-5}$	$1.550355 \cdot 10^{-7}$
7	$\{g_7(T)\} / (T^\circ)^2$	$-1.916559 \cdot 10^7$	$4.968478 \cdot 10^8$	$2.407663 \cdot 10^6$
8	$\{g_8(T)\} / (T^\circ)^3$	not used	not used	not used

^a These parameter values were obtained using matrix equation (31) to determine the standard Pitzer model parameters at $\Delta T = 10$ K temperature intervals from $T = (298.15$ to $423.15)$ K. Matrix equation (58) was used subsequently to fit temperature coefficients to these Pitzer parameter values, and the average RMSE values refer to this fit. Values of $I_{\text{sat}}(T)$, used to evaluate the coefficients of matrix equation (31), were calculated from the information tabulated by Linke [22], or estimated by interpolation when the temperatures reported by Linke did not correspond to those needed. The $g_j(T)$ functions are defined by equations (48)–(55). $m^\circ = 1 \text{ mol}\cdot\text{kg}^{-1}$ and $T^\circ = 1 \text{ K}$.

TABLE 7. Temperature coefficients a_{ij} of parameters for the standard Pitzer ion-interaction model for $\text{Ca}(\text{NO}_3)_2(\text{aq})$, derived from the extended Archer ion-interaction model of Oakes et al. [13], with constant maximum ionic strengths $I_{\text{ma}}(T) = 68.5 \text{ mol}\cdot\text{kg}^{-1}$

a

Temperature Coefficient: $\{a_{1j}(b_{\text{MX}}^{(0,P)})\}\cdot(m^\circ)$ $\{a_{2j}(b_{\text{MX}}^{(1,P)})\}\cdot(m^\circ)$ $\{a_{3j}(C_{\text{M,X}}^{(f,P)})\}\cdot(m^\circ)^2$				
$a_1^P = 0.87 \text{ kg}^{1/2}\cdot\text{mol}^{-1/2}$ (optimum value); average RMSE = $6.6735\cdot 10^{-3}$				
Index j	Basis Function	i = 1	i = 2	i = 3
1	1	0.1261160	0.4090042	$-2.647838\cdot 10^{-3}$
2	$\{g_2(T)\}\cdot(T^\circ)$	$-8.098479\cdot 10^{-2}$	-2.897730	$1.375931\cdot 10^{-2}$
3	$\{g_3(T)\}\cdot(T^\circ)^2$	$5.384184\cdot 10^{-5}$	$1.855898\cdot 10^{-3}$	$-9.781430\cdot 10^{-6}$
4	$\{g_4(T)\}/(T^\circ)$	$6.001026\cdot 10^3$	$2.231575\cdot 10^5$	$-8.815055\cdot 10^2$
5	$g_5(T)$	$3.102035\cdot 10$	$1.133882\cdot 10^3$	-4.913129
6	$\{g_6(T)\}\cdot(T^\circ)^3$	$-1.941233\cdot 10^{-8}$	$-6.384572\cdot 10^{-7}$	$3.788698\cdot 10^{-9}$
7	$\{g_7(T)\}/(T^\circ)^2$	$-2.275682\cdot 10^5$	$-8.991675\cdot 10^6$	$3.135831\cdot 10^4$
8	$\{g_8(T)\}/(T^\circ)^3$	not used	not used	not used
$a_1^P = 2.0 \text{ kg}^{1/2}\cdot\text{mol}^{-1/2}$ (standard value); average RMSE = $7.5724\cdot 10^{-2}$				
1	1	0.1344734	3.014095	$-2.934099\cdot 10^{-3}$
2	$\{g_2(T)\}\cdot(T^\circ)$	-0.1456606	-9.290062	$1.599564\cdot 10^{-2}$
3	$\{g_3(T)\}\cdot(T^\circ)^2$	$9.544499\cdot 10^{-5}$	$5.551481\cdot 10^{-3}$	$-1.122061\cdot 10^{-5}$
4	$\{g_4(T)\}/(T^\circ)$	$1.094660\cdot 10^4$	$7.931238\cdot 10^5$	$-1.052388\cdot 10^3$
5	$g_5(T)$	$5.623581\cdot 10$	$3.838806\cdot 10^3$	-5.784694
6	$\{g_6(T)\}\cdot(T^\circ)^3$	$-3.380523\cdot 10^{-8}$	$-1.731504\cdot 10^{-6}$	$4.286865\cdot 10^{-9}$
7	$\{g_7(T)\}/(T^\circ)^2$	$-4.260763\cdot 10^5$	$-3.364272\cdot 10^7$	$3.821457\cdot 10^4$
8	$\{g_8(T)\}/(T^\circ)^3$	not used	not used	not used

^a These parameter values were obtained using matrix equation (31) to determine the standard Pitzer model parameters at $\Delta T = 10$ K temperature intervals from $T = (298.15 \text{ to } 423.15)$ K. Matrix equation (58) was used subsequently to fit temperature coefficients to these Pitzer parameter values, and the average RMSE values refer to this fit. Values of $I_{\text{sat}}(T)$, used to evaluate the coefficients of matrix equation (31), were calculated from the information tabulated by Linke [22], or estimated by interpolation when the temperatures reported by Linke did not correspond to those needed. The $g_j(T)$ functions are defined by equations (48)–(55). $m^\circ = 1 \text{ mol}\cdot\text{kg}^{-1}$ and $T^\circ = 1$ K. For the 4-term temperature function fit yields $\{a_{11}(b_{\text{MX}}^{(0,P)})\}\cdot(m^\circ) = 0.1259034$, $\{a_{12}(b_{\text{MX}}^{(0,P)})\}\cdot(m^\circ) = -4.774229\cdot 10^{-4}$, $\{a_{14}(b_{\text{MX}}^{(0,P)})\}\cdot(m^\circ) = 1.442089\cdot 10^2$, $\{a_{15}(b_{\text{MX}}^{(0,P)})\}\cdot(m^\circ) = 0.5209749$, $\{a_{21}(b_{\text{MX}}^{(1,P)})\}\cdot(m^\circ) = 0.4022983$, $\{a_{22}(b_{\text{MX}}^{(1,P)})\}\cdot(m^\circ) = 3.731374\cdot 10^{-3}$, $\{a_{24}(b_{\text{MX}}^{(1,P)})\}\cdot(m^\circ) = -3.219040\cdot 10^3$, $\{a_{25}(b_{\text{MX}}^{(1,P)})\}\cdot(m^\circ) = -8.988610$, $\{a_{31}(C_{\text{MX}}^{(f,P)})\}\cdot(m^\circ)^2 = -2.608019\cdot 10^{-3}$, $\{a_{32}(C_{\text{MX}}^{(f,P)})\}\cdot(m^\circ)^2 = 2.203723\cdot 10^{-4}$, $\{a_{34}(C_{\text{MX}}^{(f,P)})\}\cdot(m^\circ)^2 = -2.968550\cdot 10^1$, and $\{a_{34}(C_{\text{MX}}^{(f,P)})\}\cdot(m^\circ)^2 = -1.623817\cdot 10^{-1}$.

TABLE 8. Temperature coefficients a_{ij} of parameters for the standard Pitzer ion-interaction model for $\text{NaNO}_3(\text{aq})$, derived from Archer's ion-interaction model [29], with maximum ionic strengths $I_{\max}(T)$ equal to the ionic strengths $I_{\text{sat}}(T)$ of the saturated solutions ^a

Temperature Coefficient: $\{a_{ij}(b_{\text{MX}}^{(0,P)})\} \cdot (m^\circ)$ $\{a_{2j}(b_{\text{MX}}^{(1,P)})\} \cdot (m^\circ)$ $\{a_{3j}(C_{\text{M,X}}^{(f,P)})\} \cdot (m^\circ)^2$				
$a_1^P = 1.43 \text{ kg}^{1/2} \cdot \text{mol}^{-1/2}$ (optimum value); average RMSE = $2.0493 \cdot 10^{-3}$				
Index j	Basis Function	i = 1	i = 2	i = 3
1	1	$-1.888186 \cdot 10^{-3}$	0.1460677	$3.308894 \cdot 10^{-4}$
2	$\{g_2(T)\} \cdot (T^\circ)$	$4.501887 \cdot 10^{-2}$	-0.8585493	$-6.711814 \cdot 10^{-4}$
3	$\{g_3(T)\} \cdot (T^\circ)^2$	$-3.612038 \cdot 10^{-5}$	$3.558161 \cdot 10^{-4}$	$8.676446 \cdot 10^{-7}$
4	$\{g_4(T)\} / (T^\circ)$	$-3.006404 \cdot 10^3$	$1.115479 \cdot 10^5$	$-2.265104 \cdot 10$
5	$g_5(T)$	$-1.578798 \cdot 10$	$4.534652 \cdot 10^2$	$8.622251 \cdot 10^{-2}$
6	$\{g_6(T)\} \cdot (T^\circ)^3$	$1.665781 \cdot 10^{-8}$	$-5.360715 \cdot 10^{-8}$	$-5.372888 \cdot 10^{-10}$
7	$\{g_7(T)\} / (T^\circ)^2$	$1.093358 \cdot 10^5$	$-5.285602 \cdot 10^6$	$3.785484 \cdot 10^3$
8	$\{g_8(T)\} / (T^\circ)^3$	not used	not used	not used
$a_1^P = 2.0 \text{ kg}^{1/2} \cdot \text{mol}^{-1/2}$ (standard value); average RMSE = $8.0052 \cdot 10^{-3}$				
1	1	$3.453151 \cdot 10^{-3}$	0.2376814	$-9.713788 \cdot 10^{-5}$
2	$\{g_2(T)\} \cdot (T^\circ)$	-0.1902405	-0.9844373	$2.736158 \cdot 10^{-2}$
3	$\{g_3(T)\} \cdot (T^\circ)^2$	$1.078947 \cdot 10^{-4}$	$5.182529 \cdot 10^{-4}$	$-1.632435 \cdot 10^{-5}$
4	$\{g_4(T)\} / (T^\circ)$	$1.630865 \cdot 10^4$	$1.135333 \cdot 10^5$	$-2.348706 \cdot 10^3$
5	$g_5(T)$	$7.964834 \cdot 10$	$4.739877 \cdot 10^2$	$-1.132943 \cdot 10$
6	$\{g_6(T)\} \cdot (T^\circ)^3$	$-2.990106 \cdot 10^{-8}$	$-1.422885 \cdot 10^{-7}$	$5.069506 \cdot 10^{-9}$
7	$\{g_7(T)\} / (T^\circ)^2$	$-6.738489 \cdot 10^5$	$-5.408732 \cdot 10^6$	$9.868867 \cdot 10^4$
8	$\{g_8(T)\} / (T^\circ)^3$	not used	not used	not used

^a These parameter values were obtained using matrix equation (31) to determine the standard Pitzer model parameters at $\Delta T = 10$ K temperature intervals from $T = (273.15$ to $423.15)$ K. Matrix equation (58) was used subsequently to fit temperature coefficients to these Pitzer parameter values, and the average RMSE values refer to this fit. Values of $I_{\text{sat}}(T)$, used to evaluate the coefficients of matrix equation (31), were calculated from the information tabulated by Linke [22] from the studies of Berkeley and Chretien, after smoothing the combined results as a function of temperature. The $g_j(T)$ functions are defined by equations (48)–(55). $m^\circ = 1 \text{ mol}\cdot\text{kg}^{-1}$ and $T^\circ = 1 \text{ K}$.

TABLE 9. Temperature dependent and average constant optimal values of exponential coefficient $a_1^p(\text{opt})$ of the standard Pitzer model for $\text{Ca}(\text{NO}_3)_2(\text{aq})$ and $\text{NaNO}_3(\text{aq})$, with maximum ionic strengths $I_{\text{max}}(T)$ equal to the ionic strength $I_{\text{sat}}(T)$ of the saturated solution.

T/K	$\text{Ca}(\text{NO}_3)_2(\text{aq})^{\text{a}}$		$\text{Mg}(\text{NO}_3)_2(\text{aq})^{\text{b}}$		$\text{NaNO}_3(\text{aq})^{\text{a}}$	
	$a_1^p(\text{opt})$	RMSE	$a_1^p(\text{opt})$	RMSE	$a_1^p(\text{opt})$	RMSE
Average ^{c,d}	0.87 ^c	$6.0964 \cdot 10^{-3c}$	n.a.	n.a.	1.43 ^c	$2.0340 \cdot 10^{-3c}$
273.15	1.74	$1.4797 \cdot 10^{-3}$	n.a.	n.a.	n.a.	n.a.
283.15	1.56	$1.4143 \cdot 10^{-3}$	n.a.	n.a.	2.60	$2.0005 \cdot 10^{-4}$
293.15	1.40	$1.3206 \cdot 10^{-3}$	n.a.	n.a.	1.96	$8.8132 \cdot 10^{-6}$
298.15	1.30	$2.0533 \cdot 10^{-3}$	1.55	$3.5733 \cdot 10^{-3}$	1.81	$2.2945 \cdot 10^{-5}$
303.15	1.25	$2.7466 \cdot 10^{-3}$	n.a.	n.a.	1.70	$4.5837 \cdot 10^{-5}$
313.15	1.10	$4.1928 \cdot 10^{-3}$	n.a.	n.a.	1.57	$1.5174 \cdot 10^{-4}$
323.15	0.95	$4.8171 \cdot 10^{-3}$	n.a.	n.a.	1.50	$3.1935 \cdot 10^{-4}$
333.15	0.90	$4.8545 \cdot 10^{-3}$	n.a.	n.a.	1.45	$5.2718 \cdot 10^{-4}$
343.15	0.88	$4.7533 \cdot 10^{-3}$	n.a.	n.a.	1.43	$7.6164 \cdot 10^{-4}$
353.15	0.86	$4.6822 \cdot 10^{-3}$	n.a.	n.a.	1.41	$1.0221 \cdot 10^{-3}$
363.15	0.86	$4.7743 \cdot 10^{-3}$	n.a.	n.a.	1.42	$1.3559 \cdot 10^{-3}$
373.15	0.85	$4.9281 \cdot 10^{-3}$	n.a.	n.a.	1.41	$1.6397 \cdot 10^{-3}$
383.15	0.85	$5.1225 \cdot 10^{-3}$	n.a.	n.a.	1.42	$1.9957 \cdot 10^{-3}$
393.15	0.85	$5.3845 \cdot 10^{-3}$	n.a.	n.a.	1.42	$2.3166 \cdot 10^{-3}$
403.15	0.85	$5.6852 \cdot 10^{-3}$	n.a.	n.a.	1.43	$2.6761 \cdot 10^{-3}$
413.15	0.86	$6.0665 \cdot 10^{-3}$	n.a.	n.a.	1.44	$3.0433 \cdot 10^{-3}$

423.15	0.87	$6.4759 \cdot 10^{-3}$	n.a.	n.a.	1.45	$3.4111 \cdot 10^{-3}$
--------	------	------------------------	------	------	------	------------------------

^a These temperature dependent optimal values of the exponential coefficient a_1^P for the standard Pitzer model were evaluated directly using as input the extended ion-interaction model parameters reported by Oakes et al [13] for $\text{Ca}(\text{NO}_3)_2(\text{aq})$ and Archer [29] for $\text{NaNO}_3(\text{aq})$. These parameter values were obtained using matrix equation (31) to determine the standard Pitzer model parameters at $\Delta T = 10$ K temperature intervals from $T = (273.15 \text{ to } 423.15)$ K for values of a_1^P increasing in steps of $\Delta a_1^P = 0.05 \text{ kg}^{1/2} \cdot \text{mol}^{-1/2}$ from $a_1^P = (0.1 \text{ to } 3.0) \text{ kg}^{1/2} \cdot \text{mol}^{-1/2}$, and the optimal value of a_1^P was determined as the value corresponding to minimum root mean square error E_I . ^b These values for $\text{Mg}(\text{NO}_3)_2(\text{aq})$ were reported by Rard et al. [17] for $T = 298.15$ K only. The equation parameters and RMSE were obtained by direct fitting of osmotic coefficients rather than from transforming the parameters of an extended ion-interaction model. n.a. denotes not available. ^c The constant optimal values of a_1^P and the corresponding constant RMSE ($E_{I,T}$) are evaluated over the ionic-strength range from zero to saturation, and $T = (298.15 \text{ to } 423.15)$ K for $\text{Ca}(\text{NO}_3)_2(\text{aq})$ and $T = (273.15 \text{ to } 423.15)$ K for $\text{NaNO}_3(\text{aq})$, respectively. Values of $I_{\text{sat}}(T)$, used to evaluate the coefficients of matrix equation (31), were calculated from the information tabulated by Linke [22].

TABLE 10. Osmotic coefficient f , activity of water a_w , mean activity coefficient g_{\pm} , and solubility product K_{sp} for solid phases of $\text{Ca}(\text{NO}_3)_2 + \text{H}_2\text{O}$ computed using the standard Pitzer ion-interaction model for $\text{Ca}(\text{NO}_3)_2(\text{aq})$ derived from the extended ion-interaction model of Oakes et al [13], and the solubility information reported by Linke [22], with temperature independent optimal exponential coefficient $a_1^p = 0.87 \text{ kg}^{1/2} \cdot \text{mol}^{-1/2}$ and maximum ionic strengths $I_{\max}(T)$ equal to those of the saturated solutions ^a

T/K	f^a	a_w^a	g_{\pm}^a	K_{sp}^a	$I_{\text{sat}}^b / m^\circ$	Solid Phase ^b
293.15	1.5399	0.51900	0.72571	$5.4279 \cdot 10$	23.640	$\text{Ca}(\text{NO}_3)_2 \cdot 4\text{H}_2\text{O}(\text{s})$
298.15	1.5687	0.49021	0.77894	$6.4916 \cdot 10$	25.227	$\text{Ca}(\text{NO}_3)_2 \cdot 4\text{H}_2\text{O}(\text{s})$
303.15	1.6183	0.44338	0.87036	$8.1962 \cdot 10$	27.897	$\text{Ca}(\text{NO}_3)_2 \cdot 4\text{H}_2\text{O}(\text{s})$
308.15	1.6634	0.39530	0.97074	$9.8300 \cdot 10$	30.971	$\text{Ca}(\text{NO}_3)_2 \cdot 4\text{H}_2\text{O}(\text{s})$
313.15	1.7219	0.32898	1.1296	$1.1515 \cdot 10^2$	35.841	$\text{Ca}(\text{NO}_3)_2 \cdot 4\text{H}_2\text{O}(\text{s})$
318.15	1.7843	0.22974	1.4251	$4.9803 \cdot 10^2$	45.755	$\text{Ca}(\text{NO}_3)_2 \cdot 3\text{H}_2\text{O}(\text{s})$
323.15	1.7499	0.19733	1.4729	$4.9627 \cdot 10^2$	51.480	$\text{Ca}(\text{NO}_3)_2 \cdot 3\text{H}_2\text{O}(\text{s})$
324.15	1.7323	0.18501	1.4928	$4.9331 \cdot 10^2$	54.067	$\text{Ca}(\text{NO}_3)_2 \cdot 3\text{H}_2\text{O}(\text{s})$
328.15	1.5705	0.15704	1.4051	$1.1512 \cdot 10^5$	65.430	$\text{Ca}(\text{NO}_3)_2(\text{s})$
353.15	1.4010	0.19104	0.98891	$4.0416 \cdot 10^4$	65.580	$\text{Ca}(\text{NO}_3)_2(\text{s})$
373.15	1.2852	0.21457	0.74225	$1.7799 \cdot 10^4$	66.480	$\text{Ca}(\text{NO}_3)_2(\text{s})$
398.15	1.1425	0.25166	0.49223	$5.3216 \cdot 10^3$	67.032	$\text{Ca}(\text{NO}_3)_2(\text{s})$
420.65	1.0154	0.28847	0.32786	$1.6386 \cdot 10^3$	67.957	$\text{Ca}(\text{NO}_3)_2(\text{s})$
424.15	0.9818	0.29626	0.30278	$1.3379 \cdot 10^3$	68.778	$\text{Ca}(\text{NO}_3)_2(\text{s})$

^a These properties are based on the derived standard Pitzer model parameters given in table 6 for constant optimal $a_1^p = 0.87 \text{ kg}^{1/2} \cdot \text{mol}^{-1/2}$. ^b Values of $I_{\text{sat}}(T)$ used to evaluate these properties, and the solid phases, are calculated from the saturated solution compositions tabulated by Linke [22]. $m^\circ = 1 \text{ mol} \cdot \text{kg}^{-1}$.

TABLE 11. Osmotic coefficient f , activity of water a_w , mean activity coefficient g_{\pm} , and solubility product K_{sp} for $\text{NaNO}_3 + \text{H}_2\text{O}$ computed using the standard Pitzer ion-interaction model parameters converted from the extended ion-interaction model of Archer [29], and solubility information reported by Linke [22], with temperature independent optimal exponential coefficient $\alpha_1^p = 1.43 \text{ kg}^{1/2} \cdot \text{mol}^{-1/2}$ and maximum ionic strengths $I_{\max}(T)$ equal to those of the saturated solutions ^a

T/K	f^a	a_w^a	g_{\pm}^a	K_{sp}^a	$I_{\text{sat}}^b / \text{m}^\circ$	Solid Phase ^b
273.15	0.72121	0.80007	0.26776	5.2827	8.584	$\text{NaNO}_3(\text{s})$
283.15	0.74603	0.77560	0.29196	7.6186	9.454	$\text{NaNO}_3(\text{s})$
293.15	0.76491	0.75152	0.31221	$1.0472 \cdot 10$	10.365	$\text{NaNO}_3(\text{s})$
298.15	0.77236	0.73961	0.32085	$1.2094 \cdot 10$	10.839	$\text{NaNO}_3(\text{s})$
303.15	0.77857	0.72778	0.32849	$1.3844 \cdot 10$	11.327	$\text{NaNO}_3(\text{s})$
313.15	0.78746	0.70436	0.34077	$1.7718 \cdot 10$	12.352	$\text{NaNO}_3(\text{s})$
323.15	0.79186	0.68125	0.34905	$2.2051 \cdot 10$	13.453	$\text{NaNO}_3(\text{s})$
333.15	0.79197	0.65845	0.35334	$2.6773 \cdot 10$	14.644	$\text{NaNO}_3(\text{s})$
353.15	0.77992	0.61375	0.35019	$3.7010 \cdot 10$	17.372	$\text{NaNO}_3(\text{s})$
373.15	0.75272	0.57039	0.33278	$4.7456 \cdot 10$	20.701	$\text{NaNO}_3(\text{s})$
393.15	0.71312	0.52870	0.30444	$5.7027 \cdot 10$	24.805	$\text{NaNO}_3(\text{s})$
423.15	0.63419	0.46971	0.24966	$6.8163 \cdot 10$	33.069	$\text{NaNO}_3(\text{s})$

^a These properties are based on the derived standard Pitzer model parameters given in table 8 for constant optimal $\alpha_1^p = 1.43 \text{ kg}^{1/2} \cdot \text{mol}^{-1/2}$. ^b Values of $I_{\text{sat}}(T)$, used to evaluate the coefficients of matrix equation (31), were calculated from the information tabulated by Linke [22] from the studies of Berkeley and Chretien, after smoothing the combined

results as a function of temperature.

Figure Captions

FIGURE 1. Variation, with respect to a_1^P , of the root mean square error (RMSE) $E_{I,T}$ for osmotic coefficient differences between the extended Archer and standard Pitzer models for $\text{Ca}(\text{NO}_3)_3(\text{aq})$ and solubility limited maximum ionic strength. \circ , RMSE for model conversion only; \diamond , RMSE for model conversion plus 4-term temperature fitting function; \bullet , RMSE for model conversion plus 7-term temperature fitting function.

FIGURE 2. Variation, with respect to a_1^P , of the root mean square error (RMSE) $E_{I,T}$ for osmotic coefficient differences between the extended Archer and standard Pitzer models for $\text{Ca}(\text{NO}_3)_2(\text{aq})$ and maximum ionic strength of $I_{\max} = 68.5 \text{ mol}\cdot\text{kg}^{-1}$. \circ , RMSE for model conversion only; \diamond , RMSE for model conversion plus 4-term temperature fitting function; \bullet , RMSE for model conversion plus 7-term temperature fitting function.

FIGURE 3. Comparison of osmotic coefficients calculated using the extended Archer and standard Pitzer models for $\text{Ca}(\text{NO}_3)_2(\text{aq})$ and solubility limited maximum ionic strength with $a_1^P = 0.20 \text{ kg}^{1/2}\cdot\text{mol}^{-1/2}$. \circ , standard Pitzer model at $T = 298.15 \text{ K}$; \bullet , extended Archer model at $T = 298.15 \text{ K}$; \triangle , standard Pitzer model at $T = 353.15 \text{ K}$; σ , extended Archer model at $T = 353.15 \text{ K}$; \square , standard Pitzer model at $T = 423.15 \text{ K}$; \blacksquare , extended Archer model at $T = 423.15 \text{ K}$.

FIGURE 4. Comparison of osmotic coefficients calculated using the extended Archer and standard Pitzer models for $\text{Ca}(\text{NO}_3)_2(\text{aq})$ and solubility limited maximum ionic strength with optimum value of $a_1^P = 0.87 \text{ kg}^{1/2}\cdot\text{mol}^{-1/2}$. \circ , standard Pitzer model at $T = 298.15 \text{ K}$; \bullet , extended Archer model at $T = 298.15 \text{ K}$; \triangle , standard Pitzer model at $T = 353.15$

K; σ , extended Archer model at $T = 353.15$ K; \square , standard Pitzer model at $T = 423.15$ K; \blacksquare , extended Archer model at $T = 423.15$ K.

FIGURE 5. Comparison of osmotic coefficients calculated using the extended Archer and standard Pitzer models for $\text{Ca}(\text{NO}_3)_2(\text{aq})$ and solubility limited maximum ionic strength with $a_1^p = 2.0 \text{ kg}^{1/2} \cdot \text{mol}^{-1/2}$. \circ , standard Pitzer model at $T = 298.15$ K; \bullet , extended Archer model at $T = 298.15$ K; \triangle , standard Pitzer model at $T = 353.15$ K; σ , extended Archer model at $T = 353.15$ K; \square , standard Pitzer model at $T = 423.15$ K; \blacksquare , extended Archer model at $T = 423.15$ K.

FIGURE 6. Comparison of Osmotic coefficients calculated using the extended Archer and standard Pitzer models for $\text{Ca}(\text{NO}_3)_2(\text{aq})$ and maximum ionic strength of $I_{\text{max}} = 68.5 \text{ mol} \cdot \text{kg}^{-1}$ with $a_1^p = 0.20 \text{ kg}^{1/2} \cdot \text{mol}^{-1/2}$. \circ , standard Pitzer model at $T = 298.15$ K; \bullet , extended Archer model at $T = 298.15$ K; \triangle , standard Pitzer model at $T = 353.15$ K; σ , extended Archer model at $T = 353.15$ K; \square , standard Pitzer model at $T = 423.15$ K; \blacksquare , extended Archer model at $T = 423.15$ K.

FIGURE 7. Comparison of osmotic coefficients calculated using the extended Archer and standard Pitzer models for $\text{Ca}(\text{NO}_3)_2(\text{aq})$ and maximum ionic strength of $I_{\text{max}} = 68.5 \text{ mol} \cdot \text{kg}^{-1}$ with optimum value of $a_1^p = 0.87 \text{ kg}^{1/2} \cdot \text{mol}^{-1/2}$. \circ , standard Pitzer model at $T = 298.15$ K; \bullet , extended Archer model at $T = 298.15$ K; \triangle , standard Pitzer model at $T = 353.15$ K; σ , extended Archer model at $T = 353.15$ K; \square , standard Pitzer model at $T = 423.15$ K; \blacksquare , extended Archer model at $T = 423.15$ K.

FIGURE 8. Comparison of osmotic coefficients calculated using the extended Archer and standard Pitzer models for $\text{Ca}(\text{NO}_3)_2(\text{aq})$ and maximum ionic strength of $I_{\text{max}} = 68.5 \text{ mol}\cdot\text{kg}^{-1}$ with $a_1^{\text{P}} = 2.0 \text{ kg}^{1/2}\cdot\text{mol}^{-1/2}$. \circ , standard Pitzer model at $T = 298.15 \text{ K}$; \bullet , extended Archer model at $T = 298.15 \text{ K}$; \triangle , standard Pitzer model at $T = 353.15 \text{ K}$; σ , extended Archer model at $T = 353.15 \text{ K}$; \square , standard Pitzer model at $T = 423.15 \text{ K}$; \blacksquare , extended Archer model at $T = 423.15 \text{ K}$.

FIGURE 9. Variation, with respect to a_1^{P} , of the root mean square error (RMSE) $E_{\text{I,T}}$ for osmotic coefficient between the Archer and standard Pitzer models for $\text{NaNO}_3(\text{aq})$ and solubility limited maximum ionic strength. \circ , RMSE for model conversion only; \diamond , RMSE for model conversion plus 4-term temperature fitting function; \bullet , RMSE for model conversion plus 7-term temperature fitting function.

FIGURE 10. Comparison of osmotic coefficients calculated using the Archer and standard Pitzer models for $\text{NaNO}_3(\text{aq})$ and solubility limited maximum ionic strength with $a_1^{\text{P}} = 0.20 \text{ kg}^{1/2}\cdot\text{mol}^{-1/2}$. \circ , standard Pitzer model at $T = 298.15 \text{ K}$; \bullet , Archer model at $T = 298.15 \text{ K}$; \triangle , standard Pitzer model at $T = 353.15 \text{ K}$; σ , Archer model at $T = 353.15 \text{ K}$; \square , standard Pitzer model at $T = 423.15 \text{ K}$; \blacksquare , Archer model at $T = 423.15 \text{ K}$.

FIGURE 11. Comparison of osmotic coefficients calculated using the Archer and standard Pitzer models for $\text{NaNO}_3(\text{aq})$ and solubility limited maximum ionic strength with optimum value of $a_1^{\text{P}} = 1.43 \text{ kg}^{1/2}\cdot\text{mol}^{-1/2}$. \circ , standard Pitzer model at $T = 298.15 \text{ K}$; \bullet , Archer model at $T = 298.15 \text{ K}$; \triangle , standard Pitzer model at $T = 353.15 \text{ K}$; σ ,

Archer model at $T = 353.15$ K; \square , standard Pitzer model at $T = 423.15$ K; \blacksquare , Archer model at $T = 423.15$ K.

FIGURE 12. Comparison of osmotic coefficients calculated using the Archer and standard Pitzer models for $\text{NaNO}_3(\text{aq})$ and solubility limited maximum ionic strength with $a_1^p = 2.0 \text{ kg}^{1/2} \cdot \text{mol}^{-1/2}$. \circ , standard Pitzer model at $T = 298.15$ K; \bullet , Archer model at $T = 298.15$ K; \triangle , standard Pitzer model at $T = 353.15$ K; σ , Archer model at $T = 353.15$ K; \square , standard Pitzer model at $T = 423.15$ K; \blacksquare , Archer model at $T = 423.15$ K.

FIGURE 13. Temperature function fits to $b_{M,X}^{(0,P)}$ values of the standard Pitzer model for $\text{Ca}(\text{NO}_3)_2(\text{aq})$ for solubility limited maximum ionic strength and optimum value of $a_1^p = 0.87 \text{ kg}^{1/2} \cdot \text{mol}^{-1/2}$. \bullet , values of $b_{M,X}^{(0,P)}$ from model conversion; \square , values of $b_{M,X}^{(0,P)}$ from 4-term temperature function; \circ , values of $b_{M,X}^{(0,P)}$ from 7-term temperature function.

FIGURE 14. Temperature function fits to $b_{M,X}^{(1,P)}$ values of the standard Pitzer model for $\text{Ca}(\text{NO}_3)_2(\text{aq})$ for solubility limited maximum ionic strength and optimum value of $a_1^p = 0.87 \text{ kg}^{1/2} \cdot \text{mol}^{-1/2}$. \bullet , values of $b_{M,X}^{(1,P)}$ from model conversion; \square , values of $b_{M,X}^{(1,P)}$ calculated with the 4-term temperature function; \circ , values of $b_{M,X}^{(1,P)}$ calculated with the 7-term temperature function.

FIGURE 15. Temperature function fits to $C_{M,X}^{(f,P)}$ values of the standard Pitzer model for $\text{Ca}(\text{NO}_3)_2(\text{aq})$ for solubility limited maximum ionic strength and optimum value of $a_1^p = 0.87 \text{ kg}^{1/2} \cdot \text{mol}^{-1/2}$. \bullet , values of $C_{M,X}^{(f,P)}$ calculated with the model conversion; \square , values of

$C_{M,X}^{(f,P)}$ calculated with the 4-term temperature function; ○, values of $C_{M,X}^{(f,P)}$ from 7-term temperature function.

FIGURE 16. Temperature function fits to $b_{M,X}^{(0,P)}$ values of the standard Pitzer model for $\text{NaNO}_3(\text{aq})$ for solubility limited maximum ionic strength and optimum value of $a_1^P = 1.43 \text{ kg}^{1/2} \cdot \text{mol}^{-1/2}$. ●, values of $b_{M,X}^{(0,P)}$ from model conversion; □, values of $b_{M,X}^{(0,P)}$ from 4-term temperature function; ○, values of $b_{M,X}^{(0,P)}$ from 7-term temperature function.

FIGURE 17. Temperature function fits to $b_{M,X}^{(1,P)}$ values of the standard Pitzer model for $\text{NaNO}_3(\text{aq})$ for solubility limited maximum ionic strength and optimum value of $a_1^P = 1.43 \text{ kg}^{1/2} \cdot \text{mol}^{-1/2}$. ●, values of $b_{M,X}^{(1,P)}$ from model conversion; □, values of $b_{M,X}^{(1,P)}$ from 4-term temperature function; ○, values of $b_{M,X}^{(1,P)}$ from 7-term temperature function.

FIGURE 18. Temperature function fits to $C_{M,X}^{(f,P)}$ values of the standard Pitzer model for $\text{NaNO}_3(\text{aq})$ for solubility limited maximum ionic strength and $a_1^P = 1.43 \text{ kg}^{1/2} \cdot \text{mol}^{-1/2}$. ●, values of $C_{M,X}^{(f,P)}$ from model conversion; □, values of $C_{M,X}^{(f,P)}$ from 4-term temperature function; ○, values of $C_{M,X}^{(f,P)}$ from 7-term temperature function.

FIGURE 19. Comparison of osmotic coefficients calculated using the extended Archer and standard Pitzer models for $\text{Ca}(\text{NO}_3)_2(\text{aq})$, solubility limited maximum ionic strength, and temperature-dependent optimal exponential coefficient $a_1^P(T)$. ○, standard Pitzer model at $T = 298.15 \text{ K}$; ●, extended Archer model at $T = 298.15 \text{ K}$; △, standard Pitzer

model at $T = 353.15$ K; σ , extended Archer model at $T = 353.15$ K; \square , standard Pitzer model at $T = 423.15$ K; \blacksquare , extended Archer model at $T = 423.15$ K.

FIGURE 20. Comparison of osmotic coefficients calculated using the extended Archer and standard Pitzer models for $\text{NaNO}_3(\text{aq})$, solubility limited maximum ionic strength, and temperature-dependent optimal exponential coefficient $a_1^p(T)$. \circ , standard Pitzer model at $T = 298.15$ K; \bullet , extended Archer model at $T = 298.15$ K; \triangle , standard Pitzer model at $T = 353.15$ K; σ , extended Archer model at $T = 353.15$ K; \square , standard Pitzer model at $T = 423.15$ K; \blacksquare , extended Archer model at $T = 423.15$ K.

FIGURE 21. Osmotic coefficient f , water activity a_w , and mean activity coefficient g_{\pm} of saturated solutions of $\text{Ca}(\text{NO}_3)_2(\text{aq})$ calculated using the standard Pitzer model with solubility limited maximum ionic strength, $a_1^p = 0.87 \text{ kg}^{1/2} \cdot \text{mol}^{-1/2}$, and 7-term temperature functions. Triangles, solid phase $\text{Ca}(\text{NO}_3)_2 \cdot 4\text{H}_2\text{O}(\text{s})$; squares, solid phase $\text{Ca}(\text{NO}_3)_2 \cdot 3\text{H}_2\text{O}(\text{s})$; circles, solid phase $\text{Ca}(\text{NO}_3)_2(\text{s})$. Top curves f , middle curves g_{\pm} , and bottom curves a_w .

FIGURE 22. Solubility m_{sat} and solubility product K_{sp} of individual solid phases of $\text{Ca}(\text{NO}_3)_2 \cdot n\text{H}_2\text{O}(\text{s})$ calculated using the standard Pitzer model with solubility limited maximum ionic strength, $a_1^p = 0.87 \text{ kg}^{1/2} \cdot \text{mol}^{-1/2}$, and 7-term temperature functions. Circles, solid phase $\text{Ca}(\text{NO}_3)_2 \cdot 4\text{H}_2\text{O}(\text{s})$; squares, solid phase $\text{Ca}(\text{NO}_3)_2 \cdot 3\text{H}_2\text{O}(\text{s})$; diamonds, solid phase $\text{Ca}(\text{NO}_3)_2(\text{s})$; filled symbols, K_{sp} ; open symbols, m_{sat} .

FIGURE 23. Osmotic coefficient f , water activity a_w , and mean activity coefficient g_{\pm} of saturated solutions of $\text{NaNO}_3(\text{aq})$ calculated using the standard Pitzer model with solubility limited maximum ionic strength, $a_1^p = 1.43 \text{ kg}^{1/2} \cdot \text{mol}^{-1/2}$, and 7-term temperature function. \square , f ; \circ , a_w ; \diamond , g_{\pm} .

FIGURE 24. Solubility m_{sat} and solubility product K_{sp} of $\text{NaNO}_3(\text{s})$ calculated using the standard Pitzer model with solubility limited maximum ionic strength, $a_1^p = 1.43 \text{ kg}^{1/2} \cdot \text{mol}^{-1/2}$, and the 7-term temperature function. \square , K_{sp} ; \circ , m_{sat} .

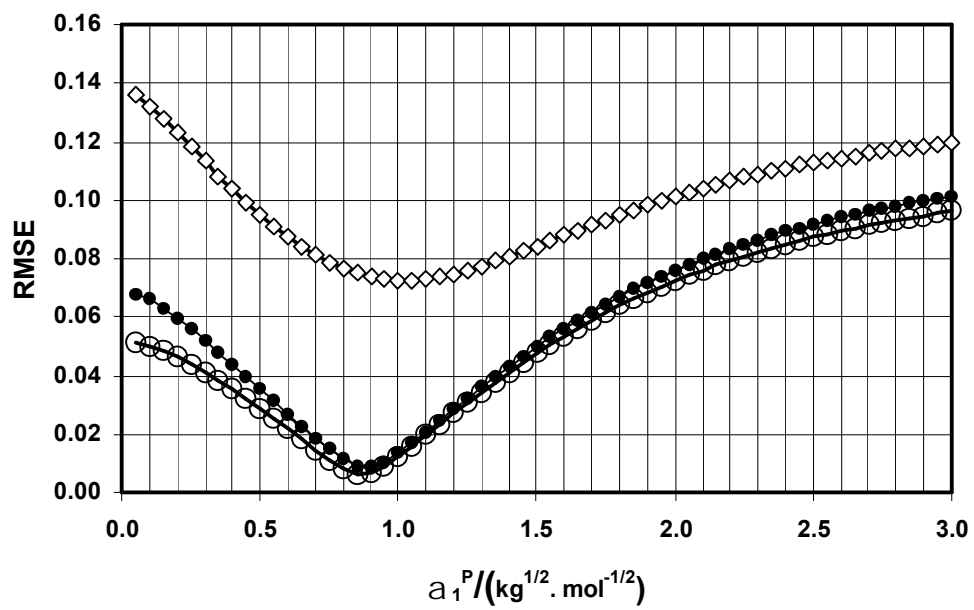


Fig 1

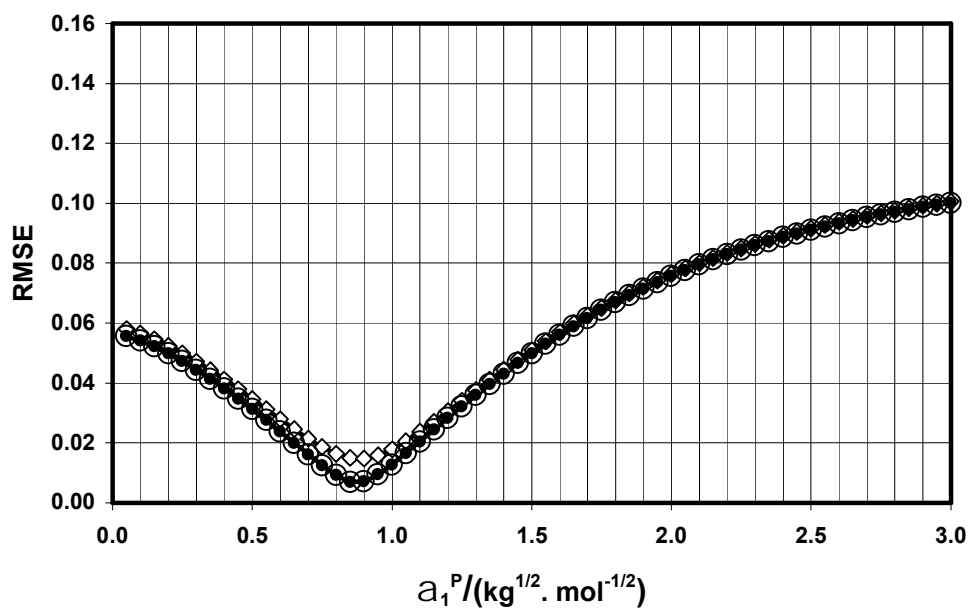


Fig 2

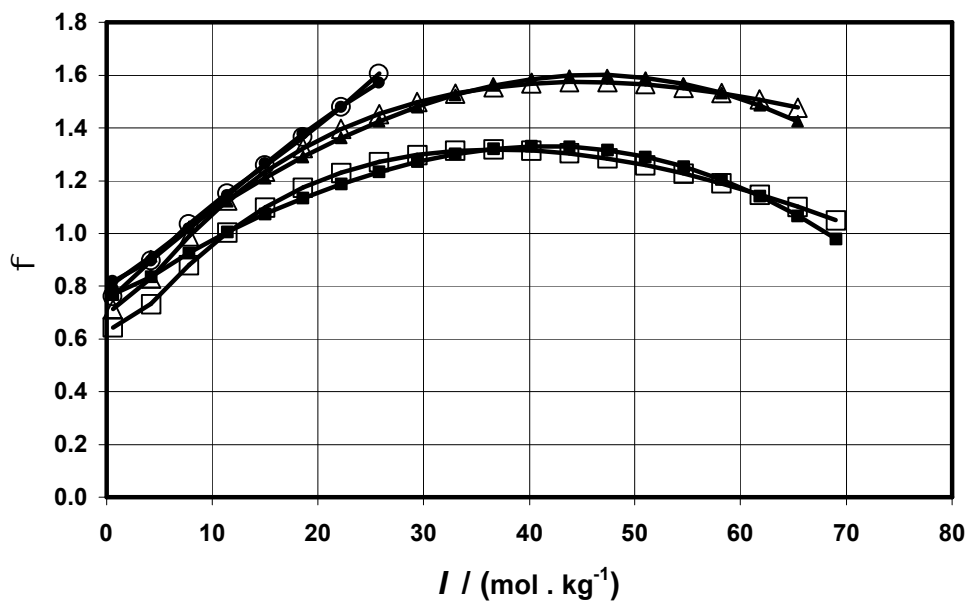


Fig 3

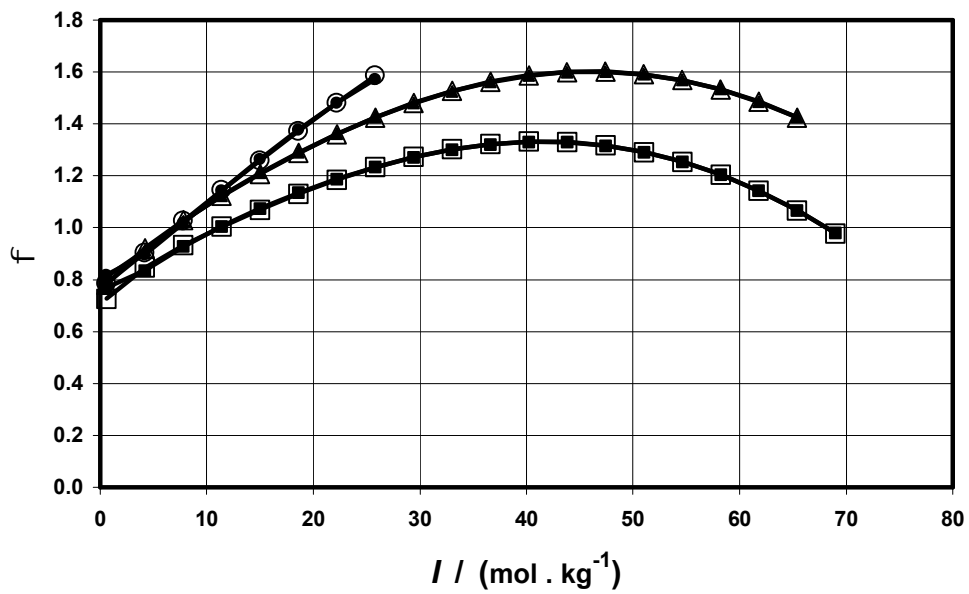


Fig 4

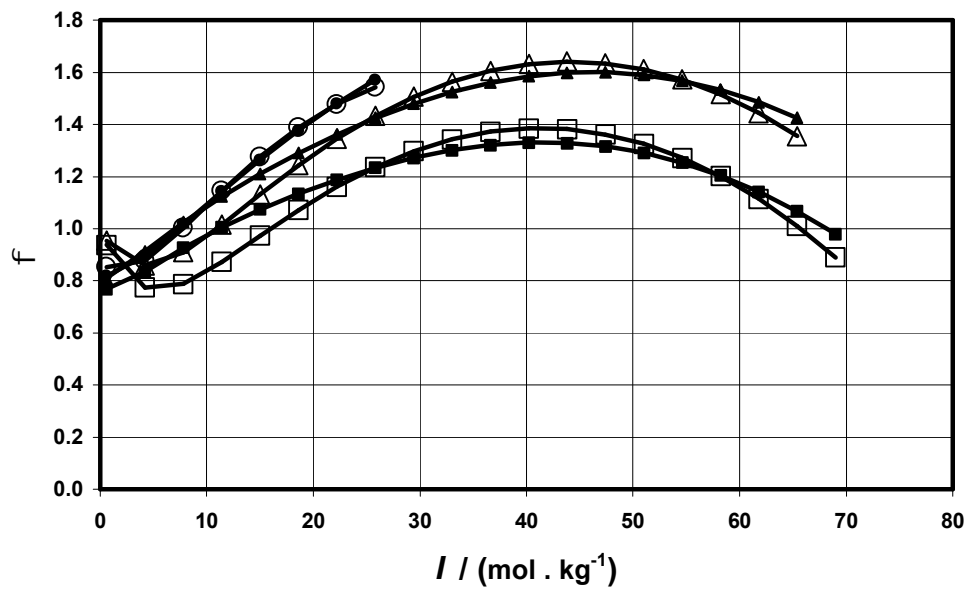


Fig 5

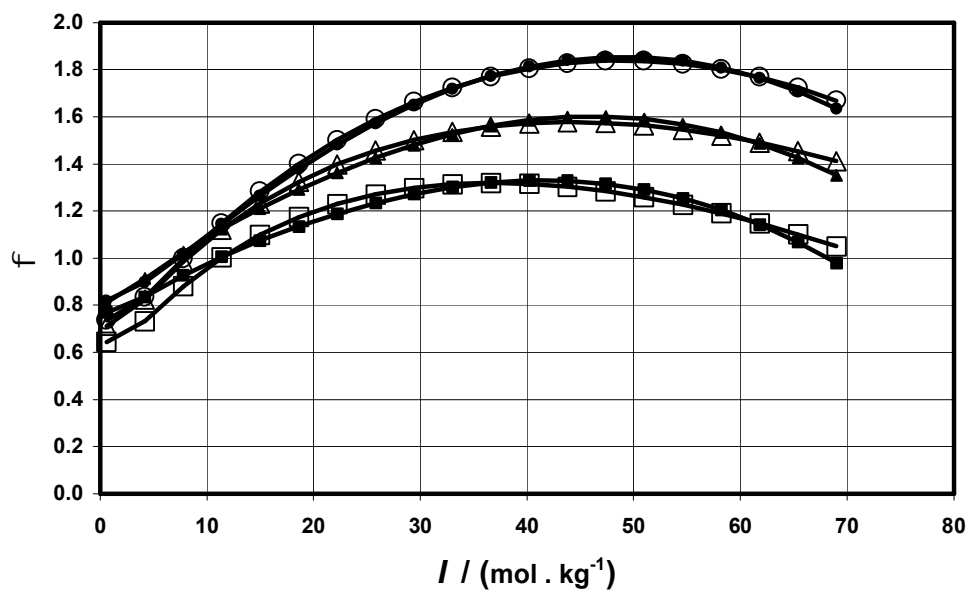


Fig 6

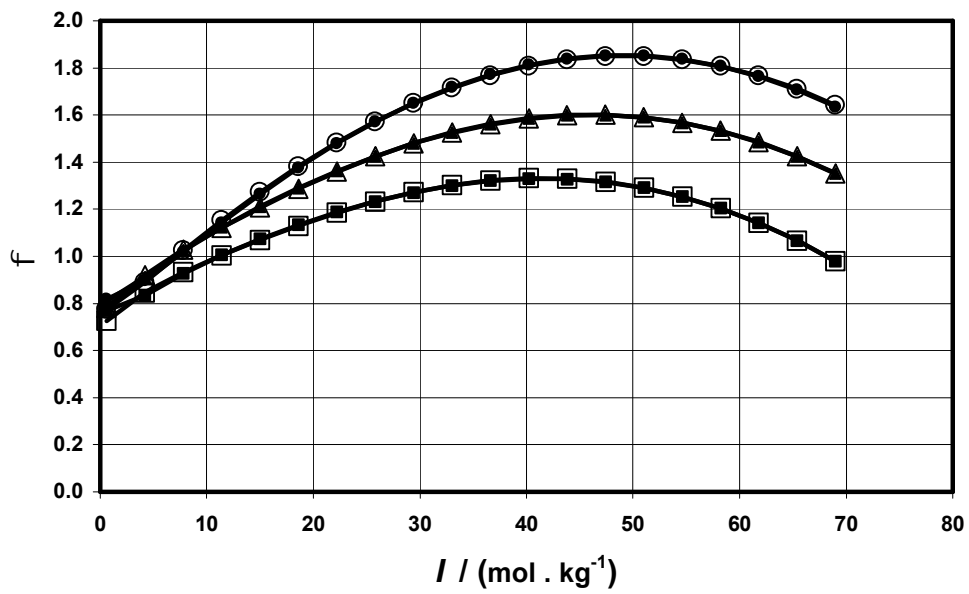


Fig 7

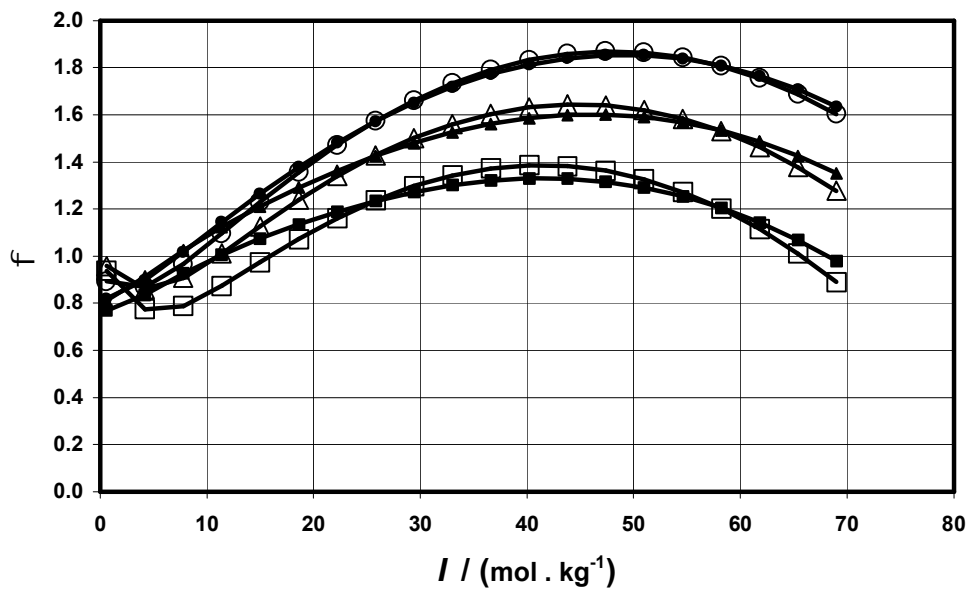


Fig 8

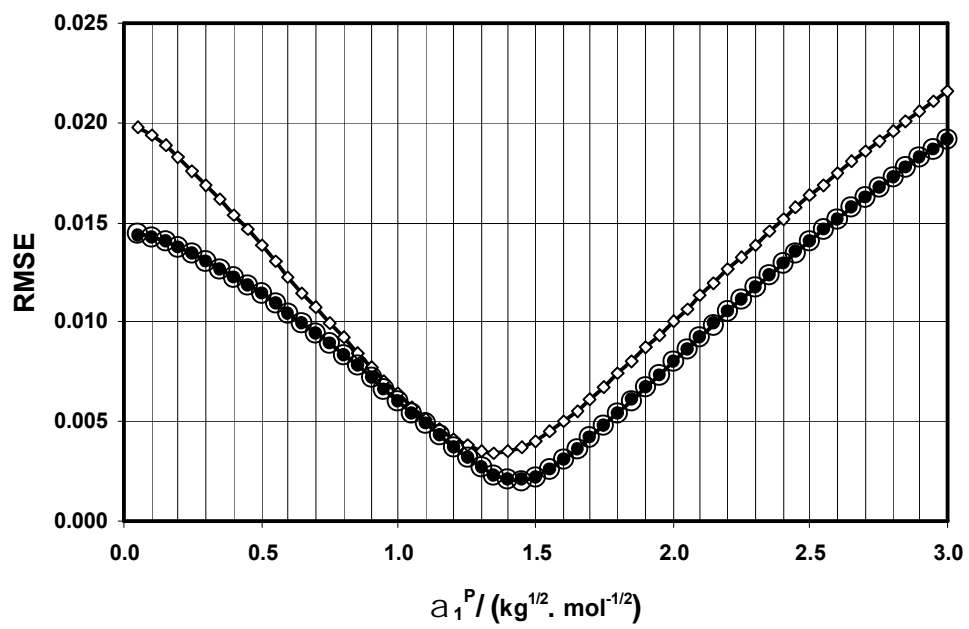


Fig 9

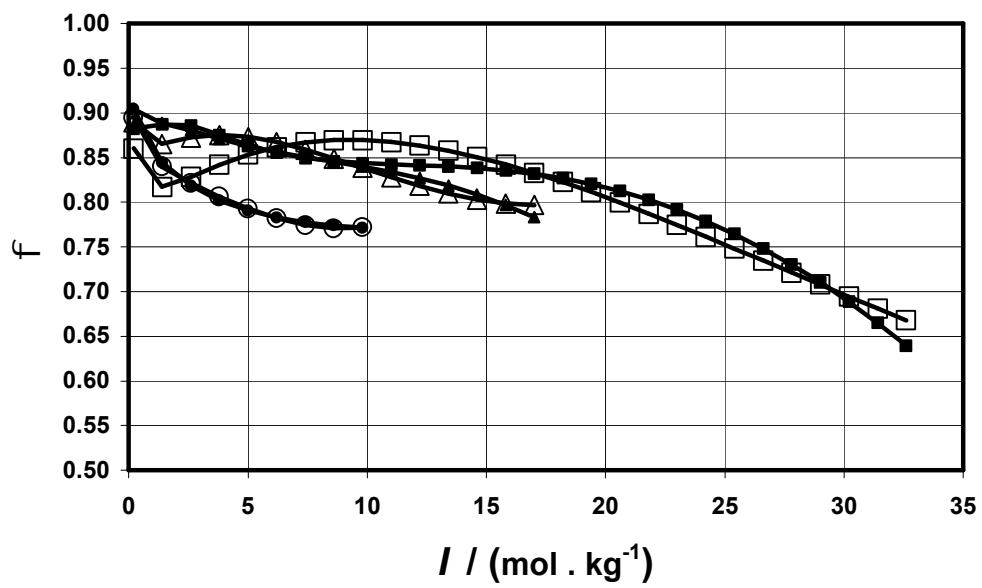


Fig 10

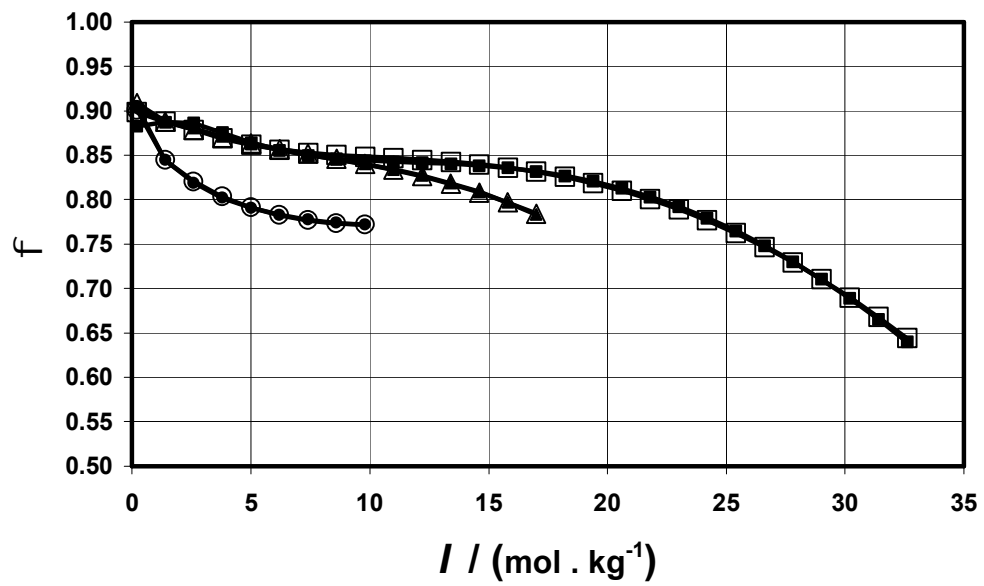


Fig 11

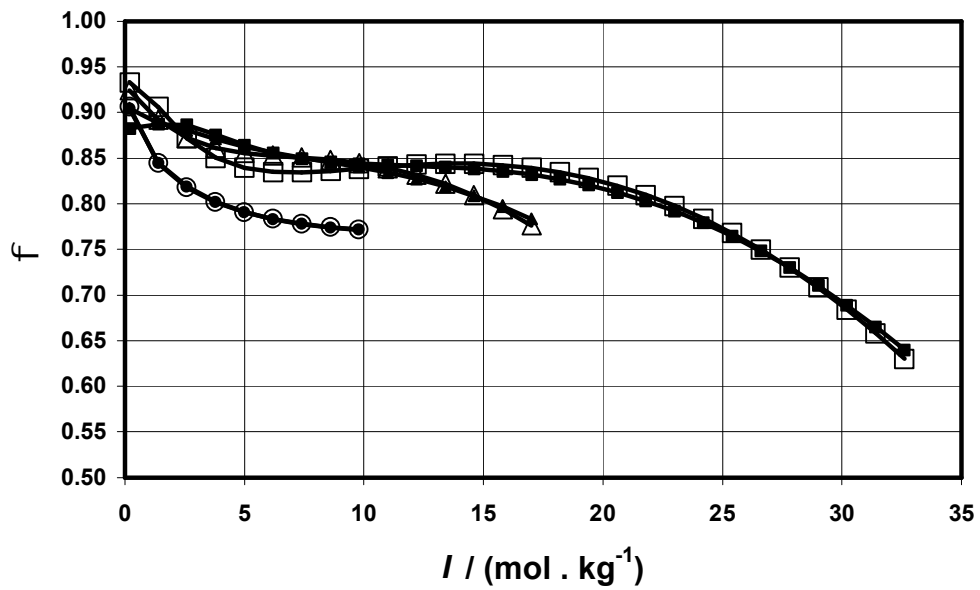


Fig 12

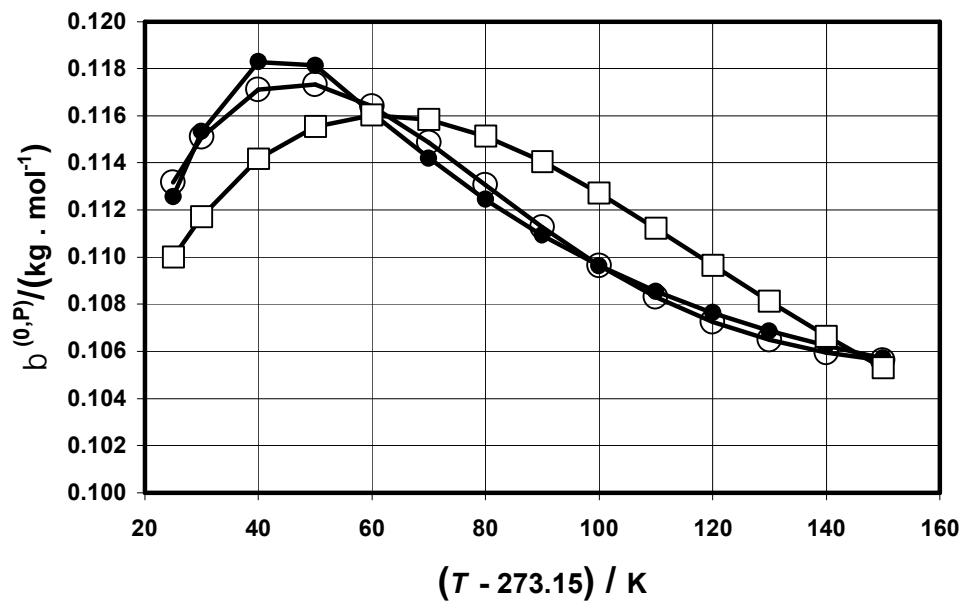


Fig 13

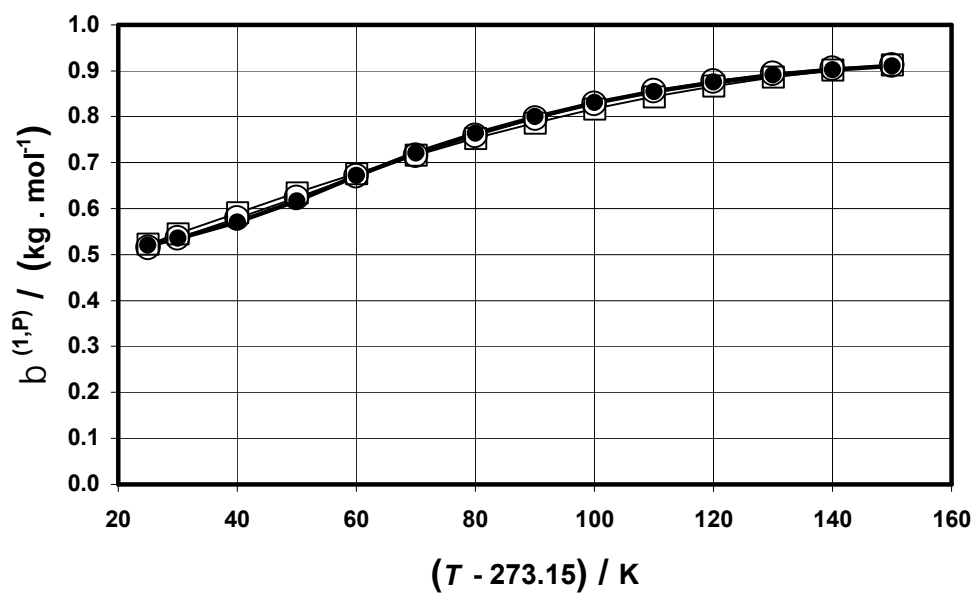


Fig 14

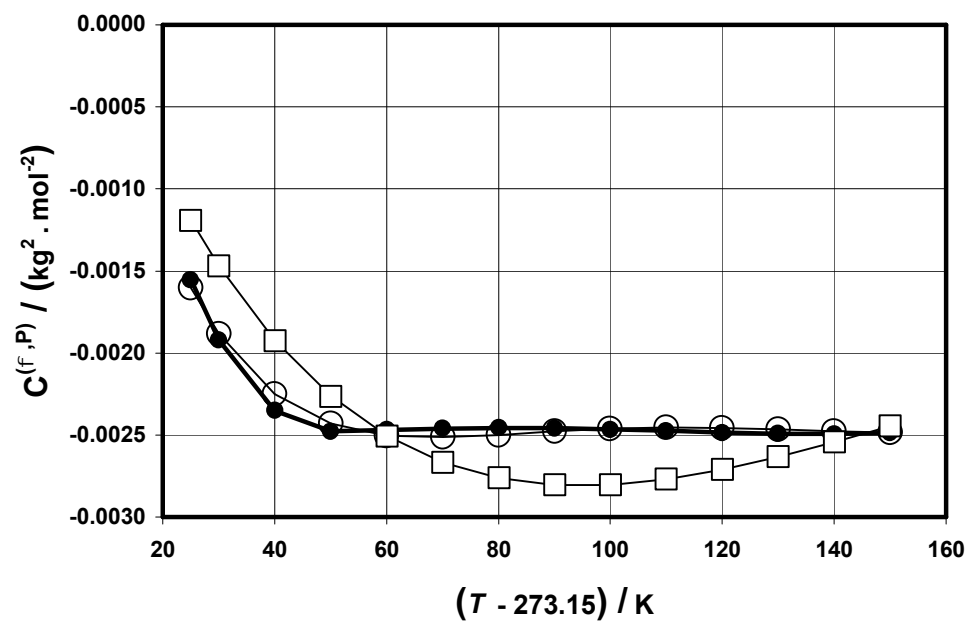


Fig 15

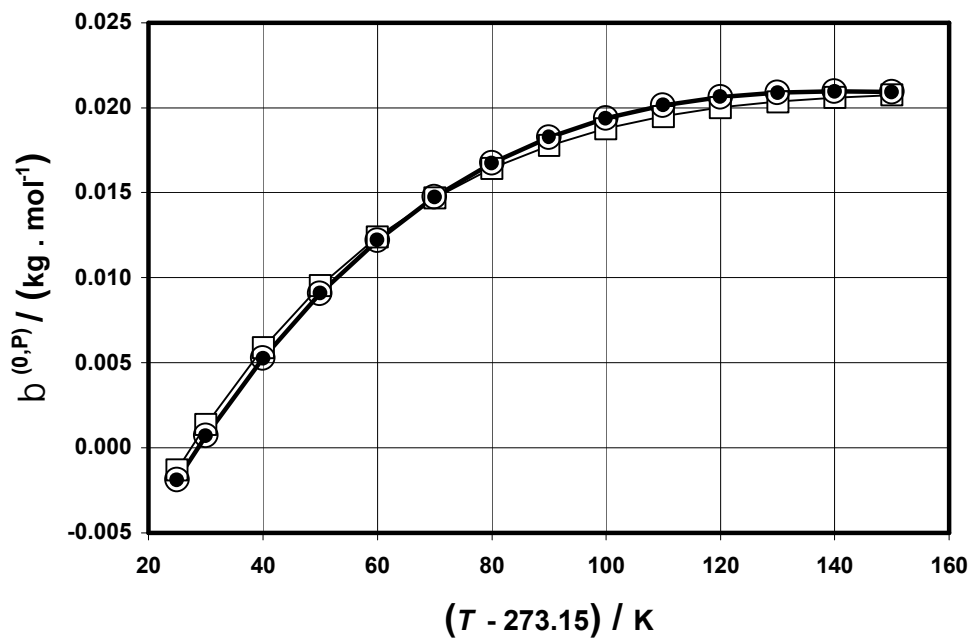


Fig 16

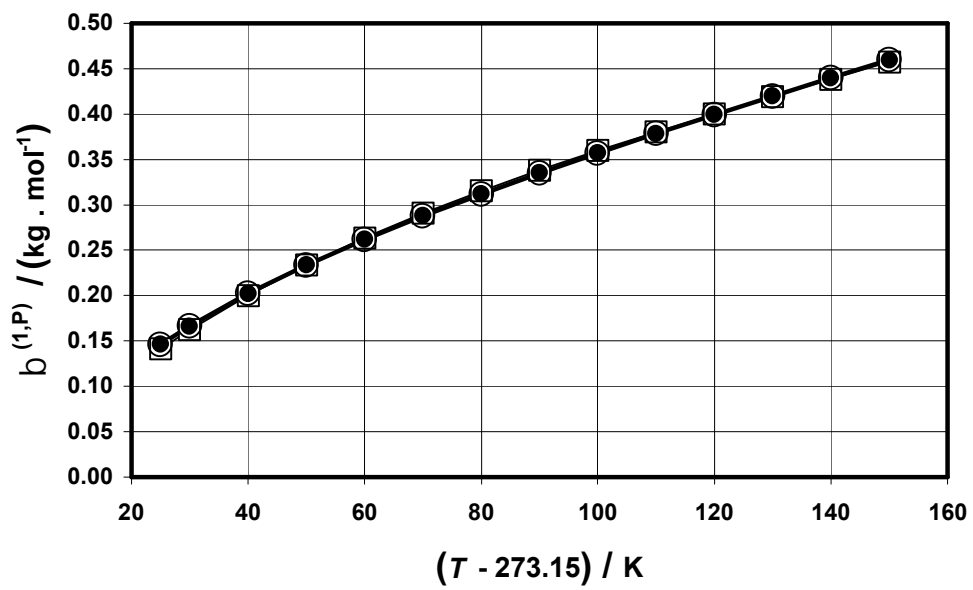


Fig 17

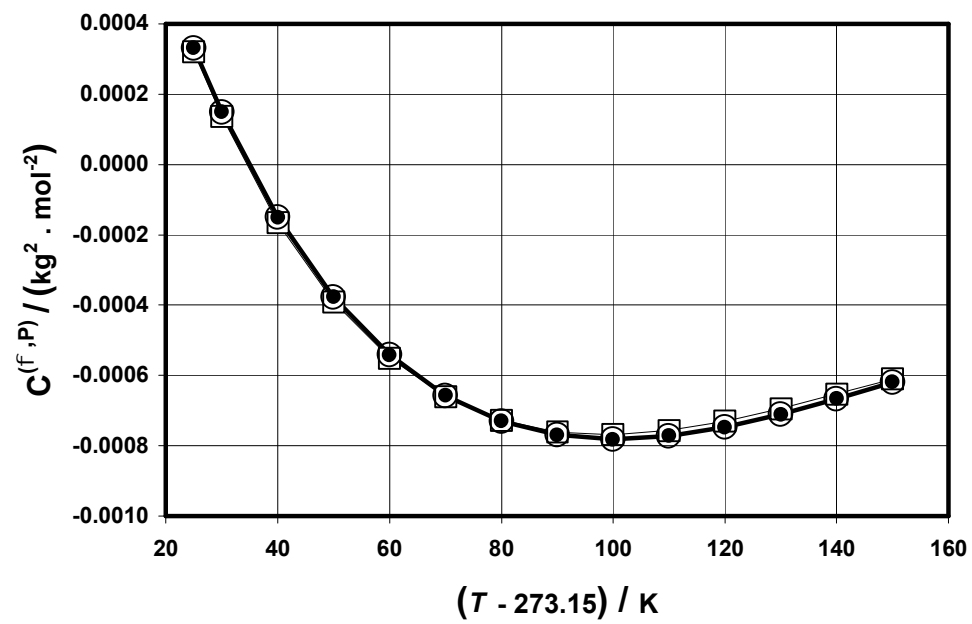


Fig 18

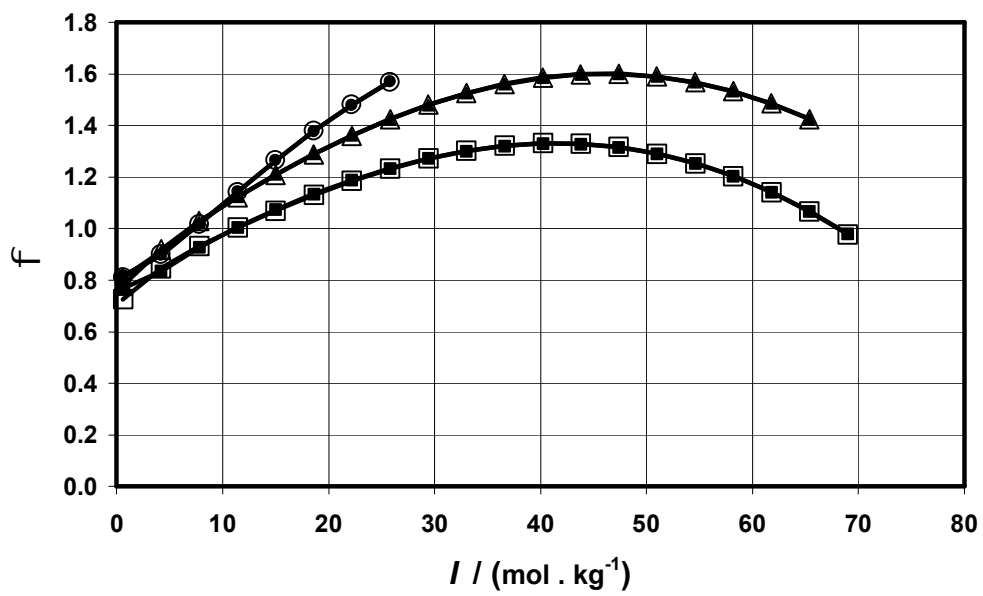


Fig 19

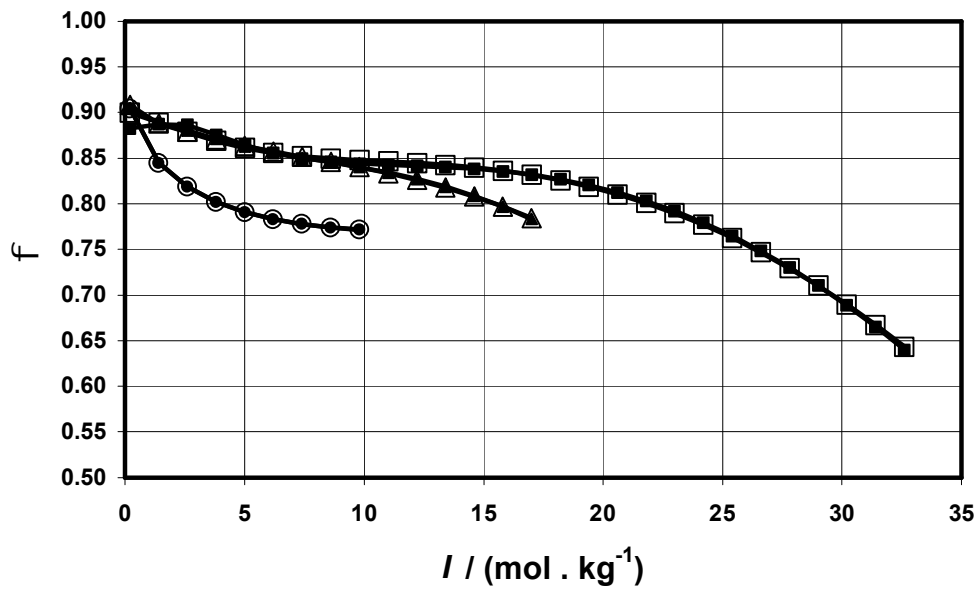


Fig 20

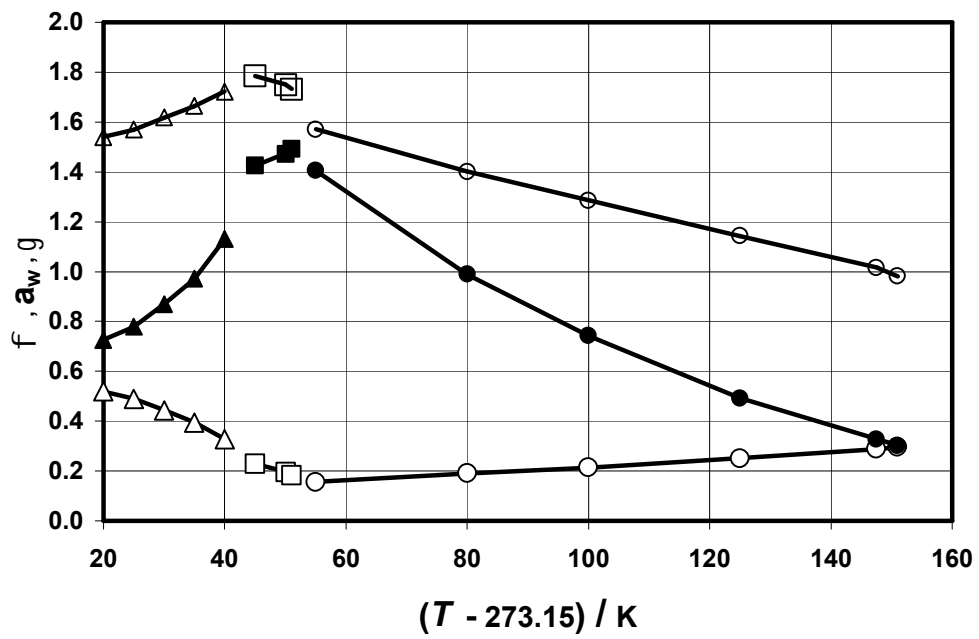


Fig 21

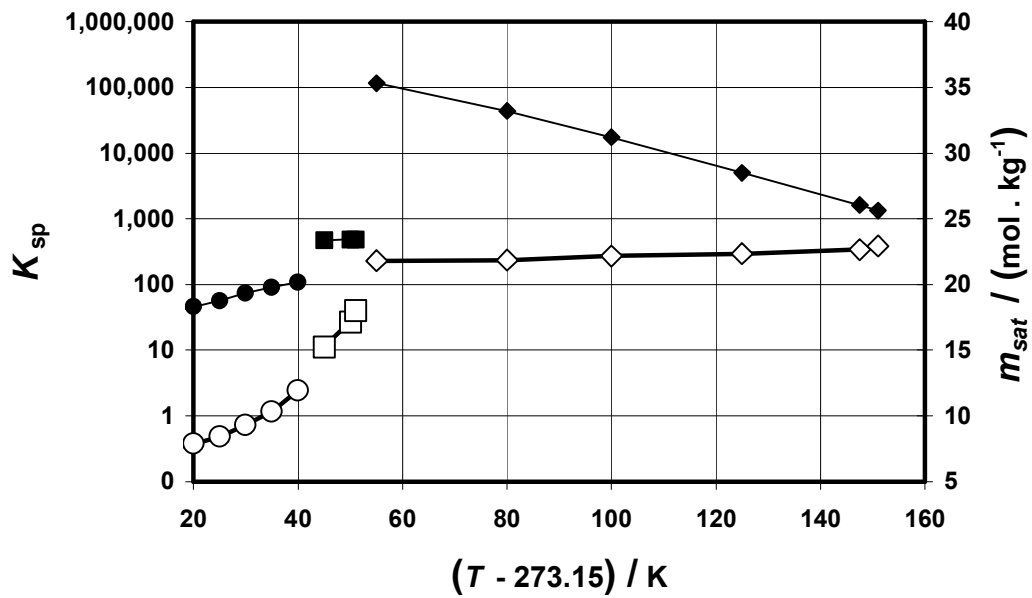


Fig 22

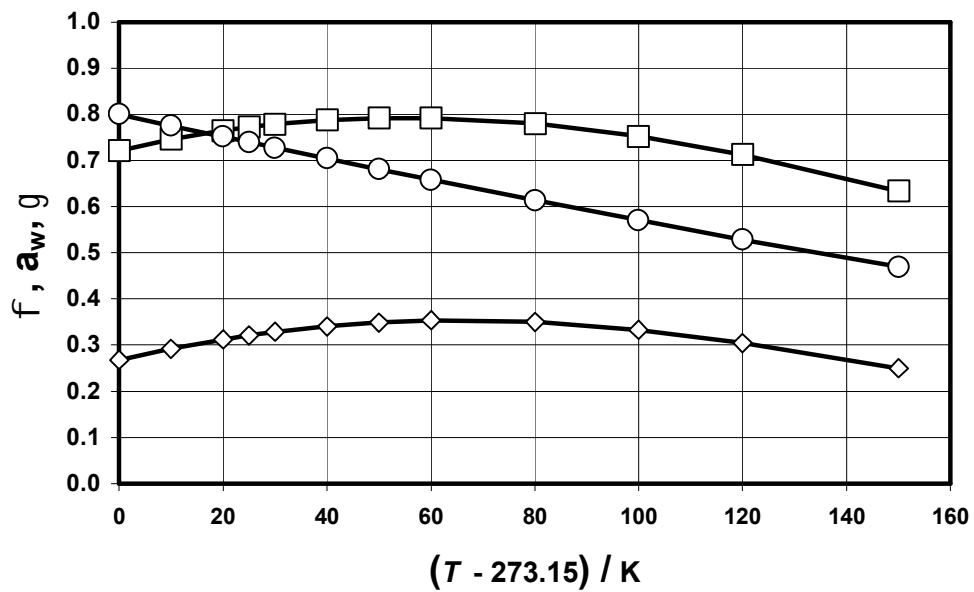


Fig 23

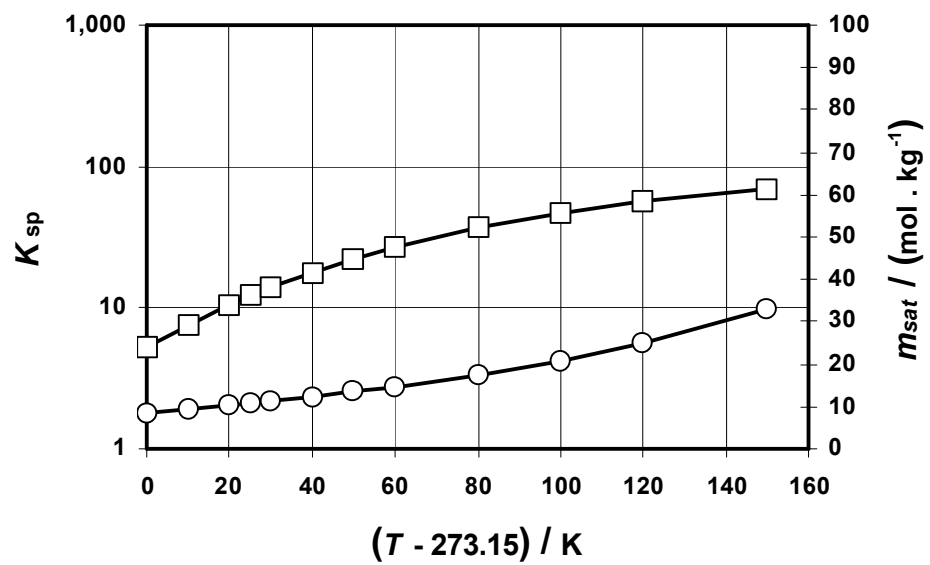


Fig 24

APPENDIX A

Analytical expressions for the elements of the coefficient matrices A_{ij} and C_{ik} , defined by equations (33) and (34), and coefficient matrices A_{nj}^a and C_{nk}^a defined by equations (41) and (42), respectively, can be obtained by substituting the results of expressions (20) – (30), (37), and (38) in these expressions and performing the indicated integrations over the range of ionic strength from $I_{\min} = 0$ to $I_{\max}(T)$. The resulting expressions are given below.

Coefficient Matrix A_{ij}

$$A_{11} = \lambda_3^2 \int_{I_{\min}=0}^{I_{\max}(T)} I^2 dI = \lambda_3^2 I_{\max}^3/3 \quad (A1)$$

$$A_{12} = A_{21} = \lambda_3^2 \int_{I_{\min}=0}^{I_{\max}(T)} I^2 \cdot \exp(-a_1^p I^{1/2}) dI \quad (A2)$$

$$A_{13} = A_{31} = \lambda_3^2 \int_{I_{\min}=0}^{I_{\max}(T)} I^2 \cdot \exp(-a_2^p I^{1/2}) dI \quad (A3)$$

$$A_{14} = A_{41} = \lambda_1 \lambda_3^2 \int_{I_{\min}=0}^{I_{\max}(T)} I^3 dI = \lambda_1 \lambda_3^2 I_{\max}^4/4 \quad (A4)$$

$$A_{22} = \lambda_3^2 \int_{I_{\min}=0}^{I_{\max}(T)} I^2 \cdot \exp(-2 a_1^p I^{1/2}) dI \quad (A5)$$

$$A_{23} = A_{32} = \lambda_3^2 \int_{I_{\min}=0}^{I_{\max}(T)} I^2 \cdot \exp\{-(a_1^p + a_2^p) I^{1/2}\} dI \quad (A6)$$

$$A_{24} = A_{42} = \lambda_1 \lambda_3^2 \int_{I_{\min}=0}^{I_{\max}(\text{T})} I^3 \cdot \exp(-a_1^p I^{1/2}) dI \quad (\text{A7})$$

$$A_{33} = \lambda_3^2 \int_{I_{\min}=0}^{I_{\max}(\text{T})} I^2 \cdot \exp(-2a_2^p I^{1/2}) dI \quad (\text{A8})$$

$$A_{34} = A_{43} = \lambda_1 \lambda_3^2 \int_{I_{\min}=0}^{I_{\max}(\text{T})} I^3 \cdot \exp(-a_2^p I^{1/2}) dI \quad (\text{A9})$$

$$A_{44} = \lambda_1^2 \lambda_3^2 \int_{I_{\min}=0}^{I_{\max}(\text{T})} I^4 dI = \lambda_1^2 \lambda_3^2 I_{\max}^5 / 5 \quad (\text{A10})$$

Coefficient Matrix C_{ik}

$$C_{11} = \lambda_3^2 \int_{I_{\min}=0}^{I_{\max}(\text{T})} I^2 dI = \lambda_3^2 I_{\max}^3 / 3 \quad (\text{A11})$$

$$C_{12} = \lambda_3^2 \int_{I_{\min}=0}^{I_{\max}(\text{T})} I^2 \cdot \exp(-a_1^{\text{EA}} I^{1/2}) dI \quad (\text{A12})$$

$$C_{13} = \lambda_3^2 \int_{I_{\min}=0}^{I_{\max}(\text{T})} I^2 \cdot \exp(-a_2^{\text{EA}} I^{1/2}) dI \quad (\text{A13})$$

$$C_{14} = \lambda_1 \lambda_2 \lambda_3^2 \int_{I_{\min}=0}^{I_{\max}(\text{T})} I^3 dI = \lambda_1 \lambda_2 \lambda_3^2 I_{\max}^4 / 4 \quad (\text{A14})$$

$$C_{15} = \lambda_1 \lambda_2 \lambda_3^2 \int_{I_{\min}=0}^{I_{\max}(\text{T})} I^3 \cdot \exp(-w_1^{\text{EA}} I^{1/2}) dI \quad (\text{A15})$$

$$C_{16} = \lambda_1 \lambda_2 \lambda_3^2 \int_{I_{\min}=0}^{I_{\max}(\text{T})} I^3 \cdot \exp(-w_2^{\text{EA}} I^{1/2}) dI \quad (\text{A16})$$

$$C_{21} = \lambda_3^2 \int_{I_{\min}=0}^{I_{\max}(T)} I^2 \cdot \exp(-a_1^P I^{1/2}) dI \quad (\text{A17})$$

$$C_{22} = \lambda_3^2 \int_{I_{\min}=0}^{I_{\max}(T)} I^2 \cdot \exp\{-(a_1^P + a_1^{\text{EA}})I^{1/2}\} dI \quad (\text{A18})$$

$$C_{23} = \lambda_3^2 \int_{I_{\min}=0}^{I_{\max}(T)} I^2 \cdot \exp\{-(a_1^P + a_2^{\text{EA}})I^{1/2}\} dI \quad (\text{A19})$$

$$C_{24} = \lambda_1 \lambda_2 \lambda_3^2 \int_{I_{\min}=0}^{I_{\max}(T)} I^3 \cdot \exp(-a_1^P I^{1/2}) dI$$

(A20)

$$C_{25} = \lambda_1 \lambda_2 \lambda_3^2 \int_{I_{\min}=0}^{I_{\max}(T)} I^3 \cdot \exp\{-(a_1^P + w_1^{\text{EA}})I^{1/2}\} dI \quad (\text{A21})$$

$$C_{26} = \lambda_1 \lambda_2 \lambda_3^2 \int_{I_{\min}=0}^{I_{\max}(T)} I^3 \cdot \exp\{-(a_1^P + w_2^{\text{EA}})I^{1/2}\} dI \quad (\text{A22})$$

$$C_{31} = \lambda_3^2 \int_{I_{\min}=0}^{I_{\max}(T)} I^2 \cdot \exp(-a_2^P I^{1/2}) dI \quad (\text{A23})$$

$$C_{32} = \lambda_3^2 \int_{I_{\min}=0}^{I_{\max}(T)} I^2 \cdot \exp\{-(a_2^P + a_1^{\text{EA}})I^{1/2}\} dI \quad (\text{A24})$$

$$C_{33} = \lambda_3^2 \int_{I_{\min}=0}^{I_{\max}(T)} I^2 \cdot \exp\{-(a_2^P + a_2^{\text{EA}})I^{1/2}\} dI \quad (\text{A25})$$

$$C_{34} = \lambda_1 \lambda_2 \lambda_3^2 \int_{I_{\min}=0}^{I_{\max}(T)} I^3 \cdot \exp(-a_2^P I^{1/2}) dI$$

(A26)

$$C_{35} = \lambda_1 \lambda_2 \lambda_3^2 \int_{I_{\min}=0}^{I_{\max}(\tau)} I^3 \cdot \exp\{-(a_2^p + w_1^{\text{EA}})I^{1/2}\} dI \quad (\text{A27})$$

$$C_{36} = \lambda_1 \lambda_2 \lambda_3^2 \int_{I_{\min}=0}^{I_{\max}(\tau)} I^3 \cdot \exp\{-(a_2^p + w_2^{\text{EA}})I^{1/2}\} dI \quad (\text{A28})$$

$$C_{41} = \lambda_1 \lambda_3^2 \int_{I_{\min}=0}^{I_{\max}(\tau)} I^3 dI = \lambda_1 \lambda_3^2 I_{\max}^4 / 4 \quad (\text{A29})$$

$$C_{42} = \lambda_1 \lambda_3^2 \int_{I_{\min}=0}^{I_{\max}(\tau)} I^3 \cdot \exp(-a_1^{\text{EA}} I^{1/2}) dI \quad (\text{A30})$$

$$C_{43} = \lambda_1 \lambda_3^2 \int_{I_{\min}=0}^{I_{\max}(\tau)} I^3 \cdot \exp(-a_2^{\text{EA}} I^{1/2}) dI \quad (\text{A31})$$

$$C_{44} = \lambda_1^2 \lambda_2 \lambda_3^2 \int_{I_{\min}=0}^{I_{\max}(\tau)} I^4 dI = \lambda_1^2 \lambda_2 \lambda_3^2 I_{\max}^5 / 5 \quad (\text{A32})$$

$$C_{45} = \lambda_1^2 \lambda_2 \lambda_3^2 \int_{I_{\min}=0}^{I_{\max}(\tau)} I^4 \cdot \exp(-w_1^{\text{EA}} I^{1/2}) dI \quad (\text{A33})$$

$$C_{46} = \lambda_1^2 \lambda_2 \lambda_3^2 \int_{I_{\min}=0}^{I_{\max}(\tau)} I^4 \cdot \exp(-w_2^{\text{EA}} I^{1/2}) dI \quad (\text{A34})$$

Coefficient Matrix \mathbf{A}_{nj}^a

$$A_{11}^a = \lambda_3^2 \int_{I_{\min}=0}^{I_{\max}(\tau)} I^{5/2} \cdot \exp(-a_1^p I^{1/2}) dI \quad (\text{A35})$$

$$A_{12}^a = \lambda_3^2 \int_{I_{\min}=0}^{I_{\max}(\tau)} I^{5/2} \cdot \exp(-2a_1^p I^{1/2}) dI \quad (\text{A36})$$

$$A_{13}^a = \lambda_3^2 \int_{I_{\min}=0}^{I_{\max}(T)} I^{5/2} \cdot \exp\{-(a_1^p + a_2^p)I^{1/2}\} dI \quad (\text{A37})$$

$$A_{14}^a = \lambda_1 \lambda_3^2 \int_{I_{\min}=0}^{I_{\max}(T)} I^{7/2} \cdot \exp(-a_1^p I^{1/2}) dI \quad (\text{A38})$$

$$A_{21}^a = \lambda_3^2 \int_{I_{\min}=0}^{I_{\max}(T)} I^{5/2} \cdot \exp(-a_2^p I^{1/2}) dI \quad (\text{A39})$$

$$A_{22}^a = \lambda_3^2 \int_{I_{\min}=0}^{I_{\max}(T)} I^{5/2} \cdot \exp\{-(a_1^p + a_2^p)I^{1/2}\} dI \quad (\text{A40})$$

$$A_{23}^a = \lambda_3^2 \int_{I_{\min}=0}^{I_{\max}(T)} I^{5/2} \cdot \exp(-2a_2^p I^{1/2}) dI$$

(A41)

$$A_{24}^a = \lambda_1 \lambda_3^2 \int_{I_{\min}=0}^{I_{\max}(T)} I^{7/2} \cdot \exp(-a_2^p I^{1/2}) dI \quad (\text{A42})$$

Coefficient Matrix C_{nk}^a

$$C_{11}^a = \lambda_3^2 \int_{I_{\min}=0}^{I_{\max}(T)} I^{5/2} \cdot \exp(-a_1^p I^{1/2}) dI \quad (\text{A43})$$

$$C_{12}^a = \lambda_3^2 \int_{I_{\min}=0}^{I_{\max}(T)} I^{5/2} \cdot \exp\{-(a_1^p + a_1^{EA})I^{1/2}\} dI \quad (\text{A44})$$

$$C_{13}^a = \lambda_3^2 \int_{I_{\min}=0}^{I_{\max}(T)} I^{5/2} \cdot \exp\{-(a_1^p + a_2^{EA})I^{1/2}\} dI \quad (\text{A45})$$

$$C_{14}^a = \lambda_1 \lambda_2 \lambda_3^2 \int_{I_{\min}=0}^{I_{\max}(\tau)} I^{7/2} \cdot \exp(-a_1^p I^{1/2}) dI \quad (\text{A46})$$

$$C_{15}^a = \lambda_1 \lambda_2 \lambda_3^2 \int_{I_{\min}=0}^{I_{\max}(\tau)} I^{7/2} \cdot \exp\{-(a_1^p + w_1^{\text{EA}})I^{1/2}\} dI \quad (\text{A47})$$

$$C_{16}^a = \lambda_1 \lambda_2 \lambda_3^2 \int_{I_{\min}=0}^{I_{\max}(\tau)} I^{7/2} \cdot \exp\{-(a_1^p + w_2^{\text{EA}})I^{1/2}\} dI \quad (\text{A48})$$

$$C_{21}^a = \lambda_3^2 \int_{I_{\min}=0}^{I_{\max}(\tau)} I^{5/2} \cdot \exp(-a_2^p I^{1/2}) dI \quad (\text{A49})$$

$$C_{22}^a = \lambda_3^2 \int_{I_{\min}=0}^{I_{\max}(\tau)} I^{5/2} \cdot \exp\{-(a_2^p + a_1^{\text{EA}})I^{1/2}\} dI \quad (\text{A50})$$

$$C_{23}^a = \lambda_3^2 \int_{I_{\min}=0}^{I_{\max}(\tau)} I^{5/2} \cdot \exp\{-(a_2^p + a_2^{\text{EA}})I^{1/2}\} dI \quad (\text{A51})$$

$$C_{24}^a = \lambda_1 \lambda_2 \lambda_3^2 \int_{I_{\min}=0}^{I_{\max}(\tau)} I^{7/2} \cdot \exp(-a_2^p I^{1/2}) dI \quad (\text{A52})$$

$$C_{25}^a = \lambda_1 \lambda_2 \lambda_3^2 \int_{I_{\min}=0}^{I_{\max}(\tau)} I^{7/2} \cdot \exp\{-(a_2^p + w_1^{\text{EA}})I^{1/2}\} dI \quad (\text{A53})$$

$$C_{26}^a = \lambda_1 \lambda_2 \lambda_3^2 \int_{I_{\min}=0}^{I_{\max}(\tau)} I^{7/2} \cdot \exp\{-(a_2^p + w_2^{\text{EA}})I^{1/2}\} dI \quad (\text{A54})$$

Evaluation of Integrals in Coefficient Matrices

The integrals involving exponential factors in the integrands in the matrices A_{ij} , C_{ik} , A_{nj}^a , and C_{nk}^a are all special cases of a generalized integral whose solution was derived

and reported by Rard and Wijesinghe [14] in their Appendix A. Their general result can be expressed in a more compact form as

$$\int_{I_{\min}=0}^{I_{\max}(\Gamma)} I^n \cdot \exp(-aI^{1/2}) dI$$

$$= 2 \{(2n + 1)!/a^{2n+2}\} \cdot [1 - \exp(-Y) \sum_{r=0}^{2n+1} \{Y^{(2n+1-r)} / (2n + 1 - r)!\}] \quad (\text{A55})$$

where we define $Y \equiv a I_{\max}^{1/2}$.